NASA TECHNICAL NOTE

NASA TN D-4972

A METHOD FOR COMPUTATION OF VIBRATION MODES AND FREQUENCIES OF ORTHOTROPIC THIN SHELLS OF REVOLUTION HAVING GENERAL MERIDIONAL CURVATURE

by Howard M. Adelman, Donnell S. Catherines, and William C. Walton, Jr.

Langley Research Center
Langley Station, Hampton, Va.

NATIONAL AERONAUTICS AND SPACE ADMINISTRATION • WASHINGTON, D. C. • JANUARY 1969

A METHOD FOR COMPUTATION OF VIBRATION MODES AND FREQUENCIES OF ORTHOTROPIC THIN SHELLS OF REVOLUTION HAVING GENERAL MERIDIONAL CURVATURE

By Howard M. Adelman, Donnell S. Catherines, and William C. Walton, Jr.

Langley Research Center
Langley Station, Hampton, Va.

NATIONAL AERONAUTICS AND SPACE ADMINISTRATION

For sale by the Clearinghouse for Federal Scientific and Technical Information
Springfield, Virginia 22151 – CFSTI price $3.00

A METHOD FOR COMPUTATION OF VIBRATION MODES AND FREQUENCIES OF ORTHOTROPIC THIN SHELLS OF REVOLUTION HAVING GENERAL MERIDIONAL CURVATURE

By Howard M. Adelman, Donnell S. Catherines,
and William C. Walton, Jr.
Langley Research Center

SUMMARY

This report describes a procedure for computing the vibration modes and frequencies of thin shells of revolution having general meridional curvature and orthotropic elastic properties. The procedure is based on the finite-element method in which the direct-stiffness approach is used. A geometrically exact finite element is employed. A computer program based on this procedure has been written and details of the program are described. The geometric characteristics of the shell are used as inputs to the program in the form of functions of the meridional coordinate. The stiffness and mass matrices are computed by numerical integration by use of the trapezoidal rule.

The computer program is applied to several shell configurations including two cylinders, two conical frustums, shells of both positive and negative Gaussian curvature, and an annular plate. Frequencies are correlated with frequencies from previous investigations for these shells. The agreement between results of the present analysis and results from the previous investigations is generally excellent.

INTRODUCTION

A problem of current interest to structural analysts in the aerospace field is that of determining the dynamic behavior of structures in which some of the components are thin shells of revolution. Understanding the modes of vibration of the individual shell components can be of fundamental importance in connection with this problem. Consequently, much effort has gone into developing techniques to determine natural frequencies and mode shapes of the commonly encountered shells of revolution. Few closed-form solutions are known and, therefore, most of the developments have been in the area of approximation methods. Among the methods that have been tried are Rayleigh-Ritz methods (refs. 1 and 2), Stodola-type iteration methods (ref. 3), finite-difference solutions (ref. 4), finite-element methods (refs. 5 to 9), and methods in which the shell boundary-value problem is reduced to an initial-value problem involving first-order differential equations which

are numerically integrated (ref. 10). The finite-difference and numerical-integration methods involve a trial-and-error search for the natural frequencies that will make a certain determinant vanish. These "search methods" are relatively slow, and analysts using them have been known to overlook modes, as noted in reference 3. Stodola-type methods also lose numerical significance in the calculation of higher modes as noted in reference 3.

The authors, in the course of developing practical procedures to analyze the forced response of structures incorporating shells of revolution, required a method for computing mode shapes and frequencies of shells of revolution having general meridional curvature and orthotropic elastic properties. These mode shapes and frequencies would be used in analyses of structures involving such shells where in the analysis the deformation of each shell is represented by superposition of a number of mode shapes of the shell. Early experience indicated that selection of representative modes for a shell would require examination of a great number of its modes some high in the frequency spectrum. It was therefore necessary that:

(1) The method should give capability for quick calculation of a large number of modes and frequencies

(2) The mode shapes and frequencies quite high in the frequency spectrum should be accurately predicted

(3) The analyst should be protected from overlooking modes in computation

In view of these objectives, search methods and Stodola methods were considered unsatisfactory for the reasons of their inadequacy to meet these requirements. Both the Rayleigh-Ritz and finite-element approaches seemed to offer better chances for success in meeting the objectives.

From the viewpoint of the analyst, the outstanding advantage of finite-element and Rayleigh-Ritz approaches is that they lead to a symmetric eigenvalue problem which is amenable to fast and accurate solution on a digital computer. In the methods available for solving symmetric eigenvalue problems, all the modes are computed simultaneously, and thus any danger of overlooking modes in computation is avoided.

A finite-element approach was selected in preference to a Rayleigh-Ritz approach for the following reasons:

(1) The computing details of the Rayleigh-Ritz methods reported in references 1 and 2 resulted in use of a large number of terms. These methods lead to relatively poorly conditioned eigenvalue formulations requiring that a large number of significant figures be carried in the calculations in order to retain significance in the results. Preliminary trials with circular plates indicated that the finite-element approach leads to very well-conditioned eigenvalue problems.

(2) It was believed that the finite-element method would converge more easily than the Rayleigh-Ritz method when local high stress gradients, such as occur for some edge conditions (ref. 11), are present.

The element most popularly employed in the finite-element analysis of shells of revolution has been the conical element (for example, refs. 8 and 9). This element can exactly fit cylinders and conical frustums. However, for shells having a curved meridian, use of this element leads to only an approximation of the shell by a series of joined conical frustums. Thus, the curved meridian is approximated by a series of straight lines. Consequently, an analysis of a shell with a curved meridian based on conical elements may give inaccurate frequencies and stresses (refs. 5 and 6).

Analysts have been aware that the use of an element which coincides with the shape of the shell being analyzed would probably improve the accuracy in computed results (ref. 5). The main impediment to the use of such a geometrically exact element has been a reluctance on the part of analysts to give up a certain computational convenience associated with the conical element. This convenience is that since the shape is fixed, quadratures required to compute the stiffness and mass matrices of the element are performed only once, and the same matrices are used in every analysis. With a geometrically exact element, the shape of the element depends on the shape of the portion of the shell which the element represents, with the result that the integration has to be an inseparable part of each analysis. It has been recognized that a natural and probably feasible approach to making the quadratures part of the analysis is to use numerical integration (ref. 5). However, the objection has remained that for each element the radius of the shell and the two radii of curvature must be specified as functions of position along the meridian of the element.

In spite of this objection, the decision was made to develop a computer program to meet the previously stated objectives based on a geometrically exact element. It was believed that the necessity for description of the geometry of an element in terms of functions rather than of numerical parameters would present no difficulties in practice if, as is nearly always the case, the geometry of the entire shell could be described by functions located in a subroutine which could be readily changed. Development has progressed to the point where the program has been applied to a variety of shells of revolution of practical interest. Detailed correlations have been made between frequencies from the program and frequencies calculated for these shells by other investigators. A cursory correlation of mode shapes including stresses has been made for some of these shells but as yet is inconclusive because of present unavailability of sufficient modal data from the methods of the previous investigators. These correlations are not presented in this report.

The main purposes of this report are as follows:

(1) To describe the analysis underlying the computer program

(2) To describe the computer program

(3) To present the frequency correlations

SYMBOLS

$a_{0,k}, a_{1,k}, a_{2,k}, a_{3,k}$ coefficients in polynomial displacement function for normal displacement w

A_k matrix which transforms displacements and rotations at ends of an element to coefficients of polynomial displacement functions (see eq. (13) and table I)

$b_{0,k}, b_{1,k}, b_{2,k}, b_{3,k}$ coefficients in polynomial displacement function for meridional displacement u

B matrix defined in equation (42)

$c_{0,k}, c_{1,k}, c_{2,k}, c_{3,k}$ coefficients in polynomial displacement function for circumferential displacement v

C_k matrix whose elements are coefficients in an expression for strain energy of a shell element in terms of coefficients of polynomial displacement functions (see eq. (20))

C_{11}, C_{12}, C_{22} membrane stiffness constants

C_{66} in-plane shear stiffness

D diagonal matrix whose elements are eigenvalues of mass matrix (see eq. (39))

D_{11}, D_{12}, D_{22} flexural stiffness constants

D_{66} torsional stiffness

e_1, e_2, e_{12} middle-surface strains (see eqs. (1a) to (1c))

E_k kinetic energy of kth element

E kinetic energy of shell; also Young's modulus

f	frequency
F_k	matrix whose elements are coefficients in an expression for kinetic energy of a shell element in terms of coefficients of polynomial displacement functions (see eq. (30))
h	shell thickness
I	identity matrix
$i = \sqrt{-1}$	
K	number of elements used to represent a shell
$K_{11},K_{12},K_{22},K_{66}$	stiffness constants representing interaction between in-plane and out-of-plane strains
L	meridional length of a shell
m	meridional wave number for a freely supported cylinder
M_k	element mass matrix
M	shell mass matrix
n	circumferential wave number
N	order of stiffness and mass matrices after edge constraints have been applied
P	matrix whose elements are coefficients in an expression for kinetic energy of a shell element in terms of displacements u, v, and w (see eq. (28))
q	index representing an integration station
Q	total number of integration intervals
r	radius of a shell measured in plane normal to shell axis
R_1,R_2	principal radii of curvature of shell

$\mathbf{R}$	matrix whose elements are coefficients in an expression for strain energy of shell element in terms of actual variables in strain energy (see eq. (16))
s	meridional coordinate
S_k	element stiffness matrix
S	shell stiffness matrix
s_0	meridional distance from origin of s to reference edge of a shell
s_k	meridional distance from reference edge of shell to center of kth element
s_{kq}	meridional distance from reference edge of shell to qth integration station of kth element
s_{ki}	meridional distance from reference edge of a shell to ith location on kth element at which mode shape is evaluated
t	time
T_k	inverse of matrix A_k
u	meridional component of middle-surface displacement
U	matrix whose columns are eigenvectors of mass matrix
v	circumferential component of middle-surface displacement
V_k	strain energy of kth element
V	strain energy of shell
w	normal component of middle-surface displacement
x	meridional coordinate measured within a single element (see eq. (5))
x_{kq}	meridional distance from center of kth element to qth integration station

$\mathbf{X}$	matrix which describes assumed form of variables appearing in strain energy
$\mathbf{y}$	column matrix containing unknown displacements and rotations
$\mathbf{Y}$	matrix which describes the assumed form of displacements u, v, and w
$\mathbf{Z}$	matrix defined in equation (43)
β	rotation of shell generator relative to unstrained direction (see eq. (10))
δ	modal column (see eq. (44))
γ	column matrix whose elements are coefficients of assumed-displacement polynomials (see eq. (18))
ϵ_k	meridional length of kth element
θ	circumferential coordinate
$\kappa_1, \kappa_2, \kappa_{12}$	changes in curvatures (see eqs. (1d) to (1f))
$\lambda_1, \lambda_2, \ldots, \lambda_N$	eigenvalues of mass matrix
ξ	column matrix whose elements are displacements and rotations at ends of an element (see eq. (22))
ρ	mass density
ω	circular frequency
Ω	nondimensional frequency
μ	Poisson's ratio

Primes denote differentiation with respect to s or x; superscript T denotes transpose of a matrix.

Special notations used in machine plots of figures 16, 17, 20, and 21:

N	circumferential wave number
S/L	nondimensional meridional distance

U,V,W middle-surface displacements in the meridional, circumferential, and normal directions, respectively

UMAX,VMAX,WMAX maximum values of U, V, and W, respectively

ω^2 = (Circular frequency)^2, sec^{-2}

DEVELOPMENT OF THE STIFFNESS MATRIX FOR A GEOMETRICALLY EXACT ELEMENT

Strain Energy in Terms of Displacements

For purposes of the following analysis, reference is made to figure 1. In this figure, u, v, and w represent displacements in the meridional, circumferential, and normal directions, respectively, R_1 and R_2 are the two principal radii of curvature of the shell, and r is the radius of the shell measured in a plane normal to the shell axis. All three radii are regarded as functions of the meridional coordinate s, measured along the shell from a reference edge.

According to Novozhilov (ref. 12), the six strain-displacement relations which describe the local state of strain for a thin shell of revolution are as follows:

Membrane strain in meridional direction:

$$e_1 = u' + \frac{w}{R_1} \tag{1a}$$

Membrane strain in circumferential direction:

$$e_2 = \frac{1}{r}\frac{\partial v}{\partial \theta} + \frac{1}{r} r'u + \frac{w}{R_2} \tag{1b}$$

In-plane shear strain:

$$e_{12} = \frac{1}{r}\frac{\partial u}{\partial \theta} + v' - \frac{1}{r} r'v \tag{1c}$$

Change of curvature in meridional direction:

$$\kappa_1 = -w'' + \frac{1}{R_1} u' - \frac{1}{R_1^2} R_1'u \tag{1d}$$

Change of curvature in circumferential direction:

$$\kappa_2 = -\frac{1}{r^2}\frac{\partial^2 w}{\partial \theta^2} + \frac{1}{rR_2}\frac{\partial v}{\partial \theta} - \frac{r'w'}{r} + \frac{1}{rR_1} r'u \tag{1e}$$

Twist of the middle surface:

$$\kappa_{12} = -\frac{1}{r}\frac{\partial w'}{\partial \theta} + \frac{1}{r^2} r' \frac{\partial w}{\partial \theta} + \frac{1}{rR_1}\frac{\partial u}{\partial \theta} + \frac{1}{R_2} v' - \frac{1}{rR_2} r'v \tag{1f}$$

For a shell which, in general, is composed of orthotropic layers, the strain energy is given in reference 13 (p. 45) as follows:

$$V = \frac{1}{2}\int\int\left(C_{11}e_1^2 + 2C_{12}e_1e_2 + C_{22}e_2^2 + C_{66}e_{12}^2\right)r\,d\theta\,ds$$

$$+ \frac{1}{2}\int\int\left(D_{11}\kappa_1^2 + 2D_{12}\kappa_1\kappa_2 + D_{22}\kappa_2^2 + D_{66}\kappa_{12}^2\right)r\,d\theta\,ds$$

$$+ \int\int\left[K_{11}e_1\kappa_1 + K_{12}\left(e_1\kappa_2 + e_2\kappa_1\right) + K_{22}e_2\kappa_2 + K_{66}e_{12}\kappa_{12}\right]r\,d\theta\,ds \qquad (2)$$

where in equation (2) the integrations are taken over the shell surface and the following definitions hold:

(1) C_{11}, C_{12}, C_{22} are membrane stiffnesses

(2) D_{11}, D_{12}, D_{22} are flexural stiffnesses

(3) C_{66} is the in-plane shear stiffness

(4) D_{66} is the torsional shear stiffness

(5) K_{11}, K_{12}, K_{22}, K_{66} are stiffnesses due to the interaction between in-plane strains and changes in curvature

All of these stiffnesses are, in general, functions of the meridional coordinate s. Reference 13 contains an excellent discussion of the derivation of the above stiffnesses for shells having various numbers of layers and composed of materials having various types of elastic properties.

The work in the present study is based on Novozhilov's strain-displacement relations (eqs. (1a) to (1f)), the energy expression of equation (2), and the definitions of the stiffnesses in reference 13 with the following single exception. The strain κ_{12} (called τ in refs. 12 and 13) is defined by Ambartsumyan (p. 25) to be double the value of this strain as defined by Novozhilov. Since the authors prefer to use Novozhilov's definition of κ_{12}, the value of D_{66} used herein is four times the value of D_{66} given in reference 13 and the value of K_{66} is twice the value of K_{66} given in reference 13.

For a shell of revolution vibrating in a natural mode with circular frequency ω, the three displacements u, v, and w can be expressed as follows:

$$\left.\begin{aligned} u(s,\theta,t) &= u(s)\cos n\theta e^{i\omega t} \\ v(s,\theta,t) &= v(s)\sin n\theta e^{i\omega t} \\ w(s,\theta,t) &= w(s)\cos n\theta e^{i\omega t} \end{aligned}\right\} \qquad (3)$$

The displacements from equations (3) are substituted into the strain-displacement relations of equations (1). Substitution of the resulting strains into the strain-energy expression of equation (2) and integration with respect to θ yields the strain energy in terms of displacements. The amplitude of the strain energy for $n \neq 0$ is as follows:

$$
\begin{aligned}
V = {} & \frac{\pi}{2}\int\left[C_{11}\left(u' + \frac{w}{R_1}\right)^2 + 2C_{12}\left(u' + \frac{w}{R_1}\right)\left(\frac{n}{r}v + \frac{r'}{r}u + \frac{w}{R_2}\right) + C_{22}\left(\frac{n}{r}v + \frac{r'}{r}u + \frac{w}{R_2}\right)^2 + C_{66}\left(-\frac{n}{r}u + v' - \frac{r'}{r}v\right)^2\right] r\,ds \\
& + \pi\int\left[K_{11}\left(u' + \frac{w}{R_1}\right)\left(-w'' + \frac{u'}{R_1} - \frac{R_1'}{R_1^2}u\right) + K_{12}\left(u' + \frac{w}{R_1}\right)\left(\frac{n^2}{r^2}w + \frac{n}{rR_2}v - \frac{r'}{r}w' + \frac{r'}{rR_1}u\right) + K_{12}\left(\frac{n}{r}v + \frac{r'}{r}u + \frac{w}{R_2}\right)\right. \\
& \left. + K_{22}\left(\frac{n}{r}v + \frac{r'}{r}u + \frac{w}{R_2}\right)\left(\frac{n^2}{r^2}w + \frac{n}{rR_2}v - \frac{r'}{r}w' + \frac{r'}{rR_1}u\right) + K_{66}\left(-\frac{n}{r}u + v' - \frac{r'}{r}v\right)\left(\frac{n}{r}w' - \frac{nr'}{r^2}w - \frac{n}{rR_1}u + \frac{v'}{R_2} - \frac{r'}{rR_2}v\right)\right] r\,ds \\
& + \frac{\pi}{2}\int\left[D_{11}\left(-w'' + \frac{u'}{R_1} - \frac{R_1'}{R_1^2}u\right)^2 + 2D_{12}\left(-w'' + \frac{u'}{R_1} - \frac{R_1'}{R_1^2}u\right)\left(\frac{n^2}{r^2}w + \frac{n}{rR_2}v - \frac{r'}{r}w' + \frac{r'}{rR_1}u\right)\right. \\
& \left. + D_{22}\left(\frac{n^2}{r^2}w + \frac{n}{rR_2}v - \frac{r'}{r}w' + \frac{r'}{rR_1}u\right)^2 + D_{66}\left(\frac{n}{r}w' - \frac{nr'}{r^2}w - \frac{n}{rR_1}u + \frac{v'}{R_2} - \frac{r'}{rR_2}v\right)^2\right] r\,ds
\end{aligned}
\tag{4}
$$

For $n = 0$ the strain energy as given by expression (4) should be doubled. The succeeding developments are carried out on the assumption that $n \neq 0$ with the understanding that for $n = 0$ appropriate expressions should be doubled.

Representation of the Shell by Geometrically Exact Finite Elements

The present analytical method follows the main steps of conventional finite-element analysis. It is noted, however, that each element coincides exactly with a slice of the actual shell. Hence, the elements are spoken of as "geometrically exact elements."

A typical idealization of a shell of revolution is shown in figure 2. Counting elements from the reference edge, the following definitions are made:

K total number of elements

ϵ_k length of kth element, measured along meridian curve of shell

x coordinate inside kth element, measured along meridian from center of kth interval so that following relationship holds:

$$-\frac{\epsilon_k}{2} \leq x \leq \frac{\epsilon_k}{2} \tag{5}$$

s_k distance along meridian from reference edge of shell to center of the kth element

From the foregoing definitions for x and s_k, it follows that

$$s = s_k + x \tag{6}$$

A numbering system has been adopted in which quantites such as displacement, derivatives of displacements, and rotations at $s = s_k - \frac{\epsilon_k}{2}$ and $s = s_k + \frac{\epsilon_k}{2}$ are indicated by subscripts k and $k+1$, respectively. Thus, for example, w_k is the normal displacement at $s = s_k - \frac{\epsilon_k}{2}$ and u_{k+1} is the meridional displacement at $s = s_k + \frac{\epsilon_k}{2}$. Also, it is necessary to have a notation for the radius of curvature R_1 at the locations $s = s_k \mp \frac{\epsilon_k}{2}$. The symbols $R_{1,k}$ and $R_{1,k+1}$ represent the respective values.

Assumed Displacement Field for Element

As an approximation, the displacements u, v, and w are assumed to have the following polynomial forms over the kth element:

$$\left.\begin{aligned} w &= a_{0,k} + a_{1,k}x + a_{2,k}x^2 + a_{3,k}x^3 \\ u &= b_{0,k} + b_{1,k}x + b_{2,k}x^2 + b_{3,k}x^3 \\ v &= c_{0,k} + c_{1,k}x + c_{2,k}x^2 + c_{3,k}x^3 \end{aligned}\right\} \tag{7}$$

where the a's, b's, and c's are undetermined coefficients. From equation (7) it follows that:

$$\begin{Bmatrix} w \\ w' \\ w'' \\ u \\ u' \\ v \\ v' \end{Bmatrix} = [X] \begin{Bmatrix} a_{0,k} \\ a_{1,k} \\ a_{2,k} \\ a_{3,k} \\ b_{0,k} \\ b_{1,k} \\ b_{2,k} \\ b_{3,k} \\ c_{0,k} \\ c_{1,k} \\ c_{2,k} \\ c_{3,k} \end{Bmatrix} \tag{8}$$

where

$$[X] = \begin{bmatrix} 1 & x & x^2 & x^3 & 0 & 0 & 0 & 0 & 0 & 0 & 0 & 0 \\ 0 & 1 & 2x & 3x^2 & 0 & 0 & 0 & 0 & 0 & 0 & 0 & 0 \\ 0 & 0 & 2 & 6x & 0 & 0 & 0 & 0 & 0 & 0 & 0 & 0 \\ 0 & 0 & 0 & 0 & 1 & x & x^2 & x^3 & 0 & 0 & 0 & 0 \\ 0 & 0 & 0 & 0 & 0 & 1 & 2x & 3x^2 & 0 & 0 & 0 & 0 \\ 0 & 0 & 0 & 0 & 0 & 0 & 0 & 0 & 1 & x & x^2 & x^3 \\ 0 & 0 & 0 & 0 & 0 & 0 & 0 & 0 & 0 & 1 & 2x & 3x^2 \end{bmatrix} \tag{9}$$

Relationship Between Undetermined Coefficients and Displacements and Rotations at Ends of Element

The rotation of the meridian curve relative to the unstrained direction is defined as β and is given by

$$\beta = w' - \frac{u}{R_1} \tag{10}$$

It follows that

$$\beta_k = w'_k - \frac{u_k}{R_{1,k}} \tag{11}$$

and

$$\beta_{k+1} = w'_{k+1} - \frac{u_{k+1}}{R_{1,k+1}} \tag{12}$$

Inserting $x = -\frac{\epsilon_k}{2}$ and $x = \frac{\epsilon_k}{2}$ into the appropriate locations in equation (8) results in the following relationship:

$$\begin{bmatrix} w_k \\ u_k \\ v_k \\ \beta_k \\ u'_k \\ v'_k \\ w_{k+1} \\ u_{k+1} \\ v_{k+1} \\ \beta_{k+1} \\ u'_{k+1} \\ v'_{k+1} \end{bmatrix} = [A_k] \begin{Bmatrix} a_{0,k} \\ a_{1,k} \\ a_{2,k} \\ a_{3,k} \\ b_{0,k} \\ b_{1,k} \\ b_{2,k} \\ b_{3,k} \\ c_{0,k} \\ c_{1,k} \\ c_{2,k} \\ c_{3,k} \end{Bmatrix} \tag{13}$$

where the elements of matrix $[A_k]$ are given in table I. When equation (13) is inverted, the following relationship results:

$$\begin{Bmatrix} a_{0,k} \\ a_{1,k} \\ a_{2,k} \\ a_{3,k} \\ b_{0,k} \\ b_{1,k} \\ b_{2,k} \\ b_{3,k} \\ c_{0,k} \\ c_{1,k} \\ c_{2,k} \\ c_{3,k} \end{Bmatrix} = [T_k] \begin{Bmatrix} w_k \\ u_k \\ v_k \\ \beta_k \\ u'_k \\ v'_k \\ w_{k+1} \\ u_{k+1} \\ v_{k+1} \\ \beta_{k+1} \\ u'_{k+1} \\ v'_{k+1} \end{Bmatrix} \tag{14}$$

where

$$[T_k] = [A_k]^{-1} \tag{15}$$

The elements of the inverse matrix $[T_k]$ are given in table II.

Formulation of Element Stiffness Matrix

From equation (4) the strain energy of an element may be written as follows:

$$V_k = \frac{\pi}{2} \int_{-\epsilon_k/2}^{\epsilon_k/2} \lfloor w, w', w'', u, u', v, v' \rfloor [R] \begin{Bmatrix} w \\ w' \\ w'' \\ u \\ u' \\ v \\ v' \end{Bmatrix} dx \tag{16}$$

where $[R]$ is a 7×7 symmetric matrix, the elements of which are known functions of the meridional coordinate x. The elements of $[R]$ are listed in the appendix. Using equation (8) in equation (16) permits the strain energy to be written in terms of the undetermined polynomial coefficients as follows:

$$V_k = \frac{\pi}{2} \int_{-\epsilon_k/2}^{\epsilon_k/2} \{\gamma\}^T [X]^T [R] [X] \{\gamma\} \, dx \tag{17}$$

where

$$\{\gamma\} = \begin{Bmatrix} a_{0,k} \\ a_{1,k} \\ a_{2,k} \\ a_{3,k} \\ b_{0,k} \\ b_{1,k} \\ b_{2,k} \\ b_{3,k} \\ c_{0,k} \\ c_{1,k} \\ c_{2,k} \\ c_{3,k} \end{Bmatrix} \tag{18}$$

or

$$V_k = \frac{1}{2}\{\gamma\}^T [C_k] \{\gamma\} \tag{19}$$

where

$$[C_k] = \pi \int_{-\epsilon_k/2}^{\epsilon_k/2} [X]^T [R] [X] \, dx \tag{20}$$

Finally, use of the transformation expressed by equation (14) gives the strain energy as

$$V_k = \frac{1}{2}\{\xi\}^T [T_k]^T [C_k] [T_k] \{\xi\} \tag{21}$$

where

$$\{\xi\} = \begin{Bmatrix} w_k \\ u_k \\ v_k \\ \beta_k \\ u'_k \\ v'_k \\ w_{k+1} \\ u_{k+1} \\ v_{k+1} \\ \beta_{k+1} \\ u'_{k+1} \\ v'_{k+1} \end{Bmatrix} \tag{22}$$

Inspection of equation (21) identifies the shell element stiffness matrix $[S_k]$ as

$$[S_k] = [T_k]^T [C_k][T_k] \tag{23}$$

DEVELOPMENT OF CONSISTENT MASS MATRIX FOR THE GEOMETRICALLY EXACT ELEMENT

If rotary inertia is neglected and if the shell is assumed to be vibrating in a natural mode, the amplitude of the kinetic energy E_k for $n \neq 0$ is

$$E_k = \frac{\pi}{2} \omega^2 \int_{-\epsilon_k/2}^{\epsilon_k/2} \rho h\left(u^2 + v^2 + w^2\right) r \, dx \tag{24}$$

where ρh is the mass per unit area of the shell. The quantity ρh is a known function of s and therefore of x. As with the strain energy, the expression for kinetic energy must be doubled for $n = 0$.

Based on the assumed displacements of equation (7), the following relation may be written:

$$\begin{Bmatrix} w \\ u \\ v \end{Bmatrix} = [Y]\{\gamma\} \tag{25}$$

where

$$[Y] = \begin{bmatrix} 1 & x & x^2 & x^3 & 0 & 0 & 0 & 0 & 0 & 0 & 0 & 0 \\ 0 & 0 & 0 & 0 & 1 & x & x^2 & x^3 & 0 & 0 & 0 & 0 \\ 0 & 0 & 0 & 0 & 0 & 0 & 0 & 0 & 1 & x & x^2 & x^3 \end{bmatrix} \tag{26}$$

Equation (24) can be rewritten in the form

$$E_k = \frac{\pi}{2} \omega^2 \int_{-\epsilon_k/2}^{\epsilon_k/2} \begin{bmatrix} w, & u, & v \end{bmatrix} [P] \begin{Bmatrix} w \\ u \\ v \end{Bmatrix} dx \tag{27}$$

where

$$[P] = \begin{bmatrix} \rho hr & 0 & 0 \\ 0 & \rho hr & 0 \\ 0 & 0 & \rho hr \end{bmatrix} \tag{28}$$

Using equation (25) with equation (27) yields

$$E_k = \frac{\omega^2}{2}\{\gamma\}^T[F_k]\{\gamma\} \tag{29}$$

where

$$F_k = \pi \int_{-\epsilon_k/2}^{\epsilon_k/2} [Y]^T[P][Y]\,dx \tag{30}$$

In view of equation (14), equation (29) may be written as follows:

$$E_k = \frac{\omega^2}{2}\{\xi\}[T_k]^T[F_k][T_k]\{\xi\} \tag{31}$$

Therefore, the element mass matrix may be identified as $[M_k]$, where

$$[M_k] = [T_k]^T[F_k][T_k] \tag{32}$$

DERIVATION OF MODAL EQUATIONS

In view of the numbering convention adopted for the elements, the second edge of the kth element coincides with the first edge of the k+1st element. In this analysis, the following conditions of compatability are assumed to hold at each such juncture:

$$\begin{Bmatrix} w_{k+1} \\ u_{k+1} \\ v_{k+1} \\ \beta_{k+1} \\ u'_{k+1} \\ v'_{k+1} \end{Bmatrix}_{\substack{\text{kth} \\ \text{element}}} = \begin{Bmatrix} w_{k+1} \\ u_{k+1} \\ v_{k+1} \\ \beta_{k+1} \\ u'_{k+1} \\ v'_{k+1} \end{Bmatrix}_{\substack{\text{k+1st} \\ \text{element}}} \qquad \text{for all} \quad k < K \tag{33}$$

Of the six equalities in equation (33), the first four are standard. The last two, however, are valid only for shells having continuous distributions of stiffness.

The total strain energy V and the kinetic energy E may be expressed as follows:

$$\left.\begin{aligned} V &= \sum_{k=1}^{K} V_k \\ E &= \sum_{k=1}^{K} E_k \end{aligned}\right\} \tag{34}$$

where V_k and E_k are given in equations (21) and (31), respectively. If the summations of equations (34) are carried out and use is made of equation (33), the strain and kinetic energies may be written as follows:

$$\left.\begin{aligned} V &= \frac{1}{2}\{y\}^T[S]\{y\} \\ E &= \frac{1}{2}\omega^2\{y\}^T[M]\{y\} \end{aligned}\right\} \tag{35}$$

where

S stiffness matrix, which is a symmetric positive semidefinite or positive definite matrix of order $6(K + 1)$

M mass or inertia matrix, which is a symmetric positive definite matrix of order $6(K + 1)$

y a vector containing all of the unknown displacements and rotations

In the present method, the matrices S and M are constructed by the well-known procedure of superimposing element matrices, illustrated in figure 3. As the figure shows, the superposition consists of placing appropriate shell element matrices in the matrices S and M so that the matrix elements in the lower right 6×6 block of the kth matrix add to the corresponding matrix elements in the upper left 6×6 block of the k+1st matrix.

The modal equations for shells with no edge constraints may be derived by minimizing the quantity $E - V$ with respect to each of the variables in the vector y. This minimization is equivalent to the following set of equations, $6(K + 1)$ in number:

$$\left.\begin{aligned} &\frac{\partial(E - V)}{\partial w_k} = 0 \qquad \frac{\partial(E - V)}{\partial \beta_k} = 0 \\ &\frac{\partial(E - V)}{\partial u_k} = 0 \qquad \frac{\partial(E - V)}{\partial u'_k} = 0 \\ &\frac{\partial(E - V)}{\partial v_k} = 0 \qquad \frac{\partial(E - V)}{\partial v'_k} = 0 \end{aligned}\right\} \quad (k = 1, 2, \ldots, K + 1) \tag{36}$$

Equations (36) can be expressed in the form

$$[S]\{y\} - \omega^2[M]\{y\} = 0 \tag{37}$$

Rigid edge constraints are incorporated by deleting from the stiffness and mass matrices of equation (37) those rows and columns which correspond to displacements and rotations that must vanish to satisfy the constraints. The form and character of equation (37) are not affected by the deletion of rows and columns from the matrices S and M, except that S may become positive definite instead of positive semidefinite. Of course, the order of matrices S and M is reduced.

Equation (37) determines $6(K + 1)$ natural frequencies and modal columns. The computation of these frequencies and modes is a standard operation. However, for completeness, some of the reductions involved in the solution are given in the section which follows.

The modal columns consist of values of displacements and rotations at each of the $K + 1$ junctures on the shell. For many purposes a more detailed mode shape is required. From equation (7) with x replaced by $s - s_k$, the following equations can be written for the mode shape within the kth element:

$$\left.\begin{aligned} w &= a_{0,k} + a_{1,k}(s - s_k) + a_{2,k}(s - s_k)^2 + a_{3,k}(s - s_k)^3 \\ u &= b_{0,k} + b_{1,k}(s - s_k) + b_{2,k}(s - s_k)^2 + b_{3,k}(s - s_k)^3 \\ v &= c_{0,k} + c_{1,k}(s - s_k) + c_{2,k}(s - s_k)^2 + c_{3,k}(s - s_k)^3 \end{aligned}\right\} \tag{38}$$

The coefficients $a_{0,k}$ through $c_{3,k}$ are computed by using equation (14).

COMPUTATIONAL METHOD AND COMPUTER PROGRAM

In this section, the details of the computing method are given. Each step is discussed and the flow of information is shown in block diagrams. The steps are intended to be specific enough to allow a digital computer program to be written by using them as a guide.

The basic organization of the computer program used in the present analysis is shown in block diagram 1.

The input which describes the geometry of the shell and its physical properties is first read, and stiffness and mass matrices referred to the coefficients of the displacement polynomials are then computed. These matrices are transformed so that they are referred to the displacements and rotations at the ends of the element. When a stiffness and a mass matrix have thus been computed for each element, the matrices are superimposed to form the shell stiffness and mass matrices. If the shell has rigid edge

constraints, then appropriate rows and columns are deleted from the stiffness and mass matrices to satisfy these constraints. The stiffness and mass matrices then constitute the ingredients to an eigenvalue problem which is solved for frequencies and modal columns. From the modal columns, the coefficients of the displacement polynomials are computed. The detailed mode shapes are then evaluated.

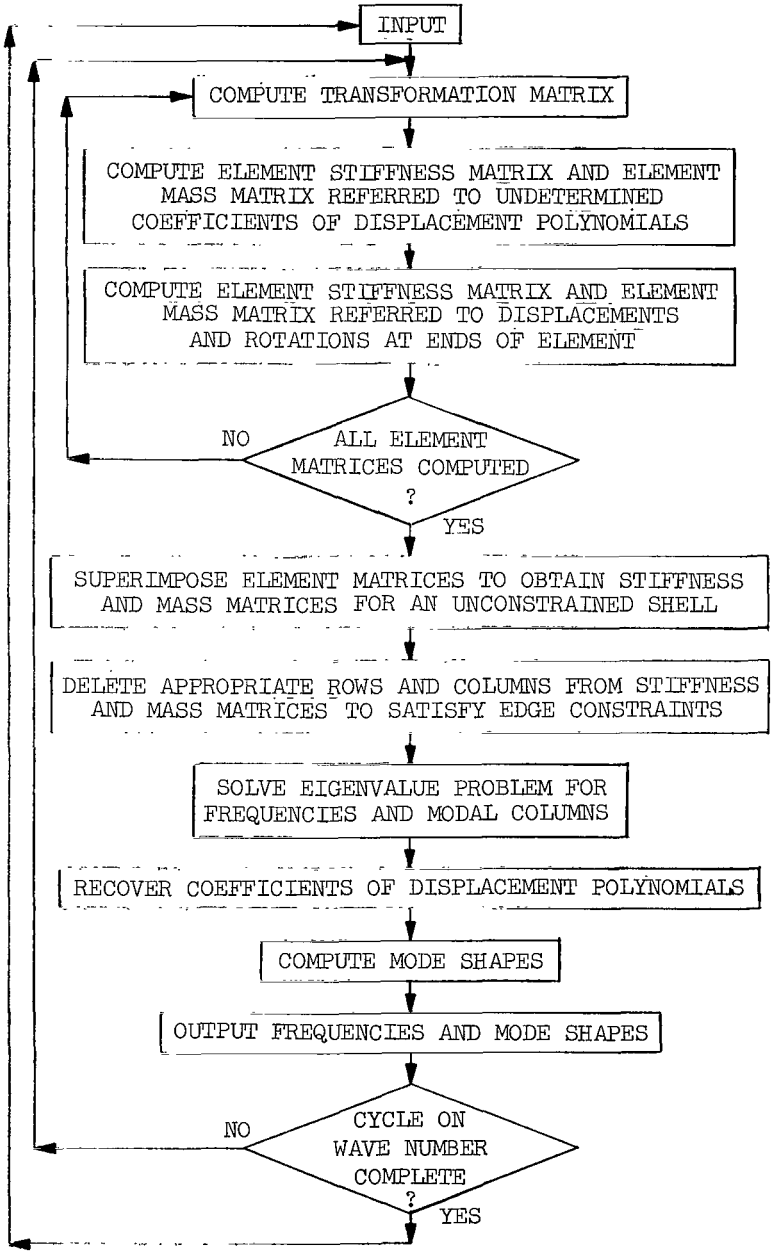

Block diagram 1.

A more detailed block diagram (see block diagram 2) is shown.

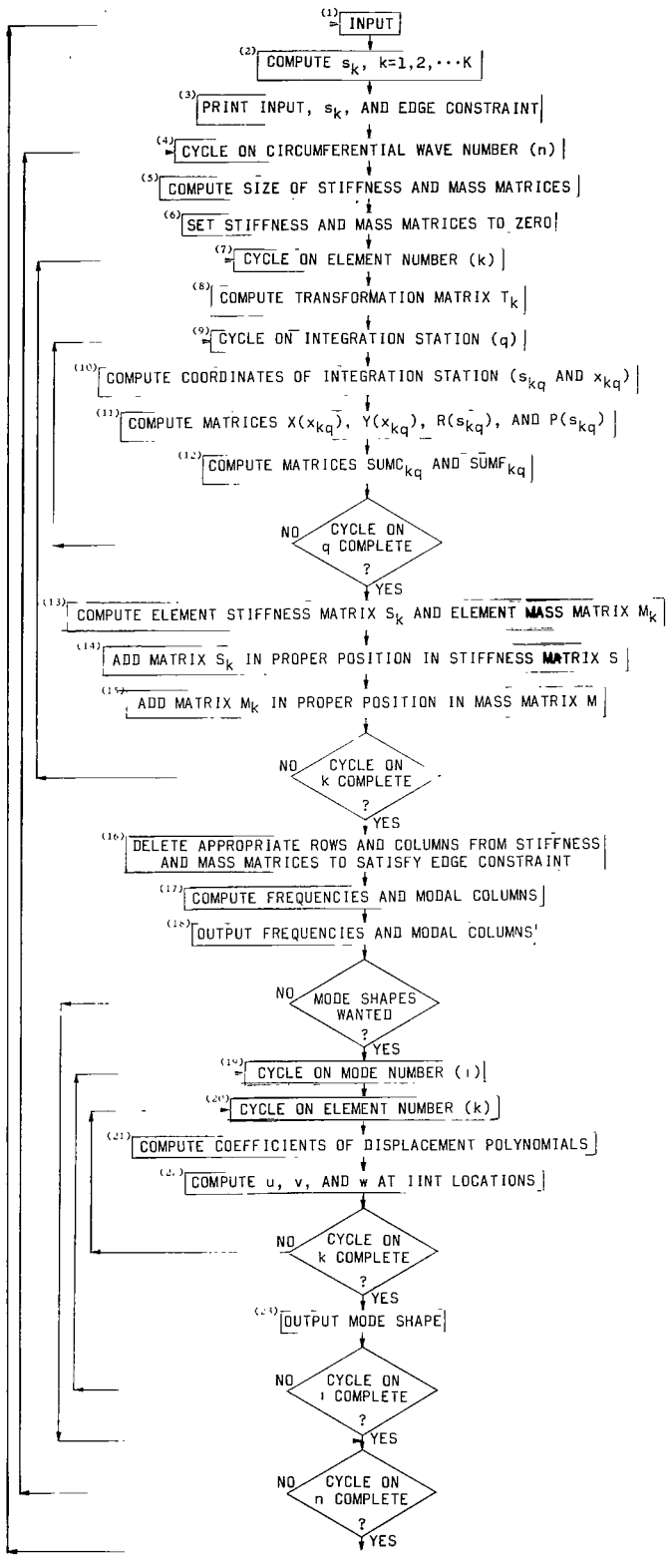

Block diagram 2.

A detailed discussion of the computing in each block of block diagram 2 is as follows:

BLOCK 1:

The following input quantities are required:

K number of elements used to represent shell

ϵ_k length of kth element, where $k = 1, 2, \ldots, K$

s_0 meridional distance from origin of s to reference edge of shell

The following input functions are required:

$1/R_1, 1/R_2$ reciprocals of principal radii of curvature

r shell radius measured in a plane normal to the shell axis

r', R_1' meridional rates of change of r and R_1

$C_{11}, C_{12}, C_{22}, C_{66}$
$D_{11}, D_{12}, D_{22}, D_{66}$
$K_{11}, K_{12}, K_{22}, K_{66}$ stiffnesses

$[\rho h]$ mass per unit area

The following control numbers are required:

NBEG initial value of n

NLAST final value of n

Q number of integration intervals to be used within each element

IPRINT if IPRINT = 0, intermediate matrices are not printed
if IPRINT $\neq$ 0, intermediate matrices are printed

NMODE number of mode shapes to be computed

IINT number of locations along each element at which mode shape is to be evaluated

ICASE edge constraint code (see table III)

BLOCK 2:

$$s_1 = s_0 + \frac{1}{2}\epsilon_1$$

$$s_k = s_0 + \frac{1}{2}\epsilon_k + \sum_{i=1}^{k-1} \epsilon_i \qquad (k = 2, \ldots, K)$$

BLOCK 4:

n = NBEG, NBEG + 1, . . ., NLAST

BLOCK 5:

KN = 6(K + 1)

BLOCK 7:

k = 1, 2, . . ., K

BLOCK 8:

The elements of $[T_k]$, a 12×12 matrix, are given in table II.

BLOCK 9:

q = 1, 2, . . ., Q + 1

BLOCK 10:

Each element is divided into Q equal intervals for the numerical integration. There are then Q + 1 integration stations. The values of x and s at the qth integration station of the kth element are, respectively, defined as

$$x_{kq} = \epsilon_k\left(\frac{q-1}{Q} - \frac{1}{2}\right) \qquad (q = 1, 2, \ldots, Q+1)$$

and

$$s_{kq} = s_k + \epsilon_k\left(\frac{q-1}{Q} - \frac{1}{2}\right) \qquad (q = 1, 2, \ldots, Q+1)$$

BLOCK 11:

The elements of $[X]$, $[Y]$, $[P]$, and $[R]$ are given in equations (9), (26), (28), and (A1) to (A28), respectively. The matrices $[X(x_{kq})]$ and $[Y(x_{kq})]$ are found by

substituting x_{kq} in equations (9) and (26), respectively. The matrices $\left[P(s_{kq})\right]$ and $\left[R(s_{kq})\right]$ are found by substituting s_{kq} into equations (28) and (A1) to (A28), respectively.

BLOCK 12:

$$\left[C_{kq}\right] = \pi\left[X(x_{kq})\right]^T\left[R(s_{kq})\right]\left[X(x_{kq})\right]$$

$$\left[SUMC_{k1}\right] = \frac{1}{2}\left[C_{k1}\right]$$

$$\left[SUMC_{kq}\right] = \left[SUMC_{k,q-1}\right] + \left[C_{kq}\right] \qquad (q = 2, 3, \ldots, Q)$$

$$\left[SUMC_{k,Q+1}\right] = \left[SUMC_{k,Q}\right] + \frac{1}{2}\left[C_{k,Q+1}\right]$$

$$\left[F_{kq}\right] = \pi\left[Y(x_{kq})\right]^T\left[P(s_{kq})\right]\left[Y(x_{kq})\right]$$

$$\left[SUMF_{k1}\right] = \frac{1}{2}\left[F_{k1}\right]$$

$$\left[SUMF_{kq}\right] = \left[SUMF_{k,q-1}\right] + \left[F_{kq}\right] \qquad (q = 2, 3, \ldots, Q)$$

$$\left[SUMF_{k,Q+1}\right] = \left[SUMF_{kQ}\right] + \frac{1}{2}\left[F_{k,Q+1}\right]$$

BLOCK 13:

$$\left[C_K\right] = \left[SUMC_{k,Q+1}\right]$$

$$\left[F_k\right] = \left[SUMF_{k,Q+1}\right]$$

$$\left[S_k\right] = \left[T_k\right]^T\left[C_k\right]\left[T_k\right]$$

$$\left[M_k\right] = \left[T_k\right]^T\left[F_k\right]\left[T_k\right]$$

BLOCKS 14 and 15:

The manner in which the matrices (either stiffness or mass) are placed in the overall matrix is illustrated in figure 3.

BLOCK 16:

Commonly encountered edge constraints along with the appropriate rows and columns to be deleted from S and M are given in table III.

BLOCK 17:

Compute by the threshold Jacobi method (ref. 14, p. 397) a modal matrix U and a set of eigenvalues $\lambda_1, \ldots, \lambda_N$ for the matrix M. Then

$$U^T M U = D = \begin{bmatrix} \lambda_1 & & & 0 \\ & \lambda_2 & & \\ & & \ddots & \\ 0 & & & \lambda_N \end{bmatrix} \tag{39}$$

and

$$U^T U = I$$

where

N order of matrix M

I identity matrix of order N

Since M is positive definite, all diagonal elements of D are positive.

Compute:

$$D^{1/2} = \begin{bmatrix} \sqrt{\lambda_1} & & & \\ & \sqrt{\lambda_2} & & \\ & & \ddots & \\ & & & \sqrt{\lambda_N} \end{bmatrix} \tag{40}$$

$$D^{-1/2} = \begin{bmatrix} 1/\sqrt{\lambda_1} & & & \\ & 1/\sqrt{\lambda_2} & & \\ & & \ddots & \\ & & & 1/\sqrt{\lambda_N} \end{bmatrix} \tag{41}$$

$$B = D^{-1/2} U^T S U D^{-1/2} \tag{42}$$

Compute Z, a modal matrix of B, by the threshold Jacobi method. Then

$$Z^T B Z = \begin{bmatrix} \omega_1^2 & & & 0 \\ & \omega_2^2 & & \\ & & \ddots & \\ 0 & & & \omega_N^2 \end{bmatrix} \tag{43}$$

$$Z^T Z = I$$

The values of ω^2 are the squares of the circular frequencies.

Compute:

$$\delta = UD^{-1/2}Z \tag{44}$$

The columns of δ are the modal columns. After the computation of the modal columns, insert zeros in the locations which correspond to rows and columns deleted from S and M.

BLOCK 18:

The output consists of the following:

(1) Lists of circular frequency squared ω^2, circular frequency ω, and frequency f.

(2) For each mode, an array of displacements and rotations as follows:

$$\begin{array}{cccccc} w_1 & u_1 & v_1 & \beta_1 & u_1' & v_1' \\ w_2 & u_2 & v_2 & \beta_2 & u_2' & v_2' \\ \vdots & \vdots & \vdots & \vdots & \vdots & \vdots \\ w_{K+1} & u_{K+1} & v_{K+1} & \beta_{K+1} & u_{K+1}' & v_{K+1}' \end{array}$$

Note that zeros again appear in the locations corresponding to deleted rows and columns in S and M.

BLOCK 19:

i = 1, 2, . . ., NMODE

BLOCK 20:

k = 1, 2, . . ., K

BLOCK 21:

$$\begin{Bmatrix} a_{0,k} \\ a_{1,k} \\ a_{2,k} \\ a_{3,k} \\ b_{0,k} \\ b_{1,k} \\ b_{2,k} \\ b_{3,k} \\ c_{0,k} \\ c_{1,k} \\ c_{2,k} \\ c_{3,k} \end{Bmatrix} = \left[T_k\right] \begin{Bmatrix} w_k \\ u_k \\ v_k \\ \beta_k \\ u'_k \\ v'_k \\ w_{k+1} \\ u_{k+1} \\ v_{k+1} \\ \beta_{k+1} \\ u'_{k+1} \\ v'_{k+1} \end{Bmatrix}$$

where the elements of T_k are given in table II.

BLOCK 22:

For the purpose of computing the detailed mode shapes, each element is divided into IINT intervals. The number of locations at which the mode shape is to be evaluated is IINT + 1. The value of s at the ith location of the kth interval is defined as s_{ki} and is given by

$$s_{ki} = s_k + \epsilon_k\left(\frac{i - 1}{IINT} - \frac{1}{2}\right) \qquad (i = 1, \ldots, IINT + 1; \quad k = 1, \ldots, K)$$

The mode shape over the portion of the shell represented by the kth element is then computed from:

$$w = a_{0,k} + a_{1,k}\left(s_{ki} - s_k\right) + a_{2,k}\left(s_{ki} - s_k\right)^2 + a_{3,k}\left(s_{ki} - s_k\right)^3$$

$$u = b_{0,k} + b_{1,k}\left(s_{ki} - s_k\right) + b_{2,k}\left(s_{ki} - s_k\right)^2 + b_{3,k}\left(s_{ki} - s_k\right)^3$$

$$v = c_{0,k} + c_{1,k}\left(s_{ki} - s_k\right) + c_{2,k}\left(s_{ki} - s_k\right)^2 + c_{3,k}\left(s_{ki} - s_k\right)^3$$

The entire mode shape is then constructed by placing the portions end to end.

BLOCK 23:

The mode shape consists of arrays of u, v, and w.

APPLICATIONS AND DISCUSSION

Description of Shells Analyzed

In order to ascertain the generality and efficacy of the present method for computing natural frequencies, a number of applications were made. The following configurations, shown in figure 4, were treated:

(1) An isotropic cylinder with freely supported edges investigated by Arnold and Warburton (ref. 15) using an exact solution.

(2) An orthotropic cylinder with freely supported edges investigated by Hoppmann (ref. 16) using an exact solution.

(3) An isotropic 120° conical frustum with both free-free and clamped-free edges, investigated by Naumann (ref. 1) using a Rayleigh-Ritz analysis.

(4) An isotropic shell having positive Gaussian curvature with freely supported edges investigated by Cooper (ref. 4) using a finite difference solution.

(5) An isotropic shell having negative Gaussian curvature with freely supported edges also investigated by Cooper (ref. 4).

(6) An isotropic annular plate with free edges, investigated by Raju (ref. 17) using an exact solution.

Correlation With Previous Investigations

Frequencies and mode shapes were computed for these shells, and the frequencies were compared with those from existing solutions. Ten elements were used to represent each shell. One hundred integration intervals within each element were used. In the correlations to follow, the quantities to be compared are called frequency parameters. For the cylinders, conical frustums, and annular plate, the parameter is the square of the circular frequency. For the shells of positive and negative Gaussian curvature, the parameter is a dimensionless frequency defined in the appropriate tables and figures.

Frequencies based on the methods of previous investigators were obtained as follows:

(1) For the cylinders and the annular plate, the methods of the previous investigators (refs. 15, 16, and 17) were automated for computation on a digital computer. Some of the physical data of the orthotropic cylinder were obtained from reference 18.

(2) For the conical frustums, the computer program of Naumann (ref. 1) was used.

(3) For the shells of positive and negative Gaussian curvature, frequencies were provided by Paul A. Cooper who obtained them by use of a computer program based on the procedure described in reference 4.

Presentation of Results

Calculations were performed with the present method for each shell using a range on the circumferential wave number n of 0 through 10 because the minimum frequencies for the shells were in this range. Since all calculations by the present method were based on representations by 10 elements, approximately 60 modes per value of n were generated. Because presentation of all these modes appeared impractical, a decision had to be made as to which modes to present for each shell. A main consideration in selection of a mode for presentation was whether a calculation of the frequency parameter was available from one of the methods of the previous investigators for comparison.

Minimum frequencies.- The minimum frequency parameter for each value of n was available for every shell. Correlations for minimum frequency parameters are presented in table IV. The information in this table is shown graphically in figures 5 to 11. The frequency parameters in these figures should be viewed both as results of the present analysis and as results of the previous investigators since the differences are too small to be seen on the plots. Some experimental results from references 16 and 1 are shown in figures 6 and 7, respectively.

Higher modes of cylinders.- The selection of which higher frequency parameters to present was made for each shell on an individual basis. For the cylinders, the solutions of Arnold and Warburton and of Hoppmann give exact frequency parameters for all modes. In order to describe which of these modes were selected for correlation, it is necessary to discuss briefly the nature of the exact mode shapes for the freely supported cylinders. The exact mode shapes have the form:

$$u = A_{mn} \cos \frac{m\pi s}{L} \cos n\theta$$

$$v = B_{mn} \sin \frac{m\pi s}{L} \sin n\theta$$

$$w = C_{mn} \sin \frac{m\pi s}{L} \cos n\theta$$

where m takes on integer values and A_{mn}, B_{mn}, and C_{mn} are constants which characterize a mode.

Thus, m is equal to the number of nodal circles in u or one plus the number of nodal circles in v or w. For a given pair of values for m and n, three modes are possible. Each mode corresponds to a different ratio of $A_{mn} : B_{mn} : C_{mn}$. For each value of n, modes were arbitrarily selected for values of m from 1 to 5. The corresponding frequency parameters computed by the present analysis were identified by inspecting the computed mode shapes and counting nodal circles. Correlations for the higher frequency parameters of the cylinders are presented in tables V and VI for the

values of n and m considered. For the purpose of illustration, the variations with m of the three frequency parameters associated with each value of m are shown in figures 12 and 13 for n = 2.

Higher modes of conical frustums.- For the conical frustums, a large number of frequency parameters were available from Naumann's Rayleigh-Ritz procedure for comparison with results of the present analysis. A correlation was made for n = 2. Modes were selected for presentation as follows: First, all modes having from one to five nodal circles in the w-displacement were examined. For the freely supported cylinders, there were exactly three modes having a given number of circumferential waves and a given number of circular node lines in the w-displacement. For the conical frustums, there are usually not exactly three. For purposes of presenting frequencies in the present analysis, an arbitrary selection of modes was made. If there are three or less modes corresponding to a given number of nodal circles in w, all are presented. If there are more than three, only three are presented. To avoid any misunderstanding, the following table tells which modes of the conical frustums having five or less nodal circles in w are not presented:

	Nodal circles in w	Nodal circles in u	Nodal circles in v
Free-free	1	0	0
Clamped-free	0	1	0
	3	0	1
	4	2	5
	3	4	7
	4	6	8

The correlations for the higher frequency parameters of the conical frustums for n = 2 are shown in tables VII and VIII. This information is also shown graphically in figures 14 and 15. As in figures 5 to 11, the results in figures 14 and 15 can be interpreted as either the results of the present analysis or the other investigation since the results are coincident for plotting purposes. As a matter of interest, the mode shapes from the present analysis corresponding to the frequency parameters in figures 14 and 15 are shown in figures 16 and 17.

Higher modes of shells having positive and negative Gaussian curvature.- For the shells of positive and negative Gaussian curvature, no higher frequency parameters were available from Cooper's method for correlation. As a matter of interest, some higher frequency parameters computed by the present analysis for these shells are presented for n = 2 in tables IX and X. Specifically, frequency parameters for modes having four or less circular node lines in w are presented. As was the case with the cylinders, there

are exactly three frequencies corresponding to each number of circular node lines in w. The variation of the three frequency parameters with the number of circular node lines in w is shown in figures 18 and 19. The mode shapes corresponding to the frequency parameters in figures 18 and 19 are shown in figures 20 and 21.

Discussion of the Applications

The correlations in tables IV to VIII can be summarized as follows: All frequency parameters presented for the two cylinders, the shells of positive and negative Gaussian curvature, and the annular plate showed agreement with the results of the previous investigators through at least the second significant figure. For the cylinders, the agreement was in most cases through six significant figures. For the free-free conical frustum, most frequency parameters predicted by the present analysis agreed with the frequency parameters from the method of reference 1 through at least the second significant figure. The exceptions were the ninth, eleventh, and twelfth values of ω^2 listed in table VII in which the frequency parameters from the present analysis were lower in the second significant figure. It is noted in reference 19 that under certain conditions (that are met by the present analysis) the finite-element method is equivalent to the Rayleigh-Ritz method in that both methods give upper bounds to the exact frequencies. Therefore, it follows that the frequency parameters predicted by the present analysis are better approximations to the corresponding exact frequency parameters than are the frequency parameters from the method of reference 1. It is believed that the first significant figure in the three frequency parameters is probably correct and that the lack of agreement for these frequency parameters does not indicate any significant inaccuracy in the results of the present analysis. For the clamped-free conical frustum, most frequency parameters predicted by the present analysis again agreed with the frequency parameters from the method of reference 1 through at least the second significant figure. The exceptions in this instance are the minimum frequency parameters in table IV for $n = 1$, 2, and 3 and the eighth and ninth values of the frequency parameters ω^2 listed in table VIII. For the eighth and ninth values of ω^2 listed in table VIII, the present analysis predicted frequency parameters which were lower than the corresponding values from the method of reference 1. As with the free-free conical frustum, these differences occurred in the second significant figure. It is again concluded that the present results are closer to the exact frequency parameters. In the case of the noted disagreement in table IV, the frequency parameters from the present analysis are higher (in the first significant figure for $n = 2$) than the corresponding result from the method of reference 1. By reasoning similar to that used in the preceding discussion, it is concluded that the present analysis is somewhat inaccurate for the minimum frequency parameters of the clamped-free conical frustum for $n = 1$, 2, and 3.

No dependence of accuracy on the circumferential wave number was noted. Furthermore, only slight degradation of accuracy was noted as modes with increasing numbers of circular node lines in w were considered. In the latter instance, significant degradation might have been expected. The only notable degradation of accuracy was with regard to edge constraint. The frequency parameters of the conical frustum with a clamped edge (tables IV and VIII) showed worse correlation with the results of the previous investigations than did the frequency parameters of shells with free or freely supported edges.

For the reasons stated in the introduction, no correlations are presented for mode shapes. However, a cursory correlation between the mode shapes from the present analysis and such mode shapes as were available from the methods of the previous investigators was made. The computed mode shapes for the cylinders appeared to coincide with the exact mode shapes which are sine and cosine curves. The computed mode shapes corresponding to some of the minimum frequencies of the free-free conical frustum appeared to agree with those mode shapes published in reference 1. The authors also made some correlations of mode shapes for a few of the higher modes of the conical frustums obtained by the method of reference 1. For these mode shapes the present analysis and the method of reference 1 appeared to agree very well.

Computational Efficiency and Reliability

As was stated in the introduction, two major objectives of the computer program were: (1) machine efficiency, that is, the ability to compute quickly a large number of frequencies and mode shapes; (2) reliability, that is, capability of predicting every mode in the range of the frequency spectrum of interest. Machine efficiency was achieved. Typically, over 600 frequencies and modal columns are computed in less than 15 minutes on the Control Data 6600 computer system. Reliability was not proven but is indicated by the correlations obtained by the exact theory for the cylinders. The eigenvalue problems generated were well conditioned, since only single-precision arithmetic was required for accurate solution.

Limitations

Experience with this computer program and with the correlations are believed to indicate that the major limitation of the program in its present form lies in the approximation of the normal displacement w by a third-order curve over each element. (See eq. (7).) From the assumption that w is a third-order curve in each element, it follows that:

(1) Certain moment resultants are discontinuous across junctures between elements.

(2) The moment distributions may be seriously in error if the moment distribution in a region represented by a single element has a variation of higher order than linear.

Some results of modal stress calculations for modes with large moment gradients are suspected to be in error. Furthermore, the errors previously noted in some minimum frequencies of the clamped-free conical frustum are believed to stem from the third-order approximation since a steep moment gradient is known to occur near a clamped edge. A possible remedy is to increase by two the order of polynomial representation of w and to require continuity of curvature across element junctures.

Another limitation which is emphasized is the restriction of the present analysis to shells for which the shell surface does not intersect the axis of the shell. Thus, this analysis is not applicable to configurations such as a hemisphere.

Finally, the reader is reminded that the analysis is restricted to shells with continuous stiffness distributions as noted from the conditions imposed by equation (33). This restriction is easily removed by replacing the last two equalities of equation (33) by appropriate conditions on the continuity of stress and moment resultants across element junctures.

CONCLUDING REMARKS

An analytical procedure based on the finite-element method is developed for computing natural frequencies and mode shapes of thin shells of revolution. The shells may have general meridional curvature and orthotropic elastic properties. The details of a computer program based on this procedure are described.

A distinguishing feature of the procedure is that it employs an element which is geometrically exact in that the actual geometry of the shell being analyzed is input to the analysis in the form of functions. The displacements of the shell within an element are approximated by third-order polynomials which are defined over the element. Inter-element compatibility is expressed by equating displacements and rotations at all junctures between elements. The required integrations for computing the element stiffness and mass matrices are performed numerically by using the trapezoidal rule. The stiffness and mass matrices for the complete shell are formed by superposition. Edge constraints are incorporated by deleting rows and columns from the complete shell stiffness and mass matrices. The resulting symmetric eigenvalue problem is solved by a standard method.

The computer program has been applied to several shells:

(1) An isotropic cylinder with freely supported edges

(2) An orthotropic cylinder with freely supported edges

(3) A 120° conical frustum with free-free edges

(4) A 120° conical frustum with clamped-free edges

(5) A shell having positive Gaussian curvature with freely supported edges

(6) A shell having negative Gaussian curvature with freely supported edges

(7) An annular plate with free-free edges

The main results and conclusions are as follows:

1. Very generally, excellent agreement was noted between frequencies from the present analysis and frequencies from the previous investigations.

2. The only inaccuracies of the present analysis which might be considered significant occurred in three minimum frequencies of the clamped-free conical frustum. This inaccuracy is believed to stem from the inability of third-order polynomials to conform to a steep stress gradient near a clamped edge, and consequently increasing the representation of the normal-displacement component to a fifth-order polynomial would be expected to result in overall excellent agreement.

3. The computer program performs with very short running times and no modes are overlooked in computation.

4. The natural frequencies and mode shapes from this method appear to constitute reliable input for forced response calculations for structures involving shells of revolution.

Langley Research Center,
National Aeronautics and Space Administration,
Langley Station, Hampton, Va., September 3, 1968,
124-08-05-08-23.

APPENDIX

ELEMENTS OF MATRIX [R]

[See eq. (16)]

The elements of matrix [R] are as follows:

$$R_{11} = \frac{C_{11}r}{R_1^2} + 2\frac{C_{12}r}{R_1R_2} + \frac{C_{22}r}{R_2^2} + \frac{D_{22}n^4}{r^3} + \frac{D_{66}n^2(r')^2}{r^3} + \frac{2K_{12}n^2}{rR_1} + \frac{2K_{22}n^2}{rR_2} \tag{A1}$$

$$R_{12} = R_{21} = -\frac{D_{22}r'n^2}{r^2} - \frac{D_{66}n^2r'}{r^2} - \frac{K_{12}r'}{R_1} - \frac{K_{22}r'}{R_2} \tag{A2}$$

$$R_{13} = R_{31} = -\frac{D_{12}n^2}{r} - \frac{K_{11}r}{R_1} - \frac{K_{12}r}{R_2} \tag{A3}$$

$$R_{14} = R_{41} = \frac{C_{12}r'}{R_1} + \frac{C_{22}r'}{R_2} - \frac{D_{12}n^2R_1'}{rR_1^2} + \frac{D_{22}r'n^2}{r^2R_1} + \frac{D_{66}n^2r'}{r^2R_1} - \frac{K_{11}R_1'r}{R_1^3} + \frac{K_{12}r'}{R_1^2}$$

$$- \frac{K_{12}rR_1'}{R_1^2R_2} + \frac{K_{22}n^2r'}{r^2} + \frac{K_{22}r'}{R_1R_2} + \frac{K_{66}n^2r'}{r^2} \tag{A4}$$

$$R_{15} = R_{51} = \frac{C_{11}r}{R_1} + \frac{C_{12}r}{R_2} + \frac{D_{12}n^2}{rR_1} + \frac{K_{11}r}{R_1^2} + \frac{K_{12}n^2}{r} + \frac{K_{12}r}{R_1R_2} \tag{A5}$$

$$R_{16} = R_{61} = \frac{C_{12}n}{R_1} + \frac{C_{22}n}{R_2} + \frac{D_{22}n^3}{r^2R_2} + \frac{D_{66}n(r')^2}{r^2R_2} + \frac{K_{12}n}{R_1R_2} + \frac{K_{22}n^3}{r^2} + \frac{K_{22}n}{R_2^2}$$

$$+ \frac{K_{66}n(r')^2}{r^2} \tag{A6}$$

$$R_{17} = R_{71} = -\frac{D_{66}nr'}{rR_2} - \frac{K_{66}nr'}{r} \tag{A7}$$

$$R_{22} = \frac{D_{22}(r')^2}{r} + \frac{D_{66}n^2}{r} \tag{A8}$$

$$R_{23} = R_{32} = D_{12}r' \tag{A9}$$

$$R_{24} = R_{42} = \frac{D_{12}R_1'r'}{R_1^2} - \frac{D_{22}(r')^2}{rR_1} - \frac{D_{66}n^2}{rR_1} - \frac{K_{22}(r')^2}{r} - \frac{K_{66}n^2}{r} \tag{A10}$$

$$R_{25} = R_{52} = -\frac{D_{12}r'}{R_1} - K_{12}r' \tag{A11}$$

$$R_{26} = R_{62} = -\frac{D_{22}nr'}{rR_2} - \frac{D_{66}r'n}{rR_2} - \frac{K_{22}nr'}{r} - \frac{K_{66}nr'}{r} \tag{A12}$$

$$R_{27} = R_{72} = \frac{D_{66}n}{R_2} + K_{66}n \tag{A13}$$

$$R_{33} = D_{11}r \tag{A14}$$

$$R_{34} = R_{43} = \frac{D_{11}R_1'r}{R_1^2} - K_{12}r' - \frac{D_{12}r'}{R_1} \tag{A15}$$

$$R_{35} = R_{53} = -\frac{D_{11}r}{R_1} - K_{11}r \tag{A16}$$

$$R_{36} = R_{63} = -\frac{D_{12}n}{R_2} - K_{12}n \tag{A17}$$

$$R_{37} = R_{73} = 0 \tag{A18}$$

$$R_{44} = \frac{C_{22}(r')^2}{r} + \frac{C_{66}n^2}{r} + \frac{D_{11}(R_1')^2r}{R_1^4} - \frac{2D_{12}R_1'r'}{R_1^3} + \frac{D_{22}(r')^2}{rR_1^2} + \frac{D_{66}n^2}{rR_1^2}$$

$$- \frac{2K_{12}r'R_1'}{R_1^2} + \frac{2K_{22}(r')^2}{rR_1} + \frac{2K_{66}n^2}{rR_1} \tag{A19}$$

$$R_{45} = R_{54} = C_{12}r' - \frac{D_{11}R_1'r}{R_1^3} + \frac{D_{12}r'}{R_1^2} - \frac{K_{11}R_1'r}{R_1^2} + \frac{2K_{12}r'}{R_1} \tag{A20}$$

$$R_{46} = R_{64} = \frac{C_{22}r'n}{r} + \frac{C_{66}nr'}{r} - \frac{D_{12}nR_1'}{R_1^2R_2} + \frac{D_{22}nr'}{rR_1R_2} + \frac{D_{66}r'n}{rR_1R_2} - \frac{K_{12}nR_1'}{R_1^2}$$

$$+ \frac{K_{22}nr'}{rR_1} + \frac{K_{22}nr'}{rR_2} + \frac{K_{66}nr'}{rR_1} + \frac{K_{66}nr'}{rR_2} \tag{A21}$$

$$R_{47} = R_{74} = -C_{66}n - \frac{D_{66}n}{R_1R_2} - \frac{K_{66}n}{R_1} - \frac{K_{66}n}{R_2} \tag{A22}$$

$$R_{55} = C_{11}r + \frac{D_{11}r}{R_1^2} + \frac{2K_{11}r}{R_1} \tag{A23}$$

$$R_{56} = R_{65} = C_{12}n + \frac{D_{12}n}{R_1R_2} + \frac{K_{12}n}{R_2} + \frac{K_{12}n}{R_1} \tag{A24}$$

$$R_{57} = R_{75} = 0 \tag{A25}$$

$$R_{66} = \frac{C_{22}n^2}{r} + \frac{C_{66}(r')^2}{r} + \frac{D_{22}n^2}{rR_2^2} + \frac{D_{66}(r')^2}{rR_2^2} + \frac{2K_{22}n^2}{rR_2} + \frac{2K_{66}(r')^2}{rR_2} \tag{A26}$$

$$R_{67} = R_{76} = -C_{66}r' - \frac{D_{66}r'}{R_2^2} - \frac{2K_{66}r'}{R_2} \tag{A27}$$

$$R_{77} = C_{66}r + \frac{D_{66}r}{R_2^2} + \frac{2K_{66}r}{R_2} \tag{A28}$$

REFERENCES

1. Naumann, Eugene C.: On the Prediction of Vibratory Behavior of Free-Free Truncated Conical Shells. NASA TN D-4772, 1968.

2. Sewall, John L.; and Naumann, Eugene C.: An Experimental and Analytical Vibration Study of Thin Cylindrical Shells With and Without Longitudinal Stiffeners. NASA TN D-4705, 1968.

3. Cohen, Gerald A.: Computer Analysis of Asymmetric Free Vibrations of Ring-Stiffened Orthotropic Shells of Revolution. AIAA J., vol. 3, no. 12, Dec. 1965, pp. 2305-2312.

4. Cooper, Paul A.: Vibration and Buckling of Prestressed Shells of Revolution. NASA TN D-3831, 1967.

5. Jones, R. E.; and Strome, D. R.: Direct Stiffness Method Analysis of Shells of Revolution Utilizing Curved Elements. AIAA J., vol. 4, no. 9, Sept. 1966, pp. 1519-1525.

6. Jones, R. E.; and Strome, D. R.: A Survey of Analysis of Shells by the Displacement Method. Matrix Methods in Structural Mechanics, AFFDL-TR-66-80, U.S. Air Force, [1965], pp. 205-229. (Available from DDC as AD 646 300.)

7. Webster, J. J.: Free Vibrations of Shells of Revolution Using Ring Finite Elements. Int. J. Mech. Sci., vol. 9, no. 8, Aug. 1967, pp. 559-570.

8. Percy, John H.; Pian, Theodore H. H.; Klein, Stanley; and Navaratna, D. R.: Application of Matrix Displacement Method to Linear Elastic Analysis of Shells of Revolution. AIAA Paper No. 65-142, Jan. 1965.

9. Bacon, Merle D.; and Bert, Charles W.: Unsymmetrical Free Vibrations of Orthotropic Sandwich Shells of Revolution. AIAA J., vol. 5, no. 3, Mar. 1967, pp. 413-417.

10. Kalnins, A.: Free Vibration of Rotationally Symmetric Shells. J. Acoust. Soc. Amer., vol. 36, no. 7, July 1964, pp. 1355-1365.

11. Forsberg, Kevin: Influence of Boundary Conditions on the Modal Characteristics of Thin Cylindrical Shells. AIAA J., vol. 2, no. 12, Dec. 1964, pp. 2150-2157.

12. Novozhilov, V. V. (P. G. Lowe, transl.): Thin Shell Theory. Second ed., P. Noordhoff Ltd. (Groningen, Neth.), c.1964, pp. 23 and 24.

13. Ambartsumyan, S. A.: Theory of Anisotropic Shells. NASA TT F-118, 1964.

14. White, Paul A.: The Computation of Eigenvalues and Eigenvectors of a Matrix. J. Soc. Ind. Appl. Math., vol. 6, no. 4, Dec. 1958, pp. 393-437.

15. Arnold, R. N.; and Warburton, G. B.: Flexural Vibrations of the Walls of Thin Cylindrical Shells Having Freely Supported Ends. Proc. Roy. Soc., Ser. A, vol. 197, no. 1049, June 7, 1949, pp. 238-256.

16. Hoppmann, W. H., II: Some Characteristics of the Flexural Vibrations of Orthogonally Stiffened Cylindrical Shells. J. Acoust. Soc. Amer., vol. 30, no. 1, Jan. 1958, pp. 77-82.

17. Raju, P. Narayana: Vibrations of Annular Plates. J. Aeronaut. Soc. of India, vol. 14, no. 2, May 1962, pp. 37-52.

18. Kunukkasseril, Vincent X.: Vibration of Multi-Layered Anisotropic Cylindrical Shells. WVT-6717, Benét Lab., U.S. Army Weapons Command, Feb. 1967. (Available from DDC as AD 649662.)

19. Zienkiewicz, O. C.: The Finite Element Method in Structural and Continuum Mechanics. McGraw-Hill Pub. Co. Ltd., c.1967, pp. 24-25.

TABLE I.- ELEMENTS OF MATRIX $[A_k]$

1	$\frac{-\epsilon_k}{2}$	$\frac{\epsilon_k^2}{4}$	$\frac{-\epsilon_k^3}{8}$	0	0	0	0	0	0	0	0
0	0	0	0	1	$\frac{-\epsilon_k}{2}$	$\frac{\epsilon_k^2}{4}$	$\frac{-\epsilon_k^3}{8}$	0	0	0	0
0	0	0	0	0	0	0	0	1	$\frac{-\epsilon_k}{2}$	$\frac{\epsilon_k^2}{4}$	$\frac{-\epsilon_k^3}{8}$
0	1	$-\epsilon_k$	$\frac{3\epsilon_k^2}{4}$	$\frac{-1}{R_{1,k}}$	$\frac{\epsilon_k}{2R_{1,k}}$	$\frac{-\epsilon_k^2}{4R_{1,k}}$	$\frac{\epsilon_k^3}{8R_{1,k}}$	0	0	0	0
0	0	0	0	0	1	$-\epsilon_k$	$\frac{3\epsilon_k^2}{4}$	0	0	0	0
0	0	0	0	0	0	0	0	0	1	$-\epsilon_k$	$\frac{3\epsilon_k^2}{4}$
1	$\frac{\epsilon_k}{2}$	$\frac{\epsilon_k^2}{4}$	$\frac{\epsilon_k^3}{8}$	0	0	0	0	0	0	0	0
0	0	0	0	1	$\frac{\epsilon_k}{2}$	$\frac{\epsilon_k^2}{4}$	$\frac{\epsilon_k^3}{8}$	0	0	0	0
0	0	0	0	0	0	0	0	1	$\frac{\epsilon_k}{2}$	$\frac{\epsilon_k^2}{4}$	$\frac{\epsilon_k^3}{8}$
0	1	ϵ_k	$\frac{3\epsilon_k^2}{4}$	$\frac{-1}{R_{1,k+1}}$	$\frac{-\epsilon_k}{2R_{1,k+1}}$	$\frac{-\epsilon_k^2}{4R_{1,k+1}}$	$\frac{-\epsilon_k^3}{8R_{1,k+1}}$	0	0	0	0
0	0	0	0	0	1	ϵ_k	$\frac{3\epsilon_k^2}{4}$	0	0	0	0
0	0	0	0	0	0	0	0	0	1	ϵ_k	$\frac{3\epsilon_k^2}{4}$

TABLE II.- ELEMENTS OF MATRIX $\left[T_k\right]$

$\frac{1}{2}$	$\frac{\epsilon_k}{8R_{1,k}}$	0	$\frac{\epsilon_k}{8}$	0	0	$\frac{1}{2}$	$\frac{-\epsilon_k}{8R_{1,k+1}}$	0	$\frac{-\epsilon_k}{8}$	0	0
$\frac{-3}{2\epsilon_k}$	$\frac{-1}{4R_{1,k}}$	0	$\frac{-1}{4}$	0	0	$\frac{3}{2\epsilon_k}$	$\frac{-1}{4R_{1,k+1}}$	0	$\frac{-1}{4}$	0	0
0	$\frac{-1}{2\epsilon_k R_{1,k}}$	0	$\frac{-1}{2\epsilon_k}$	0	0	0	$\frac{1}{2\epsilon_k R_{1,k+1}}$	0	$\frac{1}{2\epsilon_k}$	0	0
$\frac{2}{\epsilon_k^3}$	$\frac{1}{\epsilon_k^2 R_{1,k}}$	0	$\frac{1}{\epsilon_k^2}$	0	0	$\frac{-2}{\epsilon_k^3}$	$\frac{1}{\epsilon_k^2 R_{1,k+1}}$	0	$\frac{1}{\epsilon_k^2}$	0	0
0	$\frac{1}{2}$	0	0	$\frac{\epsilon_k}{8}$	0	0	$\frac{1}{2}$	0	0	$\frac{-\epsilon_k}{8}$	0
0	$\frac{-3}{2\epsilon_k}$	0	0	$\frac{-1}{4}$	0	0	$\frac{3}{2\epsilon_k}$	0	0	$\frac{-1}{4}$	0
0	0	0	0	$\frac{-1}{2\epsilon_k}$	0	0	0	0	0	$\frac{1}{2\epsilon_k}$	0
0	$\frac{2}{\epsilon_k^3}$	0	0	$\frac{1}{\epsilon_k^2}$	0	0	$\frac{-2}{\epsilon_k^3}$	0	0	$\frac{1}{\epsilon_k^2}$	0
0	0	$\frac{1}{2}$	0	0	$\frac{\epsilon_k}{8}$	0	0	$\frac{1}{2}$	0	0	$\frac{-\epsilon_k}{8}$
0	0	$\frac{-3}{2\epsilon_k}$	0	0	$\frac{-1}{4}$	0	0	$\frac{3}{2\epsilon_k}$	0	0	$\frac{-1}{4}$
0	0	0	0	0	$\frac{-1}{2\epsilon_k}$	0	0	0	0	0	$\frac{1}{2\epsilon_k}$
0	0	$\frac{2}{\epsilon_k^3}$	0	0	$\frac{1}{\epsilon_k^2}$	0	0	$\frac{-2}{\epsilon_k^3}$	0	0	$\frac{1}{\epsilon_k^2}$

TABLE III.- EDGE CONSTRAINTS

ICASE	Description	Equations for edge constraint	Rows and columns deleted
1	Free-free	None	None
2	Free—freely supported	$v(L) = w(L) = 0$	(6K + 1), (6K + 3)
3	Freely supported—free	$v(0) = w(0) = 0$	1, 3
4	Free—simply supported	$u(L) = v(L) = w(L) = 0$	(6K + 1), (6K + 2), (6K + 3)
5	Simply supported—free	$u(0) = v(0) = \omega(0) = 0$	1, 2, 3
6	Free-clamped	$u(L) = v(L) = w(L) = \beta(L) = 0$	(6K + 1), (6K + 2), (6K + 3), (6K + 4)
7	Clamped-free	$u(0) = v(0) = w(0) = \beta(0) = 0$	1, 2, 3, 4
8	Freely supported—freely supported	$v(0) = w(0) = 0$ $v(L) = w(L) = 0$	1, 3, (6K + 1), (6K + 3)
9	Simply supported—simply supported	$u(0) = v(0) = w(0) = 0$ $u(L) = v(L) = w(L) = 0$	1, 2, 3, (6K + 1), (6K + 2), (6K + 3)
10	Clamped-clamped	$u(0) = v(0) = w(0) = \beta(0) = 0$ $u(L) = v(L) = w(L) = \beta(L) = 0$	1, 2, 3, 4, (6K + 1), (6K + 2), (6K + 3), (6K + 4)
11	Freely supported—simply supported	$v(0) = w(0) = 0$ $u(L) = v(L) = w(L) = 0$	1, 3, (6K + 1), (6K + 2), (6K + 3)
12	Freely supported—clamped	$v(0) = w(0) = 0$ $u(L) = v(L) = w(L) = \beta(L) = 0$	1, 3, (6K + 1), (6K + 2), (6K + 3), (6K + 4)
13	Simply supported—freely supported	$u(0) = v(0) = w(0) = 0$ $v(L) = w(L) = 0$	1, 2, 3, (6K + 1), (6K + 3)
14	Simply supported—clamped	$u(0) = v(0) = w(0) = 0$ $u(L) = v(L) = w(L) = \beta(L) = 0$	1, 2, 3, (6K + 1), (6K + 2), (6K + 3), (6K + 4)
15	Clamped—freely supported	$u(0) = v(0) = w(0) = \beta(0) = 0$ $v(L) = w(L) = 0$	1, 2, 3, 4, (6K + 1), (6K + 3)
16	Clamped—simply supported	$u(0) = v(0) = w(0) = \beta(0) = 0$ $u(L) = v(L) = w(L) = 0$	1, 2, 3, 4, (6K + 1), (6K + 2), (6K + 3)

TABLE IV.- COMPARISON OF MINIMUM FREQUENCY PARAMETERS AS COMPUTED BY PRESENT METHODS WITH THOSE OF PREVIOUS INVESTIGATIONS

Circumferential wave number, n	ω^2, sec^{-2}			
	Freely supported—freely supported cylinder			
	Isotropic		Orthotropic	
	Present analysis	Reference 15	Present analysis	Reference 16
0	3.86111×10^8	3.86111×10^8	8.01167×10^8	8.01167×10^8
1	1.17339×10^8	1.17339×10^8	1.09559×10^8	1.09559×10^8
2	2.25430×10^7	2.25430×10^7	2.15504×10^7	2.15504×10^7
3	5.95827×10^7	5.95827×10^7	5.53142×10^7	5.53142×10^7
4	2.17401×10^6	2.17401×10^6	1.85439×10^8	1.85439×10^8
5	1.11765×10^6	1.11765×10^6	4.74829×10^8	4.74829×10^8
6	9.09145×10^5	9.09145×10^5	1.01231×10^9	1.01231×10^9
7	1.11505×10^6	1.11505×10^6	1.90756×10^9	1.90756×10^9
8	1.64300×10^6	1.64300×10^6	3.29043×10^9	3.29043×10^9
9	2.50514×10^6	2.50514×10^6	5.31084×10^9	5.31084×10^9
10	3.75508×10^6	3.75508×10^6	8.13868×10^9	8.13868×10^9
Circumferential wave number, n	ω^2, sec^{-2}			
	120^o conical frustum			
	Free-free		Clamped-free	
	Present analysis	Reference 1	Present analysis	Reference 1
0	0	0	2.5380×10^4	2.5378×10^4
1	0	0	3.7049×10^5	3.6125×10^5
2	2.8727×10^2	2.8725×10^2	7.2558×10^4	6.9075×10^4
3	1.9154×10^3	1.9149×10^3	2.2666×10^4	2.1638×10^4
4	6.3759×10^3	6.3728×10^3	1.3694×10^4	1.3434×10^4
5	1.5047×10^4	1.5038×10^4	1.7636×10^4	1.7611×10^4
6	2.7824×10^4	2.7815×10^4	2.8529×10^4	2.8520×10^4
7	4.4394×10^4	4.4387×10^4	4.4524×10^4	4.4507×10^4
8	6.6322×10^4	6.6310×10^4	6.6338×10^4	6.6324×10^4
9	9.5417×10^4	9.5394×10^4	9.5418×10^4	9.539×10^4
10	1.3333×10^5	1.3329×10^5	1.3333×10^5	1.3329×10^5

TABLE IV.- COMPARISON OF MINIMUM FREQUENCY PARAMETERS AS COMPUTED BY PRESENT METHODS WITH THOSE OF PREVIOUS INVESTIGATIONS – Concluded

Circumferential wave number, n	Dimensionless frequency parameter, $\Omega = \omega R\left[(\rho/E)(1 - \mu^2)\right]^{1/2}$			
	Shell of positive Gaussian curvature, freely supported edges		Shell of negative Gaussian curvature, freely supported edges	
	Present analysis	Reference 4	Present analysis	Reference 4
0	----	----	0.640	0.640
1	0.411	0.412	.368	.368
2	.360	.362	.157	.157
3	.340	.340	.0628	.0628
4	.331	.331	.01970	.01972
5	.327	.327	.00779	.00784
6	.324	.324	.01923	.01924
7	.323	.322	.02804	.02805
8	.322	.321	.02580	.02609
9	.321	.321	.0240	.0241
10	.321	.321	.0292	.0292

Circumferential wave number, n	ω^2, sec^{-2}	
	Plates	
	Present analysis	Reference 17
0	86.74	86.74
1	295.8	295.8
2	18.24	18.24
3	130.5	130.5
4	443.8	443.8
5	1 087	1 087
6	2 215	2 215
7	4 003	4 003
8	6 660	6 660
9	10 415	10 415
10	15 532	15 532

TABLE V.- CORRELATION OF FREQUENCY PARAMETER ω^2 OF FREELY SUPPORTED CYLINDER AS COMPUTED BY PRESENT ANALYSIS AND EXACT SOLUTION OF REFERENCE 15

m	ω^2, sec^{-2}					
	Present analysis	Reference 15	Present analysis	Reference 15	Present analysis	Reference 15
	n = 0		n = 1		n = 2	
1	1.950193×10^9	1.950193×10^9	1.17339×10^8	1.17339×10^8	2.25430×10^7	2.25430×10^7
	9.00656×10^8	9.00656×10^8	1.41017×10^9	1.41017×10^9	3.1160×10^9	3.116×10^9
	3.86111×10^8	3.86111×10^8	4.09860×10^9	4.09860×10^9	9.65443×10^9	9.65443×10^9
2	1.53415×10^9	1.53415×10^9	5.83357×10^8	5.83356×10^8	1.90073×10^8	1.90073×10^8
	4.57961×10^9	4.47961×10^9	2.78500×10^9	2.78500×10^9	4.59200×10^9	4.59200×10^9
	1.54445×10^9	1.54445×10^9	6.67902×10^9	6.67902×10^9	1.24328×10^{10}	1.24328×10^{10}
3	1.58626×10^9	1.58626×10^9	1.02452×10^9	1.02451×10^9	4.75299×10^8	4.75290×10^8
	9.96586×10^9	9.96570×10^9	1.18772×10^{10}	1.18772×10^{10}	6.60278×10^9	6.60268×10^9
	3.47507×10^9	3.47500×10^9	4.51464×10^9	4.51457×10^9	1.75057×10^{10}	1.75056×10^{10}
4	1.59995×10^9	1.59995×10^9	1.26785×10^9	1.26782×10^9	7.55161×10^8	7.55117×10^8
	1.75668×10^8	1.75655×10^8	1.94100×10^{10}	1.94088×10^{10}	2.49175×10^{10}	2.49164×10^{10}
	6.17832×10^9	6.17778×10^9	7.05640×10^9	7.95582×10^9	9.22905×10^9	9.22834×10^9
5	1.60572×10^9	1.60571×10^9	1.39208×10^9	1.39201×10^9	9.73034×10^8	9.72909×10^8
	2.73552×10^{10}	2.73485×10^{10}	2.91681×10^{10}	2.91617×10^{10}	3.46020×10^{10}	3.45961×10^{10}
	9.65539×10^9	9.65279×10^9	1.04453×10^{10}	1.04425×10^{10}	1.25978×10^{10}	1.25946×10^{10}
m	n = 3		n = 4		n = 5	
1	5.95827×10^6	5.95827×10^6	2.17401×10^6	2.17401×10^6	1.11765×10^6	1.11765×10^6
	6.15055×10^9	6.15055×10^9	1.04833×10^{10}	1.04833×10^{10}	1.60902×10^{10}	1.60902×10^{10}
	1.85829×10^{10}	1.85829×10^{10}	3.09779×10^{10}	3.09779×10^{10}	4.68747×10^{10}	4.68747×10^{10}
2	6.66567×10^7	6.66563×10^7	2.70603×10^7	2.70601×10^7	1.27354×10^7	1.27352×10^7
	7.56577×10^9	7.56576×10^9	1.18310×10^{10}	1.18310×10^{10}	1.73881×10^{10}	1.73881×10^{10}
	2.15282×10^{10}	2.15282×10^{10}	3.40266×10^{10}	3.40266×10^{10}	4.99865×10^{10}	4.99865×10^{10}
3	2.13124×10^8	2.13118×10^8	1.00599×10^8	1.00594×10^8	5.13733×10^7	5.13704×10^7
	9.67973×10^9	9.67963×10^9	1.39500×10^{10}	1.39499×10^{10}	1.94829×10^{10}	1.94828×10^{10}
	2.66367×10^{10}	2.66367×10^{10}	3.92032×10^{10}	3.92031×10^{10}	5.52220×10^{10}	5.52219×10^{10}
4	4.10749×10^8	4.10708×10^8	2.22493×10^8	2.22462×10^8	1.24623×10^8	1.24601×10^8
	1.24380×10^{10}	1.24372×10^{10}	1.67738×10^{10}	1.67733×10^{10}	2.23239×10^{10}	2.23230×10^{10}
	3.39988×10^{10}	3.39978×10^{10}	4.65653×10^{10}	4.65745×10^{10}	6.26256×10^{10}	6.26249×10^{10}
5	6.12256×10^8	6.12119×10^8	3.72329×10^8	3.72208×10^8	2.27379×10^8	2.27282×10^8
	4.36214×10^{10}	4.36131×10^{10}	2.02963×10^{10}	2.02922×10^{10}	7.22276×10^{10}	7.22237×10^{10}
	1.58850×10^{10}	1.58813×10^{10}	5.61740×10^{10}	5.61693×10^{10}	2.58897×10^{10}	2.58853×10^{10}

TABLE V.- CORRELATION OF FREQUENCY PARAMETER ω^2 OF FREELY SUPPORTED CYLINDER AS COMPUTED BY PRESENT ANALYSIS AND EXACT SOLUTION OF REFERENCE 15 – Concluded

m	ω^2, sec^{-2}					
	Present analysis	Reference 15	Present analysis	Reference 15	Present analysis	Reference 15
	n = 6		n = 7		n = 8	
1	9.09145×10^5	9.09145×10^5	1.11505×10^6	1.11505×10^6	1.64300×10^6	1.64300×10^6
	2.29598×10^{10}	2.29598×10^{10}	3.10870×10^{10}	3.10870×10^{10}	4.04694×10^{10}	4.04694×10^{10}
	6.62863×10^{10}	6.62863×10^{10}	8.92182×10^{10}	8.92182×10^{10}	1.15673×10^{11}	1.15673×10^{11}
2	6.96234×10^6	6.96226×10^6	4.56899×10^6	4.56892×10^6	3.77396×10^6	3.77391×10^6
	2.42233×10^{10}	2.42233×10^{10}	3.23267×10^{10}	3.23267×10^{10}	4.16922×10^{10}	4.16922×10^{10}
	6.94380×10^{10}	6.94380×10^{10}	9.23964×10^{10}	9.23964×10^{10}	1.18870×10^{11}	1.18870×10^{11}
3	2.85635×10^7	2.85615×10^7	1.74106×10^7	1.74092×10^7	1.18524×10^7	1.18514×10^7
	2.62905×10^{10}	2.62903×10^{10}	3.43697×10^{10}	3.43696×10^{10}	4.37157×10^{10}	4.37156×10^{10}
	7.47182×10^{10}	7.47182×10^{10}	9.77096×10^{10}	9.77096×10^{10}	1.24207×10^{11}	1.24207×10^{11}
4	7.33039×10^7	7.32876×10^7	4.56222×10^7	4.56103×10^7	3.03024×10^7	3.02935×10^7
	2.91264×10^{10}	2.91254×10^{10}	3.71926×10^{10}	3.71916×10^{10}	4.65240×10^{10}	4.65231×10^{10}
	8.21554×10^{10}	8.21548×10^{10}	1.05176×10^{11}	1.05176×10^{11}	1.31698×10^{11}	1.31698×10^{11}
5	1.42224×10^8	1.42150×10^8	9.20757×10^7	9.20184×10^7	6.21633×10^7	6.21190×10^7
	3.27094×10^{10}	3.27049×10^{10}	4.07780×10^{10}	4.07733×10^{10}	5.01043×10^{10}	5.00996×10^{10}
	9.17738×10^{10}	9.17704×10^{10}	1.14813×10^{11}	1.14812×10^{11}	1.41378×10^{11}	1.41353×10^{11}
m	n = 9		n = 10			
1	2.50514×10^6	2.50514×10^6	3.75508×10^6	3.75508×10^6		
	5.11057×10^{10}	5.11057×10^{10}	6.29952×10^{10}	6.29952×10^{10}		
	1.45653×10^{11}	1.45653×10^{11}	1.79157×10^{11}	1.79157×10^{11}		
2	3.91728×10^6	3.91725×10^6	4.75813×10^6	4.75810×10^6		
	5.23161×10^{10}	5.23162×10^{10}	6.41965×10^{10}	6.41965×10^{10}		
	1.48862×10^{11}	1.48862×10^{11}	1.82376×10^{11}	1.82376×10^{11}		
3	9.27100×10^6	9.27021×10^6	8.48546×10^6	8.48484×10^6		
	5.43242×10^{10}	5.43241×10^{10}	6.61922×10^{10}	6.61921×10^{10}		
	1.54218×10^{11}	1.54218×10^{11}	1.87746×10^{11}	1.87746×10^{11}		
4	2.17922×10^7	2.17854×10^7	1.72993×10^7	1.72939×10^7		
	5.71189×10^{10}	5.71180×10^{10}	6.89750×10^{10}	6.89741×10^{10}		
	1.61727×10^{11}	1.61727×10^{11}	1.95275×10^{11}	1.95272×10^{11}		
5	4.41539×10^7	4.41191×10^7	3.34003×10^7	3.33725×10^7		
	6.06912×10^{10}	6.06864×10^{10}	7.25384×10^{10}	7.25336×10^{10}		
	1.71401×10^{11}	1.71401×10^{11}	2.04966×10^{11}	2.04960×10^{11}		

TABLE VI.- COMPARISON OF FREQUENCY PARAMETER ω^2 OF AN ORTHOTROPIC CYLINDER WITH FREELY SUPPORTED EDGES AS COMPUTED BY PRESENT ANALYSIS AND EXACT METHOD OF REFERENCE 16

m	ω^2, sec^{-2}					
	Present analysis	Reference 16	Present analysis	Reference 16	Present analysis	Reference 16
	n = 0		n = 1		n = 2	
1	8.37907×10^9	8.37907×10^9	1.09559×10^8	1.09559×10^8	2.15504×10^7	2.15504×10^7
	2.00989×10^9	2.00989×10^9	6.98986×10^9	6.98986×10^9	2.18774×10^{10}	2.18774×10^{10}
	8.01167×10^8	8.01167×10^8	1.76461×10^{10}	1.76461×10^{10}	4.35227×10^{10}	4.35227×10^{10}
2	6.73909×10^9	6.73909×10^9	9.33628×10^8	9.33624×10^8	1.96173×10^8	1.96170×10^8
	1.00045×10^{10}	1.00045×10^{10}	1.05341×10^{10}	1.05341×10^{10}	2.39218×10^{10}	2.39218×10^{10}
	3.20467×10^9	3.20467×10^9	2.20377×10^{10}	2.20377×10^{10}	5.00686×10^{10}	5.00686×10^{10}
3	7.77840×10^9	7.77835×10^9	2.47618×10^9	2.47610×10^9	7.07832×10^8	7.07771×10^8
	1.95747×10^{10}	1.95744×10^{10}	3.14843×10^{10}	3.14841×10^{10}	2.70286×10^{10}	2.70284×10^{10}
	7.21064×10^9	7.21050×10^9	1.41632×10^{10}	1.41630×10^{10}	6.10771×10^{10}	6.10769×10^{10}
4	7.97769×10^9	7.97727×10^9	4.14783×10^9	4.14727×10^9	1.56673×10^9	1.56621×10^9
	3.42687×10^{10}	3.42661×10^{10}	4.59040×10^{10}	4.59018×10^{10}	7.64494×10^{10}	7.64474×10^{10}
	1.28198×10^{10}	1.28198×10^{10}	1.85782×10^{10}	1.85770×10^{10}	3.13158×10^{10}	3.13143×10^{10}
5	8.18535×10^9	8.18303×10^9	5.52799×10^9	5.52532×10^9	2.66133×10^9	2.65858×10^9
	5.32836×10^{10}	5.32704×10^{10}	6.48262×10^{10}	6.48142×10^{10}	9.60704×10^{10}	9.60598×10^{10}
	2.00346×10^{10}	2.00292×10^{10}	2.47182×10^{10}	2.47122×10^{10}	3.70574×10^{10}	3.70507×10^{10}
m	n = 3		n = 4		n = 5	
1	5.53142×10^7	5.53142×10^7	1.85439×10^8	1.85439×10^8	4.74829×10^8	4.74829×10^8
	4.77293×10^{10}	4.77293×10^{10}	8.43972×10^{10}	8.43972×10^{10}	1.31754×10^{11}	1.31754×10^{11}
	8.54639×10^{10}	8.54639×10^{10}	1.43693×10^{11}	1.43693×10^{11}	2.18346×10^{11}	2.18346×10^{11}
2	1.16635×10^8	1.16633×10^8	2.30036×10^8	2.30034×10^8	5.25903×10^8	5.25901×10^8
	4.85733×10^{10}	4.85733×10^{10}	8.44403×10^{10}	8.44403×10^{10}	1.31272×10^{11}	1.31272×10^{11}
	9.33321×10^{10}	9.33321×10^{10}	1.52391×10^{11}	1.52391×10^{11}	2.27577×10^{11}	2.27577×10^{11}
3	3.18483×10^8	3.18432×10^8	3.55839×10^8	3.55792×10^8	6.44414×10^8	6.44369×10^8
	5.04809×10^{10}	5.04807×10^{10}	8.52479×10^{10}	8.52477×10^{10}	1.31219×10^{11}	1.31219×10^{11}
	1.05863×10^{11}	1.05864×10^{11}	1.66119×10^{11}	1.66119×10^{11}	2.42199×10^{11}	2.42198×10^{11}
4	7.36447×10^8	7.35971×10^8	6.21337×10^8	6.20889×10^8	8.74824×10^8	8.74385×10^8
	5.37677×10^{10}	5.37662×10^{10}	8.73284×10^{10}	8.73268×10^{10}	1.32196×10^{11}	1.32194×10^{11}
	1.22697×10^{11}	1.22696×10^{11}	1.84339×10^{11}	1.84338×10^{11}	2.61593×10^{11}	2.61592×10^{11}
5	1.40603×10^9	1.40340×10^9	1.08415×10^9	1.08160×10^9	1.27123×10^9	1.26872×10^9
	1.43650×10^{11}	1.43641×10^{11}	9.09817×10^{10}	9.09739×10^{10}	1.34611×10^{11}	1.34603×10^{11}
	5.86279×10^{10}	5.86202×10^{10}	2.06739×10^{11}	2.06733×10^{11}	2.85407×10^{11}	2.85339×10^{11}

TABLE VI.- COMPARISON OF FREQUENCY PARAMETER ω^2 OF AN ORTHOTROPIC CYLINDER WITH FREELY SUPPORTED EDGES AS COMPUTED BY PRESENT ANALYSIS AND EXACT METHOD OF REFERENCE 16 – Concluded

m	ω^2, sec^{-2}					
	Present analysis	Reference 16	Present analysis	Reference 16	Present analysis	Reference 16
	n = 6		n = 7		n = 8	
1	1.01231×10^9	1.01231×10^9	1.90756×10^9	1.90756×10^9	3.29043×10^9	3.29043×10^9
	1.89737×10^{11}	1.89737×10^{11}	2.58318×10^{11}	2.58318×10^{11}	3.37482×10^{11}	3.37482×10^{11}
	3.09484×10^{11}	3.09484×10^{11}	4.17137×10^{11}	4.17137×10^{11}	5.41321×10^{11}	5.41321×10^{11}
2	1.07881×10^9	1.07880×10^9	1.99482×10^9	1.99481×10^9	3.40265×10^9	3.40265×10^9
	1.88906×10^{11}	1.88906×10^{11}	2.47246×10^{11}	2.47246×10^{11}	3.36238×10^{11}	3.36238×10^{11}
	3.19069×10^{11}	3.19069×10^{11}	4.26965×10^{11}	4.26965×10^{11}	5.51321×10^{11}	5.51321×10^{11}
3	1.21550×10^9	1.215546×10^9	2.16263×10^9	2.16258×10^9	3.61029×10^9	3.61024×10^9
	1.88205×10^{11}	1.88205×10^{11}	2.56061×10^{11}	2.56061×10^{11}	3.34688×10^{11}	3.34688×10^{11}
	3.34351×10^{11}	3.34351×10^{11}	4.42737×10^{11}	4.42737×10^{11}	5.67465×10^{11}	5.67462×10^{11}
4	1.45929×10^9	1.45885×10^9	2.44390×10^9	2.44346×10^9	3.94411×10^9	3.94365×10^9
	1.88257×10^{11}	1.88256×10^{11}	2.55363×10^{11}	2.55362×10^{11}	3.33389×10^{11}	3.33387×10^{11}
	3.54695×10^{11}	3.54700×10^{11}	4.63855×10^{11}	4.63851×10^{11}	5.89187×10^{11}	5.89184×10^{11}
5	1.85912×10^9	1.85661×10^9	2.88407×10^9	2.88152×10^9	4.44733×10^9	4.44473×10^9
	1.89540×10^{11}	1.89533×10^{11}	2.55664×10^{11}	2.55657×10^{11}	3.32856×10^{11}	3.32849×10^{11}
	3.79646×10^{11}	3.79631×10^{11}	4.89809×10^{11}	4.89791×10^{11}	6.15984×10^{11}	6.15972×10^{11}
m	n = 9		n = 10			
1	5.31084×10^9	5.31084×10^9	8.13868×10^9	8.13868×10^9		
	4.27220×10^{11}	4.27220×10^{11}	5.27528×10^{11}	5.27528×10^{11}		
	6.82044×10^{11}	6.82044×10^{11}	8.39310×10^{11}	8.39310×10^{11}		
2	5.45179×10^9	5.45179×10^9	8.31196×10^9	8.31196×10^9		
	4.25852×10^{11}	4.25852×10^{11}	5.26066×10^{11}	5.26066×10^{11}		
	6.92169×10^{11}	6.92169×10^{11}	8.49529×10^{11}	8.49529×10^{11}		
3	5.70636×10^9	5.70631×10^9	8.61988×10^9	8.61982×10^9		
	4.24463×10^{11}	4.24022×10^{11}	5.24019×10^{11}	5.24019×10^{11}		
	7.08592×10^{11}	7.08591×10^{11}	8.66169×10^{11}	8.66169×10^{11}		
4	6.10407×10^9	6.10360×10^9	9.09120×10^9	9.09072×10^9		
	4.22240×10^{11}	4.22239×10^{11}	5.21849×10^{11}	5.21849×10^{11}		
	7.30801×10^{11}	7.30800×10^{11}	8.88772×10^{11}	8.88769×10^{11}		
5	6.68682×10^9	6.68415×10^9	9.76702×10^9	9.76427×10^9		
	4.21001×10^{11}	4.21001×10^{11}	5.20031×10^{11}	5.20024×10^{11}		
	7.58307×10^{11}	7.58295×10^{11}	9.16865×10^{11}	9.16854×10^{11}		

TABLE VII.- NATURAL FREQUENCIES OF A FREE-FREE 120° CONICAL FRUSTUM SHELL AS A FUNCTION OF NUMBER OF CIRCULAR NODE LINES IN NORMAL DISPLACEMENT w

[n = 2]

Number of circular node lines in w	Mode-identification figure	ω^2, sec^{-2}	
		Present analysis	Reference 1
1	16(a)	3.903×10^4	3.900×10^4
1	16(f)	1.780×10^9	1.781×10^9
1	16(j)	4.337×10^9	4.337×10^9
2	16(b)	1.858×10^7	1.861×10^7
2	16(k)	8.045×10^9	8.045×10^9
3	16(c)	2.267×10^7	2.286×10^7
3	16(g)	2.422×10^9	2.422×10^9
3	16(l)	1.311×10^{10}	1.314×10^{10}
4	16(d)	2.754×10^7	2.831×10^7
4	16(h)	4.127×10^9	4.127×10^9
4	16(m)	1.874×10^{10}	1.951×10^{10}
5	16(e)	3.314×10^7	3.654×10^7
5	16(i)	6.342×10^9	6.342×10^9
5	16(n)	2.019×10^{10}	----------

TABLE VIII.- NATURAL FREQUENCIES OF A CLAMPED-FREE 120° CONICAL FRUSTUM SHELL AS A FUNCTION OF NUMBER OF CIRCULAR NODE LINES IN NORMAL DISPLACEMENT w

[n = 2]

Number of circular node lines in w	Mode-identification figure	ω^2, sec^{-2}	
		Present analysis	Reference 1
1	17(a)	1.199×10^7	1.195×10^7
1	17(f)	1.794×10^9	1.795×10^9
1	17(k)	4.290×10^9	4.290×10^9
2	17(b)	1.948×10^7	1.953×10^7
2	17(g)	1.420×10^9	1.420×10^9
3	17(c)	2.420×10^7	2.453×10^7
3	17(h)	3.069×10^9	3.076×10^9
3	17(l)	8.695×10^9	8.702×10^9
4	17(d)	2.940×10^7	3.076×10^7
4	17(m)	1.304×10^{10}	1.325×10^{10}
4	17(i)	5.224×10^{10}	----------
5	17(e)	3.545×10^7	----------
5	17(j)	1.025×10^{10}	----------
5	17(n)	1.760×10^{10}	----------

TABLE IX.- NATURAL FREQUENCIES OF A FREELY SUPPORTED SHELL HAVING POSITIVE GAUSSIAN CURVATURE AS A FUNCTION OF THE NODAL CIRCLES IN NORMAL DISPLACEMENT w

[n = 2]

Number of circular node lines in w	Mode-identification figure	Ω^2, sec^{-2} (present analysis)
0	20(a)	0.1425
0	20(f)	.2340
0	20(k)	5.659
1	20(b)	0.3607
1	20(g)	3.918
1	20(l)	9.754
2	20(c)	0.5507
2	20(h)	5.914
2	20(m)	15.90
3	20(d)	0.6641
3	20(i)	8.571
3	20(n)	24.40
4	20(e)	0.7260
4	20(j)	12.26
4	20(o)	35.24

TABLE X.- NATURAL FREQUENCIES OF A FREELY SUPPORTED SHELL WITH NEGATIVE GAUSSIAN CURVATURE AS A FUNCTION OF THE NUMBER OF CIRCULAR NODE LINES IN NORMAL DISPLACEMENT w

[n = 2]

Number of circular node lines in w	Mode-identification figure	Ω^2, sec^{-2} (present analysis)
0	21(a)	0.0246
0	21(f)	1.888
0	21(k)	5.804
1	21(b)	0.1950
1	21(g)	3.243
1	21(l)	8.660
2	21(c)	0.403
2	21(h)	5.128
2	21(m)	13.96
3	21(d)	0.5547
3	21(i)	1.347
3	21(n)	7.738
4	21(e)	0.6499
4	21(j)	11.13
4	21(o)	31.39

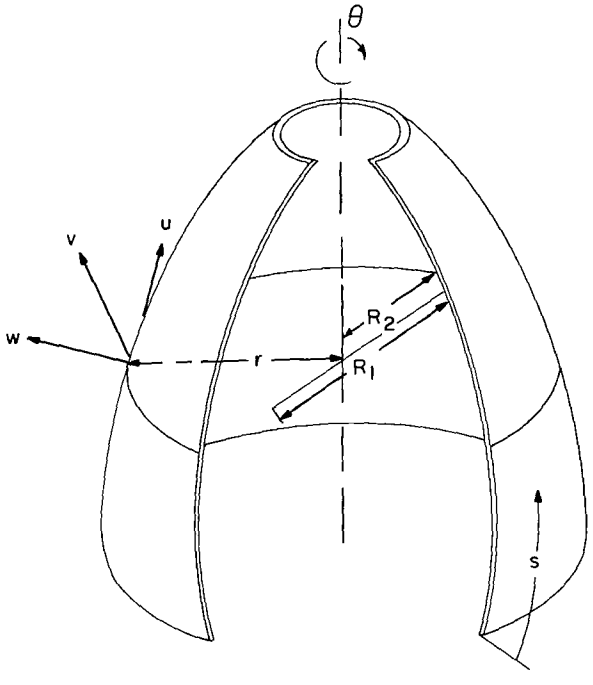

Figure 1.- Geometry of a shell of revolution.

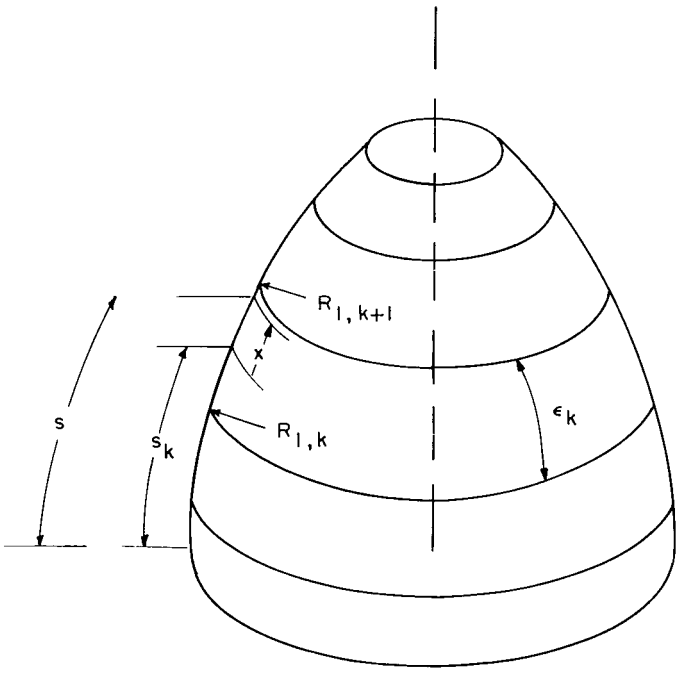

Figure 2.- Typical idealization of shell of revolution showing geometrically exact finite elements.

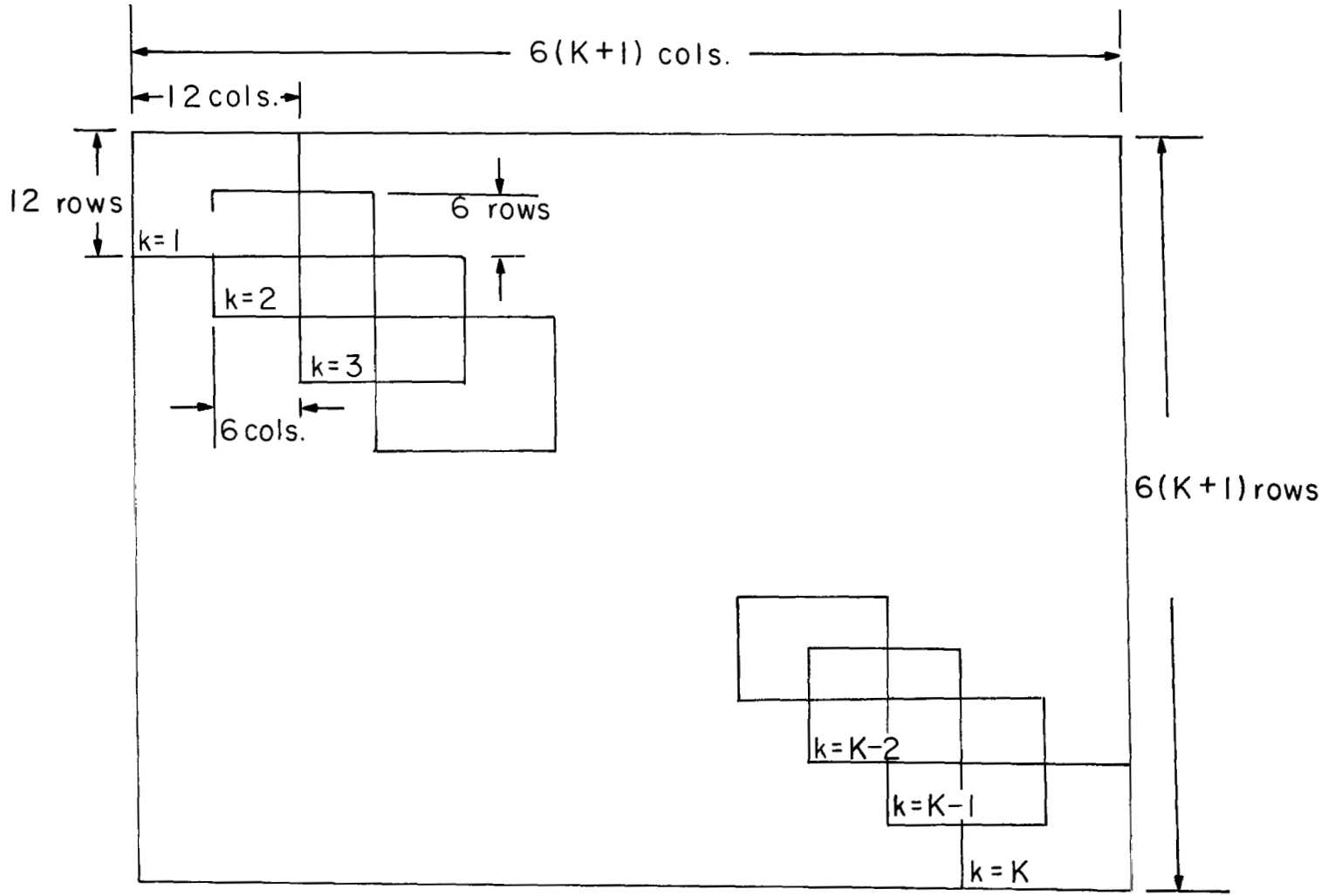

Figure 3.- Illustration of synthesis of stiffness and mass matrices.

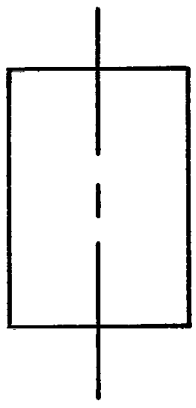

$r = 5$ in. $= 12.7$ cm

$1/R_1 = 0$

$1/R_2 = 0.2$ in.$^{-1} = 0.07874$ cm^{-1}

$r' = 0$

$R_1' = 0$

$L = 20$ in. $= 50.8$ cm

$E = 2.96 \times 10^7$ lb/in^2 $= 2.0408 \times 10^7$ N/cm^2

$\mu = 0.29$

$\rho = 7.33 \times 10^{-4}$ lb-sec^2/in^4 $= 0.78335 \times 10^{-4}$ N-sec^2/cm^4

$h = 0.008$ in. $= 0.02032$ cm

(a) Isotropic cylinder.

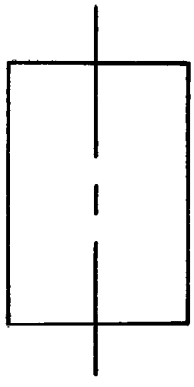

$r = 1.925$ in. $= 4.8895$ cm

$1/R_1 = 0$

$1/R_2 = 0.5195$ in.$^{-1} = 0.2045$ cm^{-1}

$r' = 0$

$R_1' = 0$

$h = 0.065$ in. $= 0.165$ cm

$L = 15.53$ in. $= 39.4462$ cm

$\rho h = 0.1211 \times 10^{-4}$ lb-sec^2/in^3 $= 0.3287 \times 10^{-5}$ N-sec^2/cm^3

$C_{11} = 1.25 \times 10^6$ lb/in. $= 2.189 \times 10^6$ N/cm

$C_{12} = 0.187 \times 10^6$ lb/in. $= 0.327 \times 10^6$ N/cm

$C_{22} = 0.742 \times 10^6$ lb/in. $= 1.299 \times 10^6$ N/cm

$C_{66} = 0.473 \times 10^6$ lb/in. $= 0.828 \times 10^6$ N/cm

$D_{11} = 0.652 \times 10^6$ lb-in. $= 7.367 \times 10^6$ N-cm

$D_{12} = 1.767 \times 10^6$ lb-in. $= 19.964 \times 10^6$ N-cm

$D_{22} = 2.767 \times 10^6$ lb-in. $= 31.263 \times 10^6$ N-cm

$D_{66} = 9 \times 10^6$ lb-in. $= 101.686 \times 10^6$ N-cm

(b) Orthotropic cylinder.

Figure 4.- Properties of the shells analyzed for sample calculations.

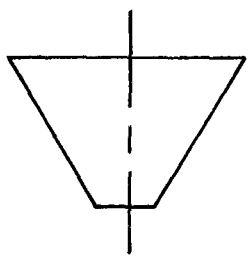

$$r = 3 + s\sqrt{3}/2 \text{ (in.)} = 7.62 + s\sqrt{3}/2 \text{ (cm)}$$

$$1/R_1 = 0$$

$$1/R_2 = \frac{1}{0.1667 + s\sqrt{3}} \text{ (in}^{-1}\text{)} = \frac{1}{0.06562 + s\sqrt{3}} \text{ (cm}^{-1}\text{)}$$

$$r' = \sqrt{3}/2$$

$$R_1' = 0$$

$$L = \frac{42}{\sqrt{3}} \text{ (in.)} = \frac{106.7}{\sqrt{3}} \text{ (cm)}$$

$$E = 1 \times 10^7 \text{ lb/in}^2 = 6.8948 \times 10^6 \text{ N/cm}^2$$

$$\mu = 0.315$$

$$\rho = 2.54 \times 10^{-4} \text{ lb-sec}^2/\text{in}^4 = 0.2714 \times 10^{-4} \text{ N-sec}^2/\text{cm}^4$$

$$h = 0.025 \text{ in.} = 0.0635 \text{ cm}$$

(c) Isotropic 120^0 conical frustum.

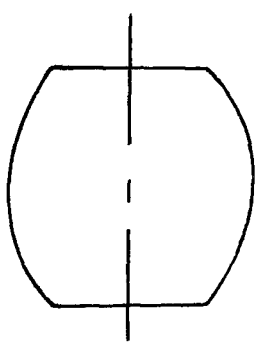

$$r = 3\cos\left(0.5 - \frac{s}{3}\right) - 1.879 \text{ (in.)} = 7.62\cos\left(0.5 - \frac{s}{7.62}\right) - 4.773 \text{ (cm)}$$

$$1/R_1 = 0.333 \text{ in}^{-1} = 0.131 \text{ cm}^{-1}$$

$$1/R_2 = \frac{\cos\left(0.5 - \frac{s}{3}\right)}{3\cos\left(0.5 - \frac{s}{3}\right) - 1.879} \text{ (in}^{-1}\text{)} = \frac{\cos\left(0.5 - \frac{s}{7.62}\right)}{7.62\cos\left(0.5 - \frac{s}{7.62}\right) - 4.773} \text{ (cm}^{-1}\text{)}$$

$$r' = \sin\left(0.5 - \frac{s}{3}\right) = \sin\left(1.27 - \frac{s}{7.62}\right)$$

$$R_1' = 0$$

$$L = 3 \text{ in.} = 7.62 \text{ cm}$$

$$E = 1 \text{ lb/in}^2 = 0.68948 \text{ N/cm}^2$$

$$\mu = 0.30$$

$$\rho = 1 \text{ lb-sec}^2/\text{in}^4 = 0.10687 \text{ N-sec}^2/\text{cm}^4$$

$$h = 0.001 \text{ in.} = 0.00254 \text{ cm}$$

(d) Isotropic shell of positive Gaussian curvature.

Figure 4.- Continued.

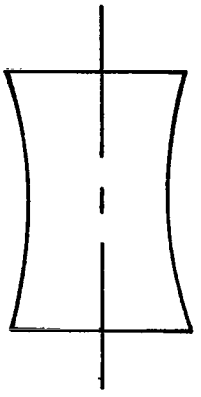

$$r = 1 - 20\left\{\cos\left[-(1.5 - s)0.5\right] - 1\right\} \text{ (in.)}$$

$$= 2.54 - 50.8\left\{\cos\left[-(3.81 - s)0.01969\right] - 1\right\} \text{ (cm)}$$

$$1/R_1 = -0.05 \text{ in}^{-1} = -0.01969 \text{ cm}^{-1}$$

$$1/R_2 = \frac{-\cos\left[-(1.5 - s)0.05\right]}{-1 + 20\left\{\cos\left[-(1.5 - s)0.05\right] - 1\right\}} \text{ in}^{-1}$$

$$= \frac{-\cos\left[-(3.81 - s)0.01969\right]}{-2.54 + 50.8\left\{\cos\left[-(3.81 - s)0.01969\right] - 1\right\}} \text{ cm}^{-1}$$

$$r' = \sin\left[-(1.5 - s)0.05\right] = \sin\left[-(3.81 - s)0.01969\right]$$

$$R_1' = 0$$

$$L = 3 \text{ in.} = 7.62 \text{ cm}$$

$$E = 0.91 \text{ lb/in}^2 = 0.6274 \text{ N/cm}^2$$

$$\mu = 0.30$$

$$\rho = 1 \text{ lb-sec}^2/\text{in}^4 = 0.10687 \text{ N-sec}^2/\text{cm}^4$$

$$h = 0.001 \text{ in.} = 0.00254 \text{ cm}$$

(e) Isotropic shell of negative Gaussian curvature.

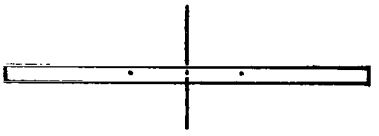

$$r = 0.5 + s \text{ (in.)} = 1.27 + s \text{ (cm)}$$

$$1/R_1 = 0$$

$$1/R_2 = 0$$

$$r' = 1$$

$$R_1' = 0$$

$$L = 0.5 \text{ in.} = 1.27 \text{ cm}$$

$$E = 10.92 \text{ lb/in}^2 = 7.5291 \text{ N/cm}^2$$

$$\mu = 0.30$$

$$\rho = 1 \text{ lb-sec}^2/\text{in}^4 = 0.10687 \text{ N-sec}^2/\text{cm}^4$$

$$h = 1 \text{ in.} = 2.54 \text{ cm}$$

(f) Isotropic annular plate.

Figure 4.- Concluded.

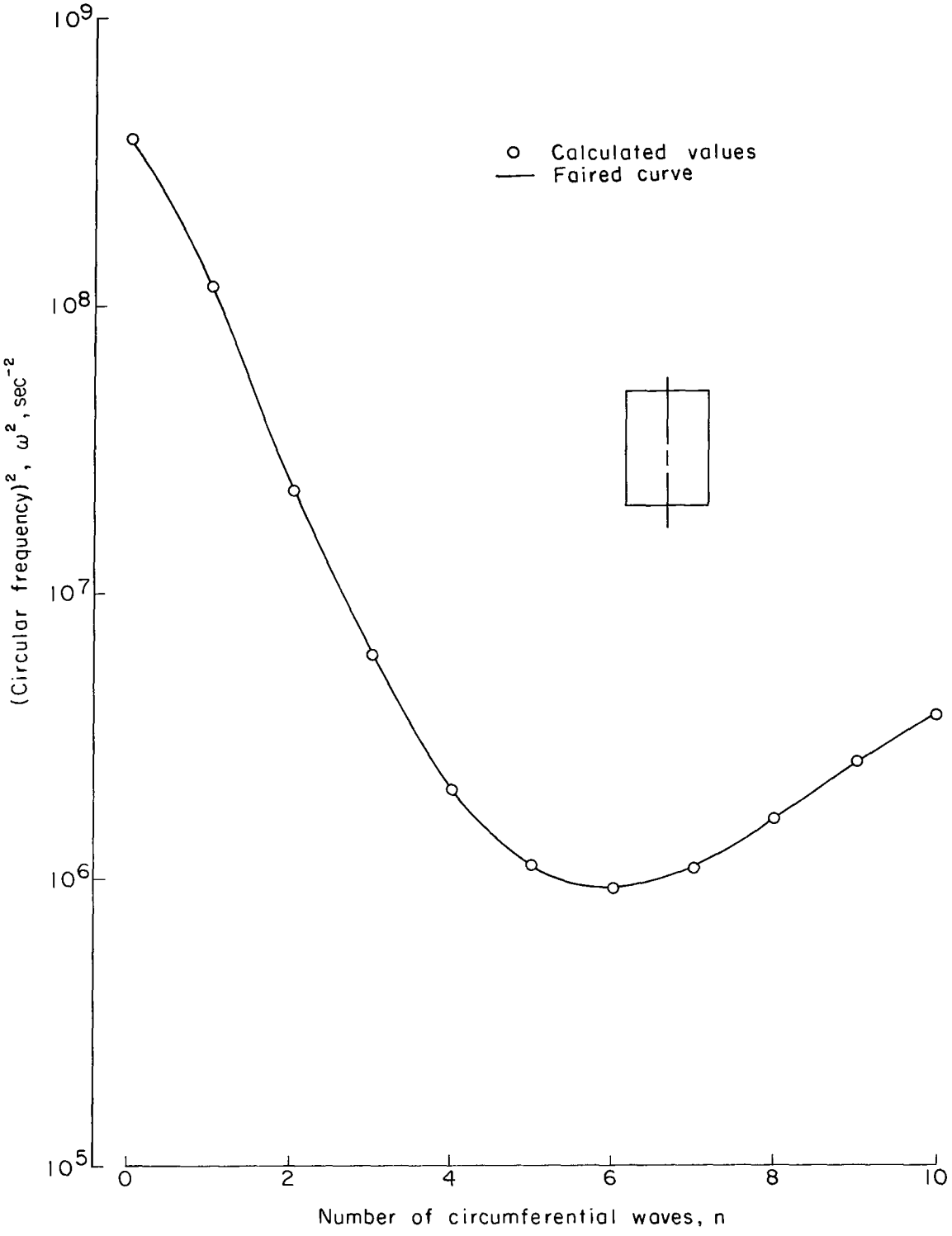

Figure 5.- Minimum circular frequencies of a cylindrical shell computed by present method and method of reference 15. Freely supported edges.

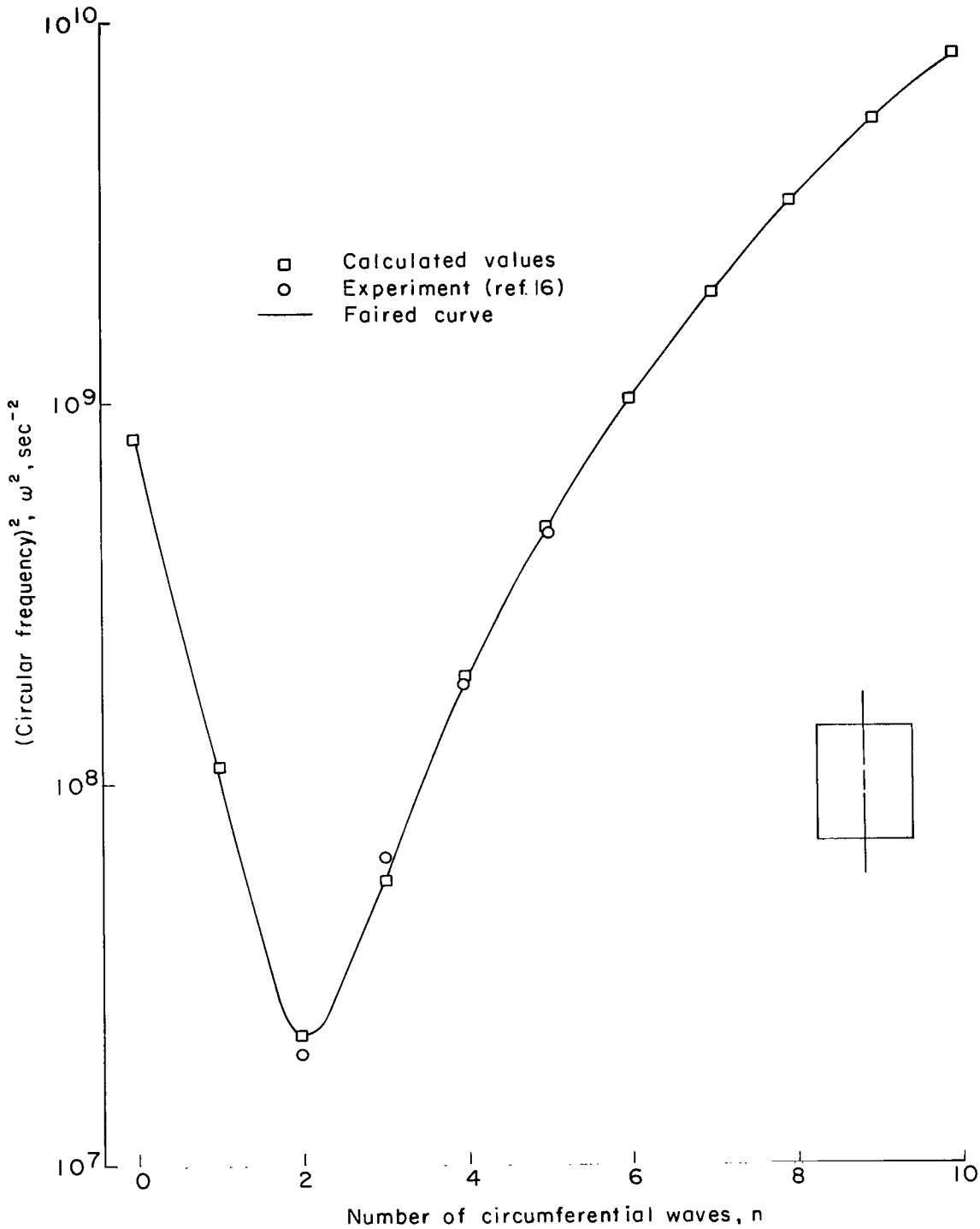

Figure 6.- Minimum circular frequencies of an orthotropic cylindrical shell computed by present method and method of reference 16. Freely supported edges.

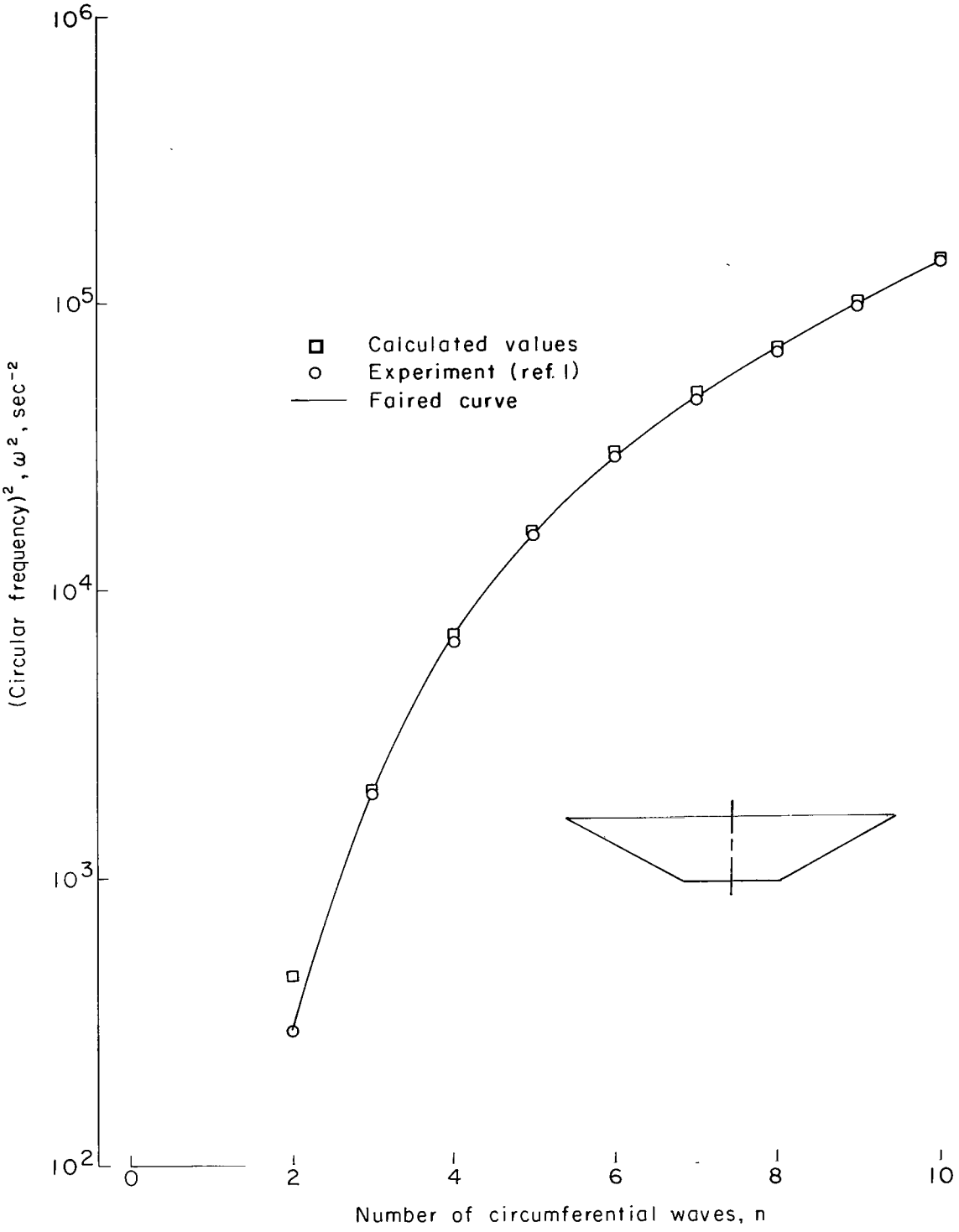

Figure 7.- Minimum circular frequencies of a 120^0 conical frustum by present method and method of reference 1. Free-free edge conditions.

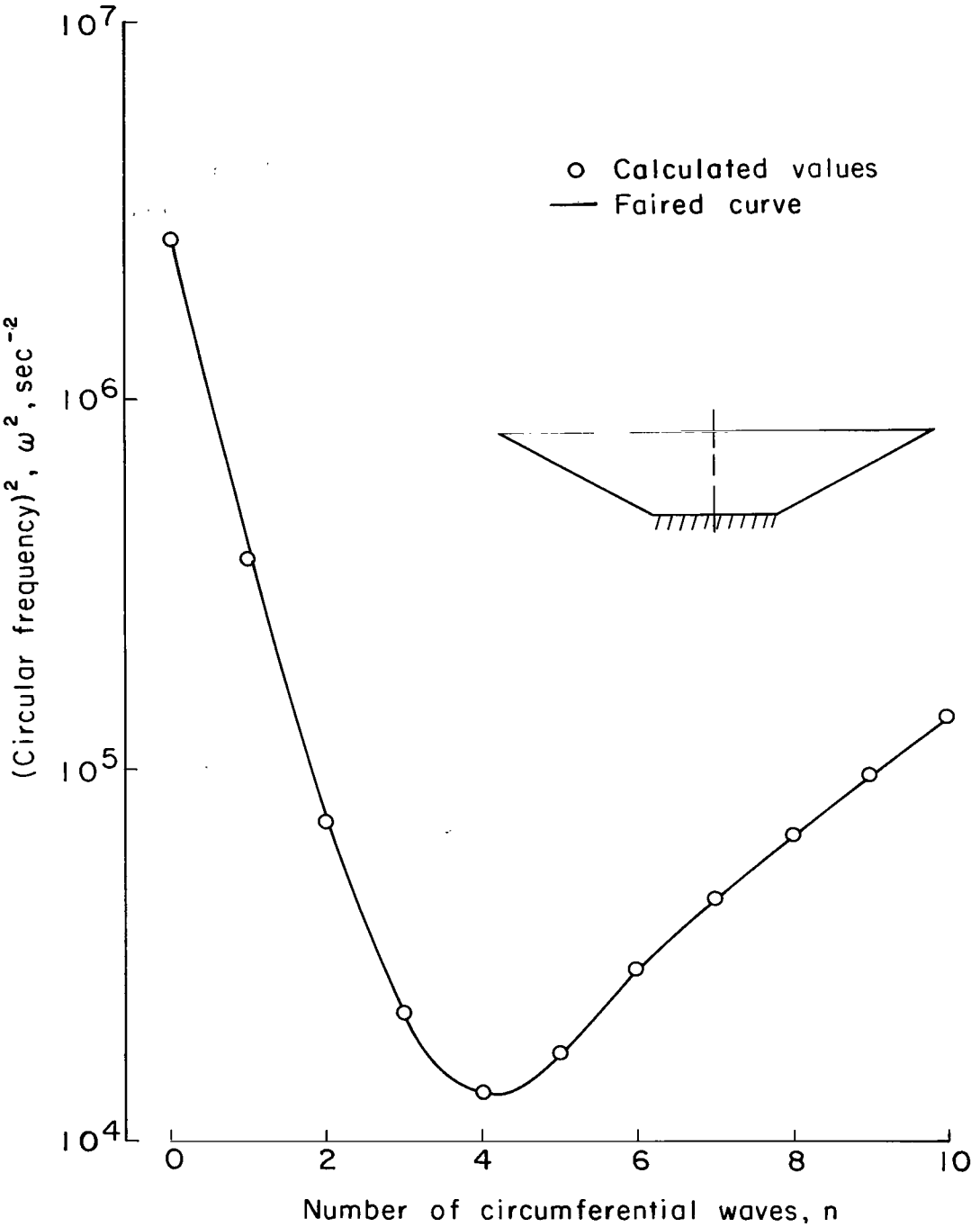

Figure 8.- Minimum circular frequencies of a 120° conical frustum by present method and method of reference 1. Clamped-free edge conditions.

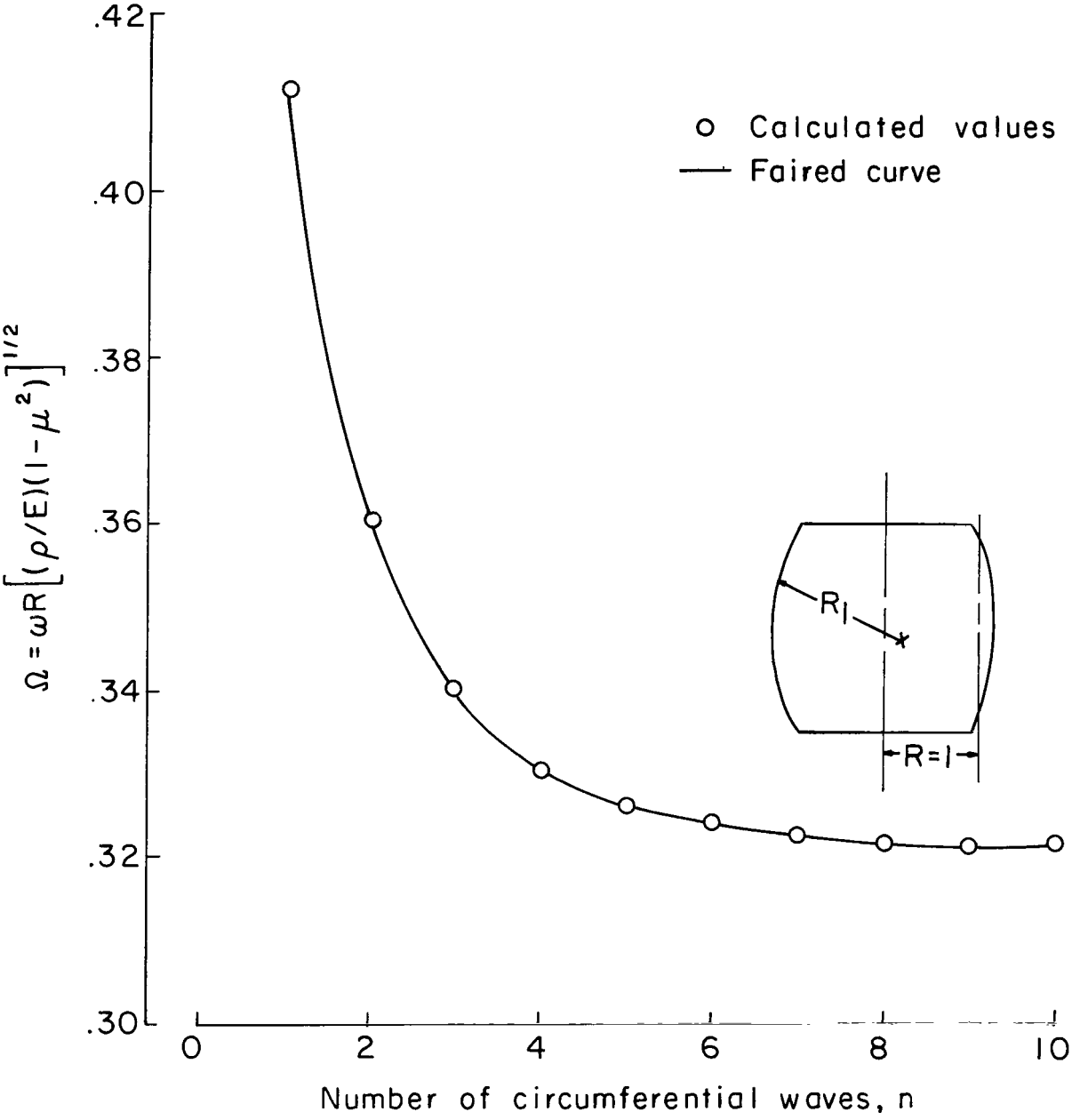

Figure 9.- Minimum nondimensional frequencies of a shell of positive Gaussian curvature as computed by present method and method of reference 4. Freely supported edges.

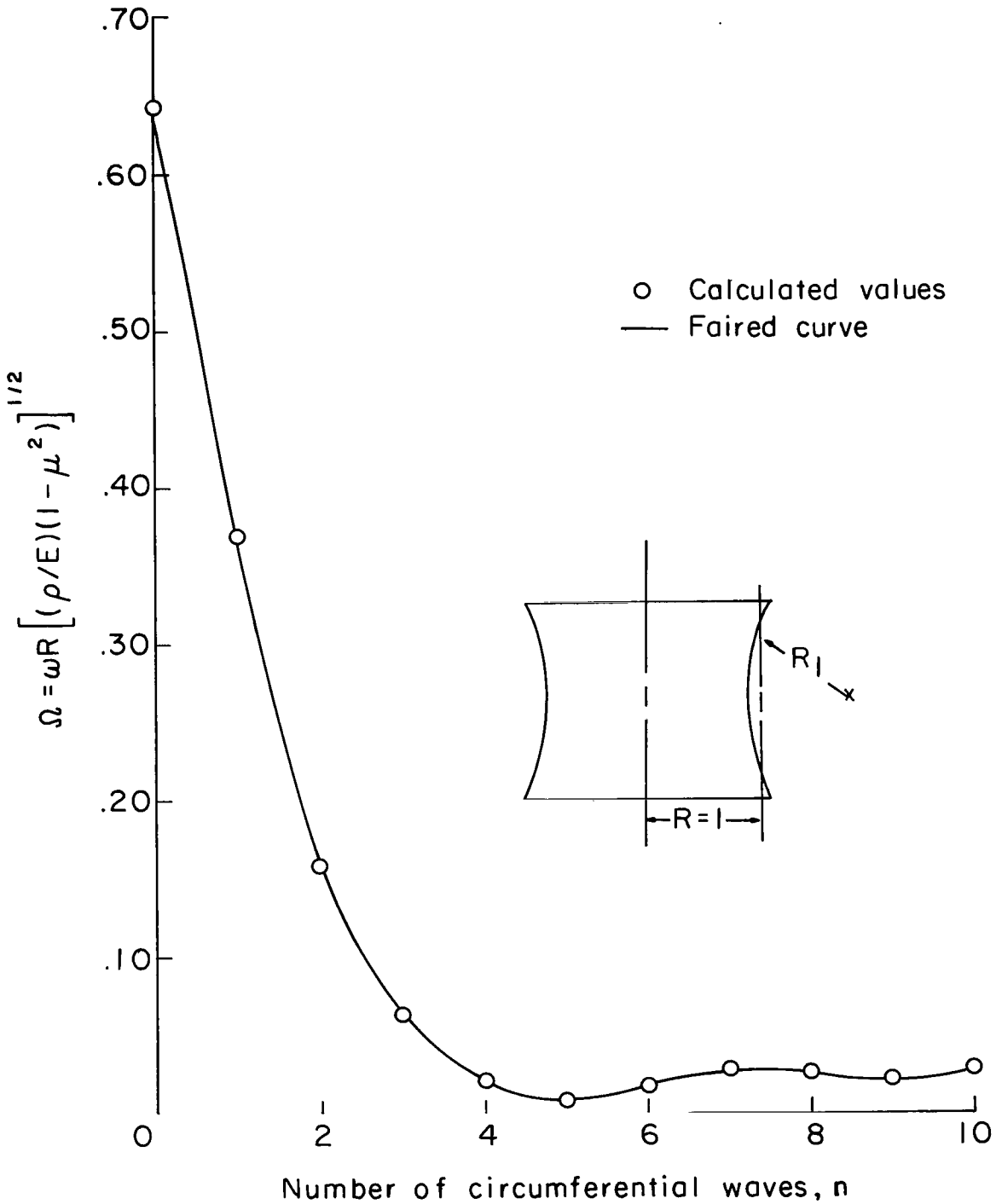

Figure 10.- Minimum nondimensional frequencies of a shell of negative Gaussian curvature as computed by present method and method of reference 4. Freely supported edges.

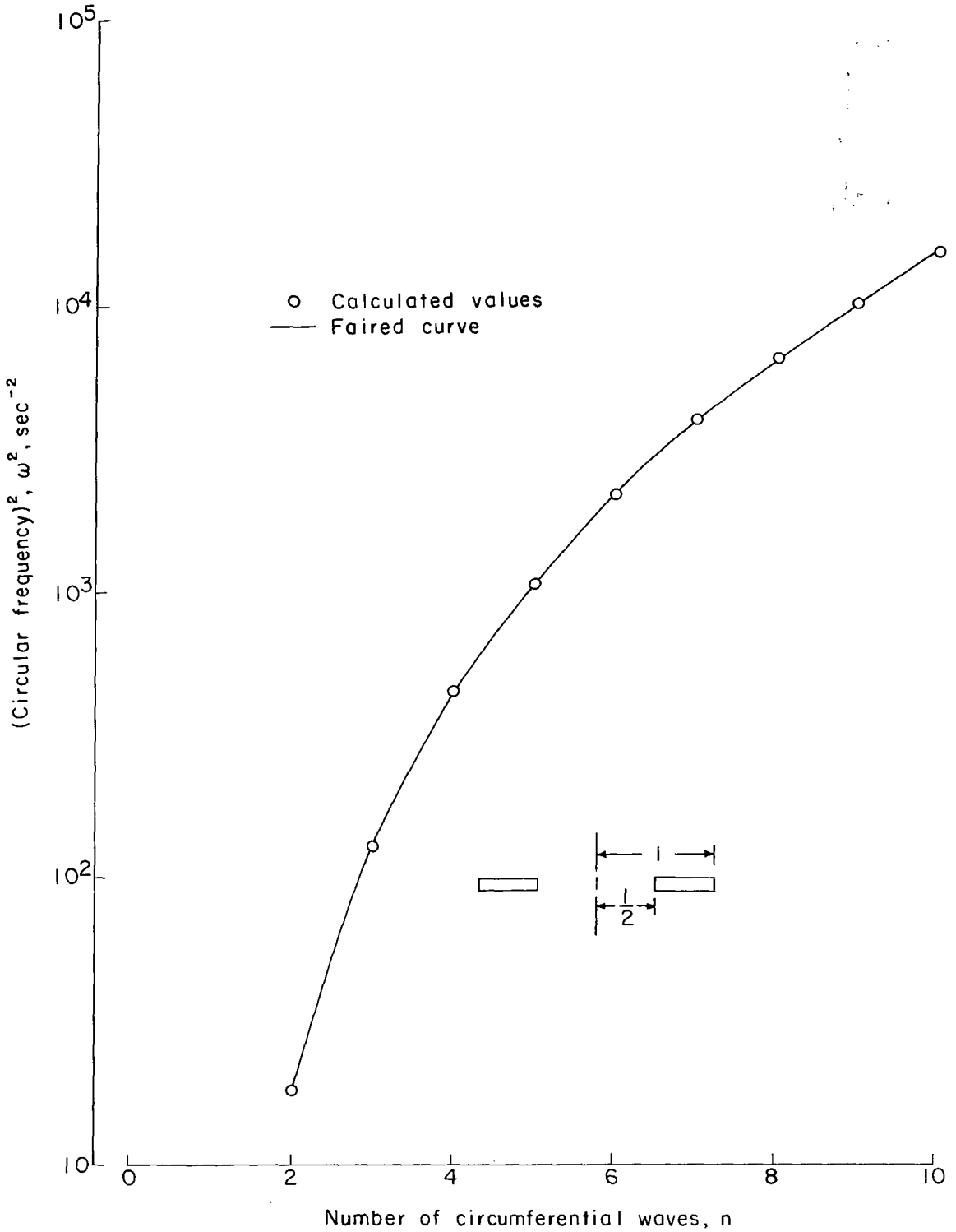

Figure 11.- Minimum circular frequencies of an annular plate as computed by present method and method of reference 17. Free-free edges.

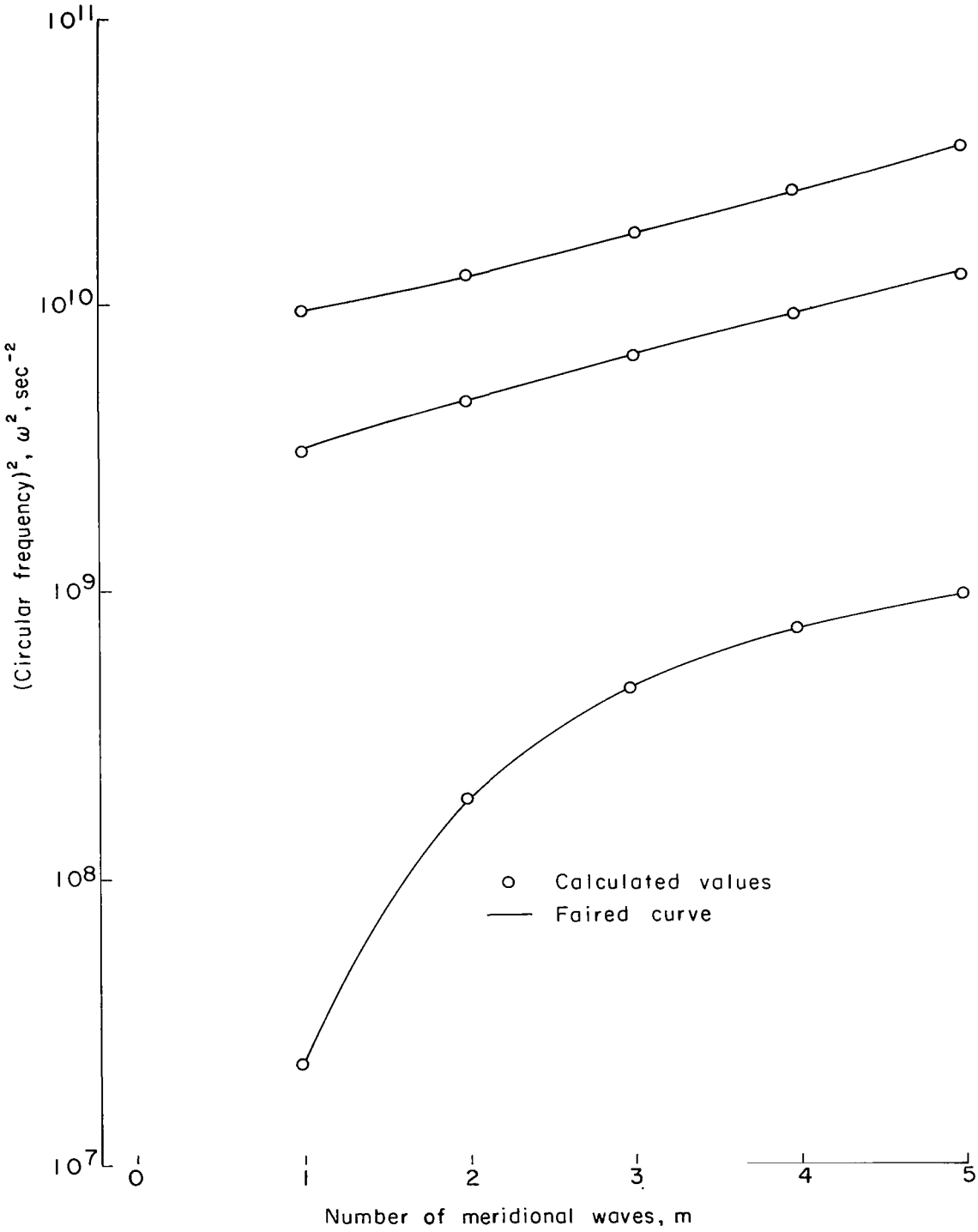

Figure 12.- Frequencies of an isotropic cylinder as computed by present method and method of reference 15. Freely supported edges; n = 2.

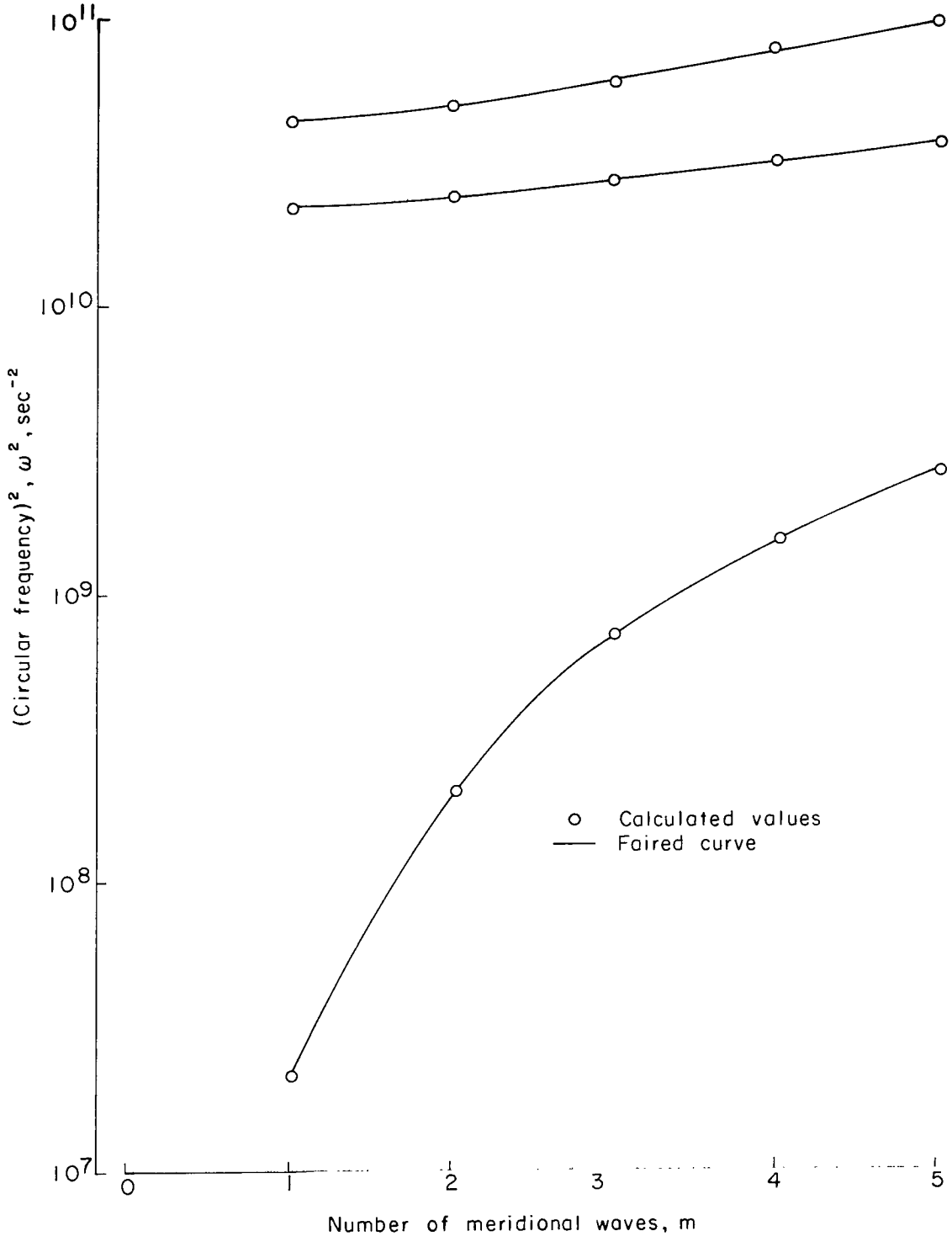

Figure 13.- Frequencies of an orthotropic cylinder as computed by present method and method of reference 16. Freely supported edges; n = 2.

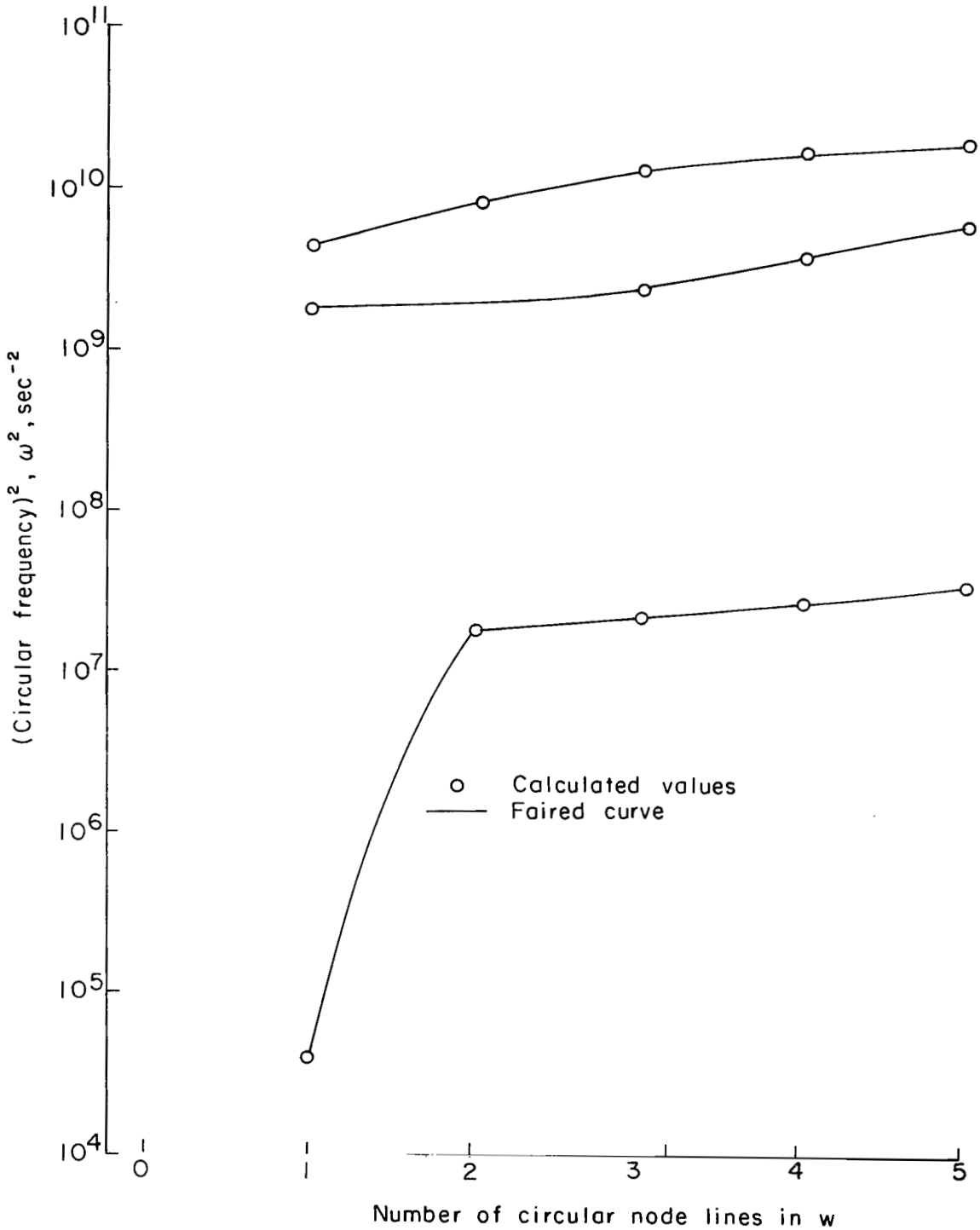

Figure 14.- Circular frequencies of a free-free 120° conical frustum as computed by present method and method of reference 1.

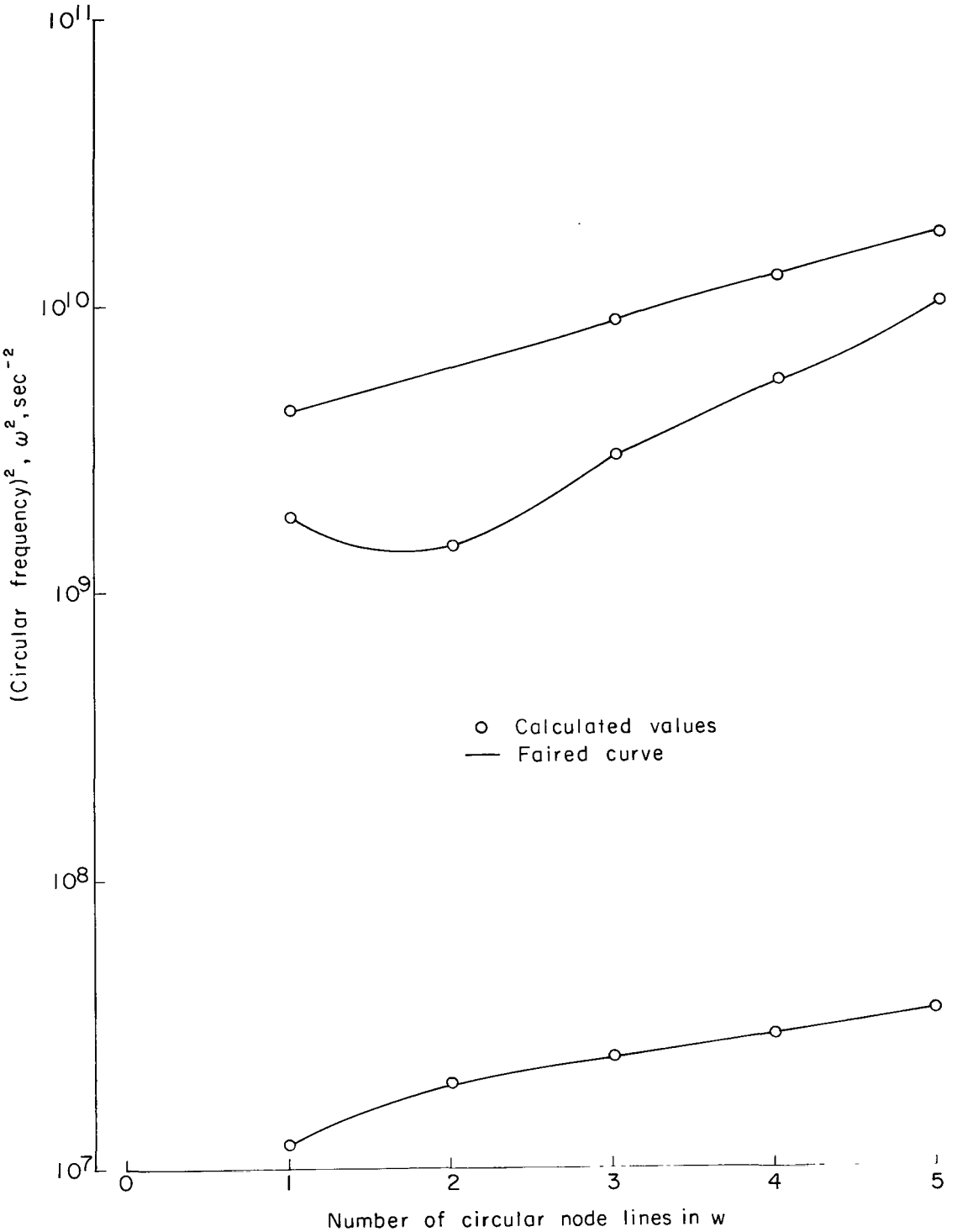

Figure 15.- Frequencies of a 120° conical frustum shell as computed by present method and method of reference 1. Clamped at smaller end; n = 2.

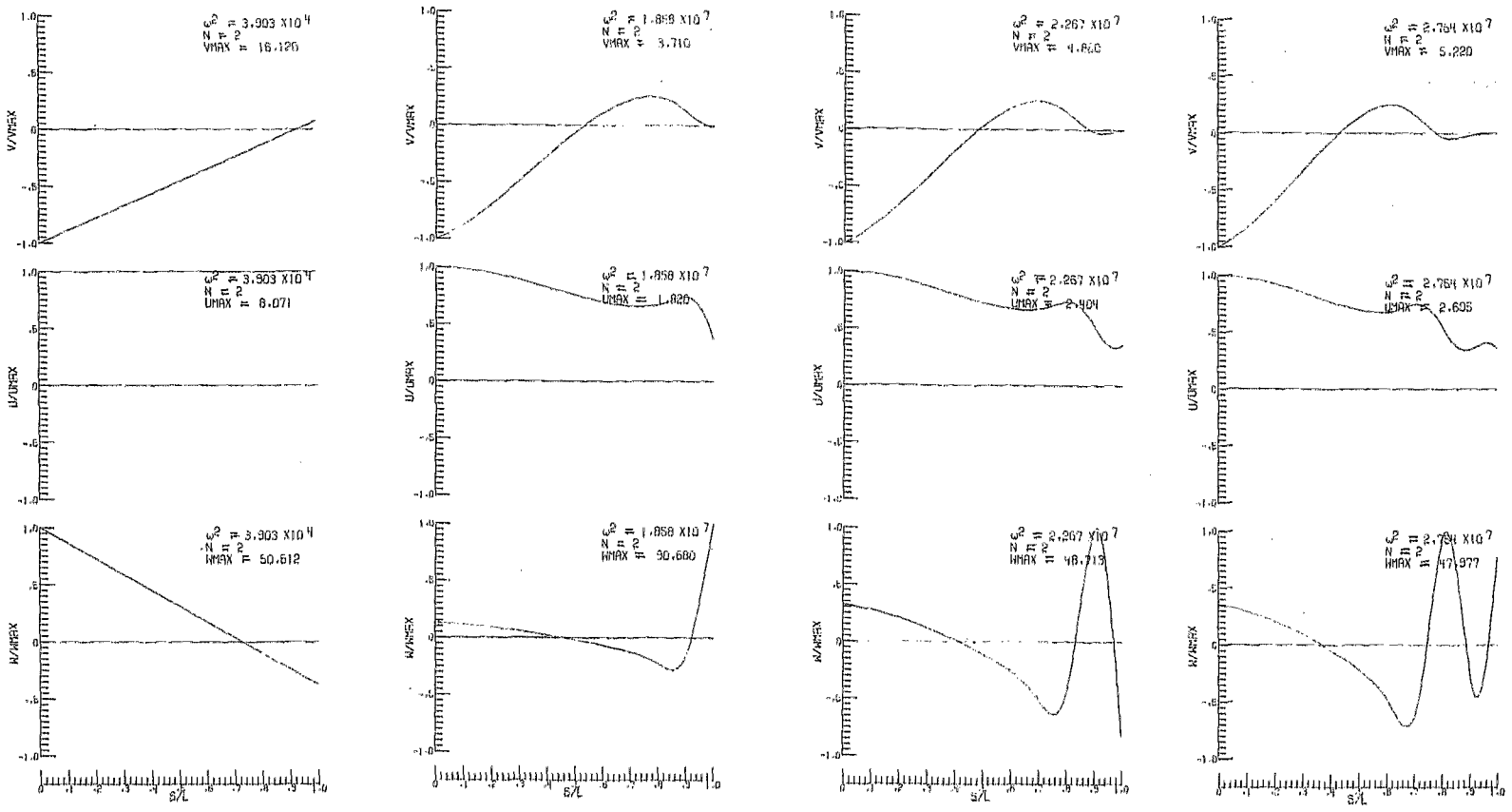

(a) One nodal circle in w displacement.

(b) Two nodal circles in w displacement.

(c) Three nodal circles in w displacement.

(d) Four nodal circles in w displacement.

Figure 16.- Natural mode shapes of a free-free 120° conical frustum corresponding to the frequencies shown in figure 14.

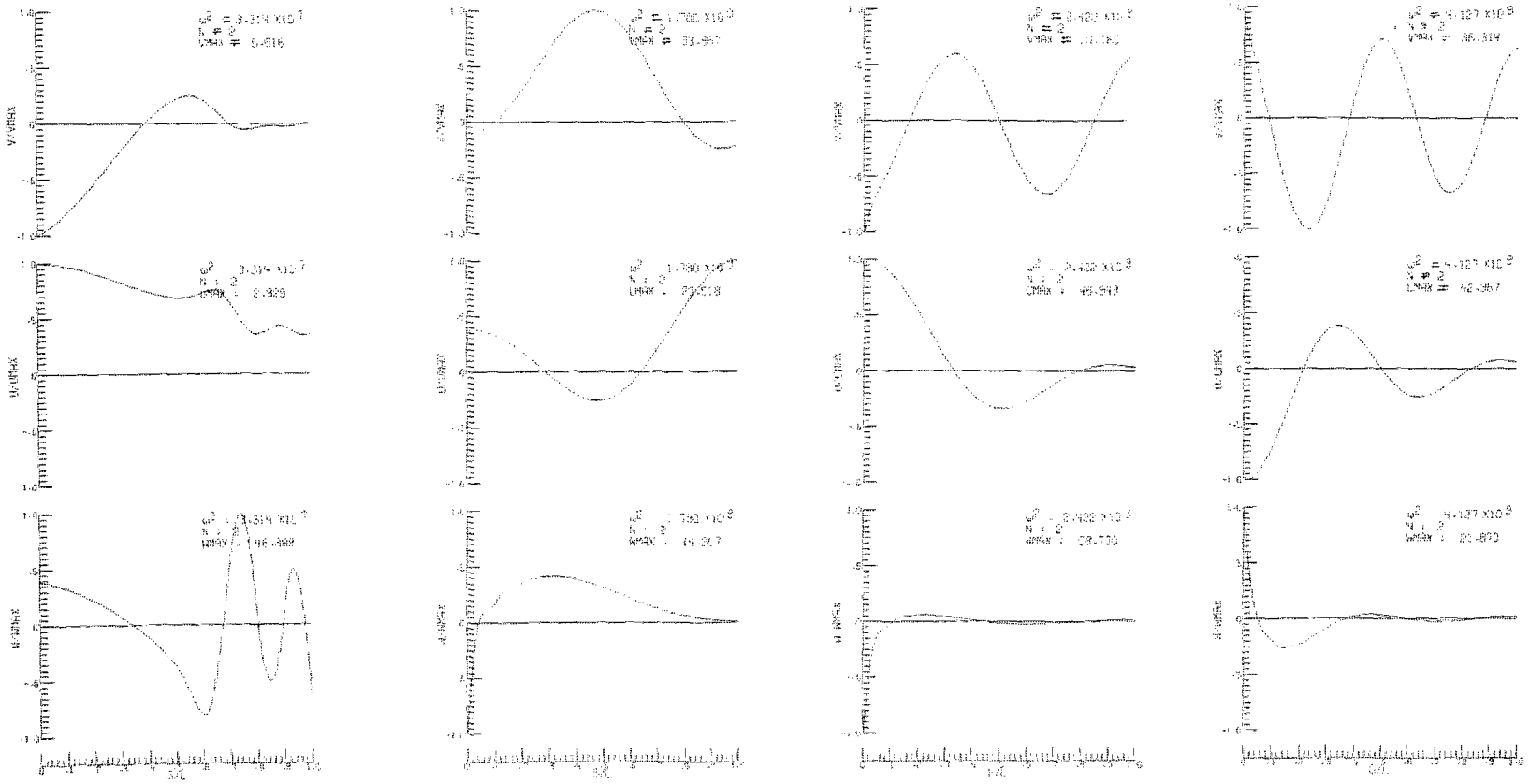

(e) Five nodal circles in w displacement.

(f) One nodal circle in w displacement.

(g) Three nodal circles in w displacement.

(h) Four nodal circles in w displacement.

Figure 16.- Continued.

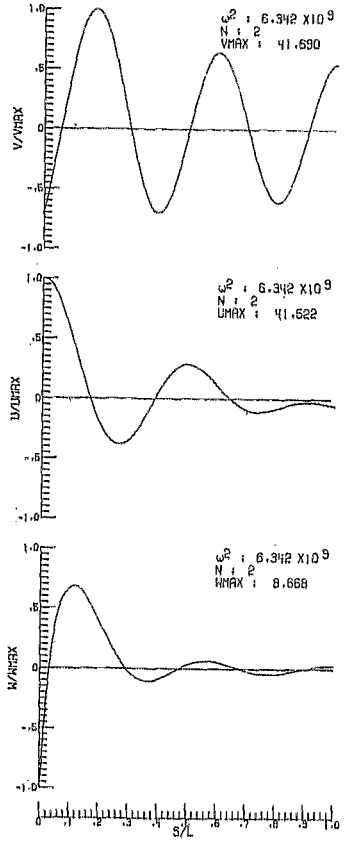

(I) Five nodal circles in w displacement.

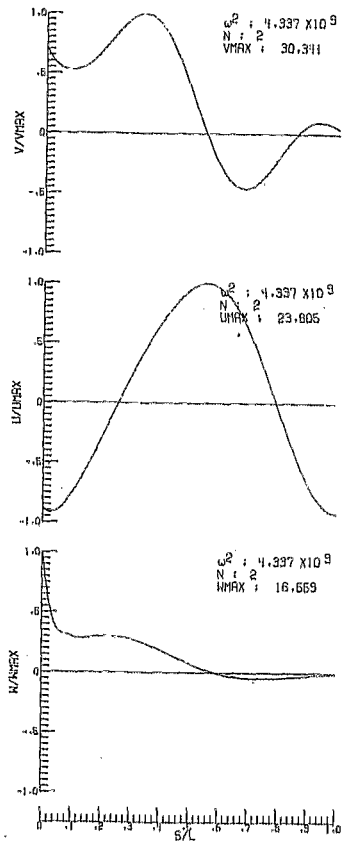

(J) One nodal circle in w displacement.

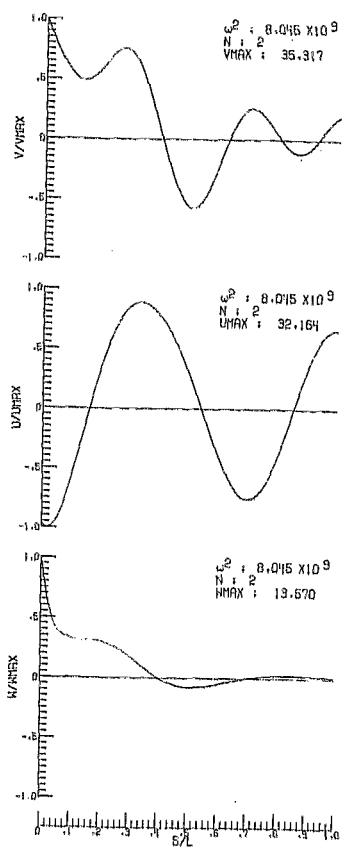

(K) Two nodal circles in w displacement.

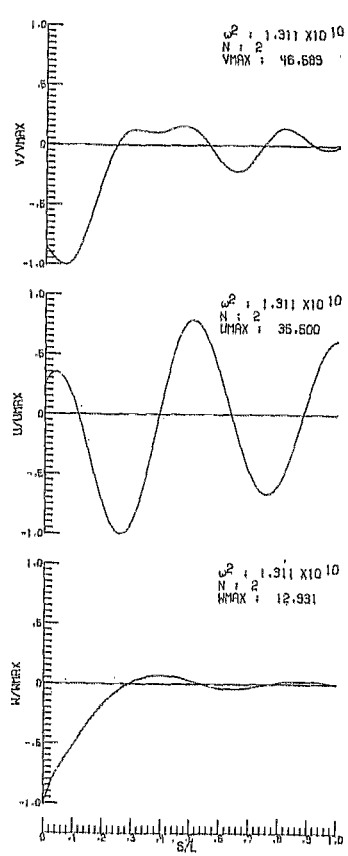

(L) Three nodal circles in w displacement.

Figure 16.- Continued.

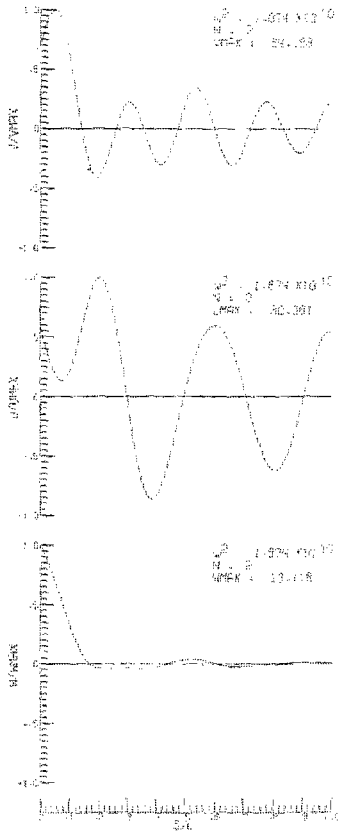

(m) Four nodal circles in w displacement.

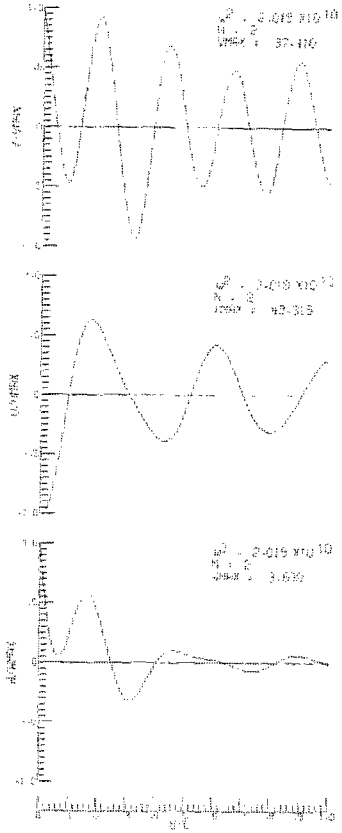

(n) Five nodal circles in w displacement.

Figure 16.- Concluded.

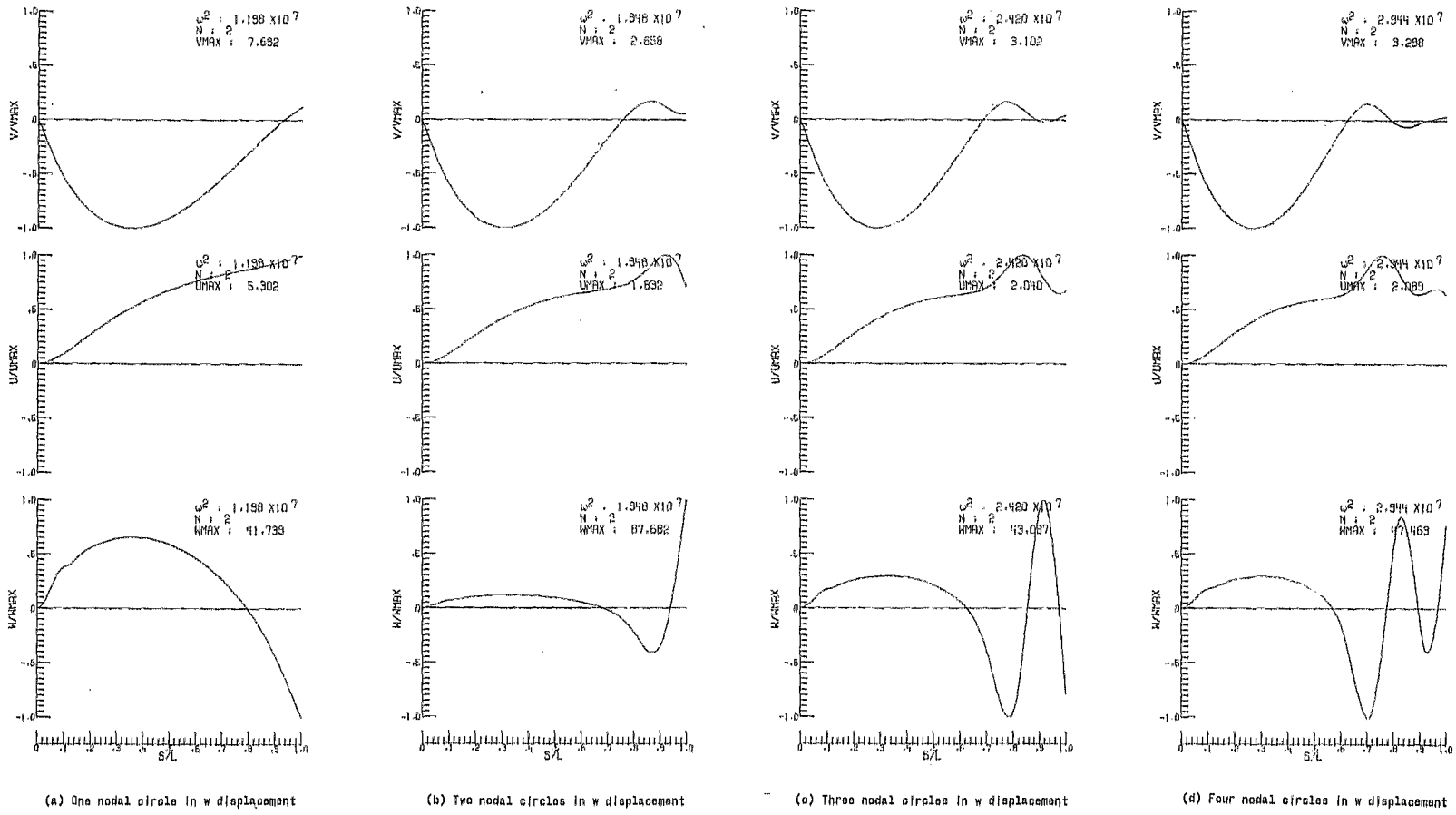

(a) One nodal circle in w displacement

(b) Two nodal circles in w displacement

(c) Three nodal circles in w displacement

(d) Four nodal circles in w displacement

Figure 17.- Natural mode shapes of a clamped-free 120° conical frustum corresponding to the frequencies shown in figure 15.

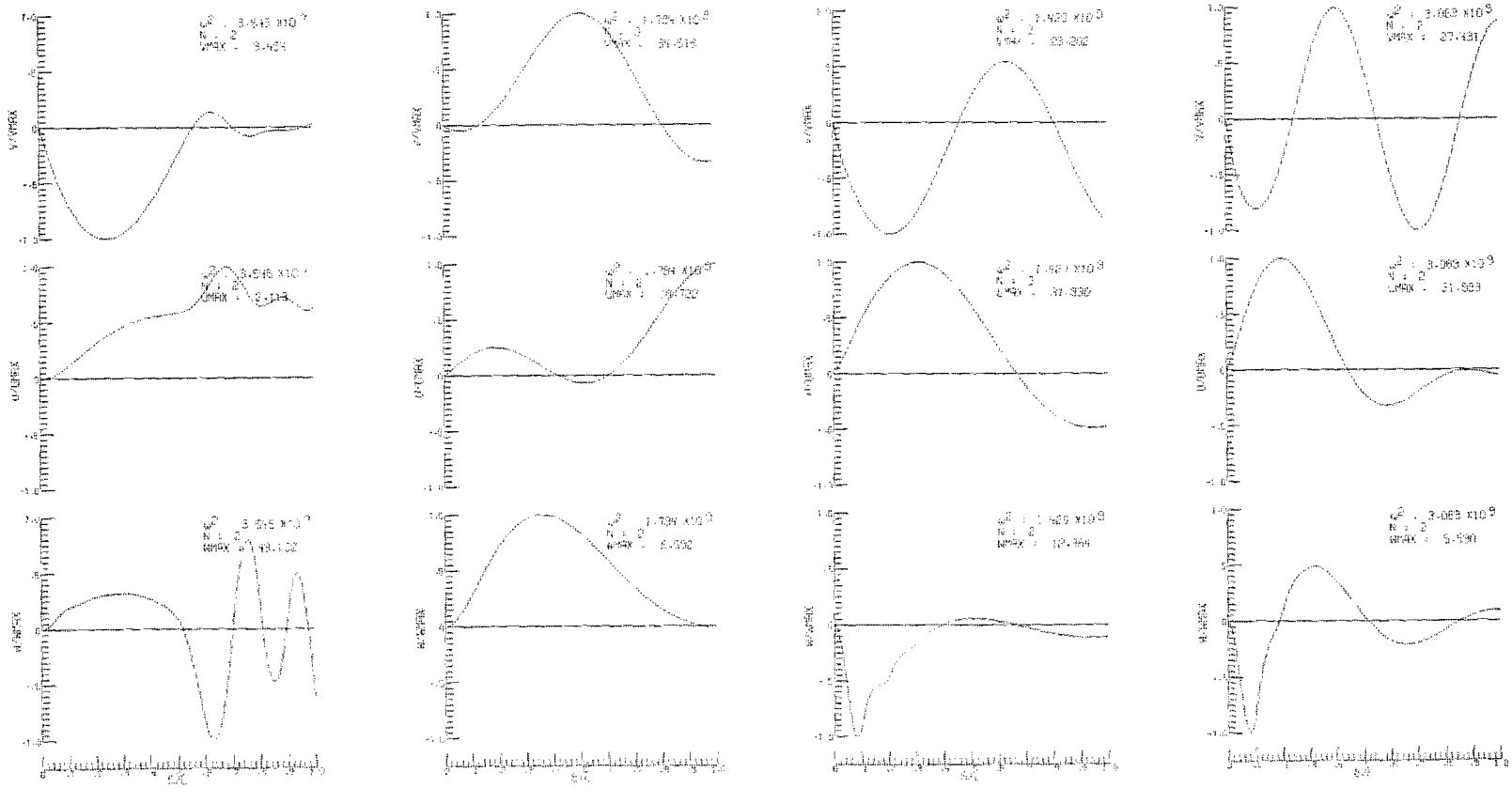

(e) Five nodal circles in w displacement

(f) One nodal circle in w displacement

(g) Two nodal circles in w displacement

(h) Three nodal circles in w displacement

Figure 17.- Continued.

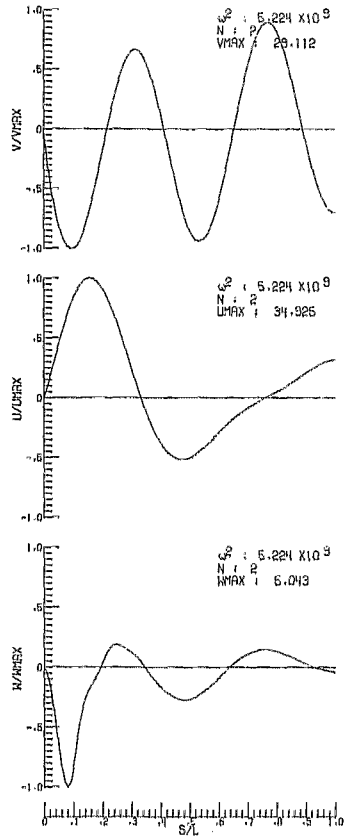

(i) Four nodal circles in w displacement

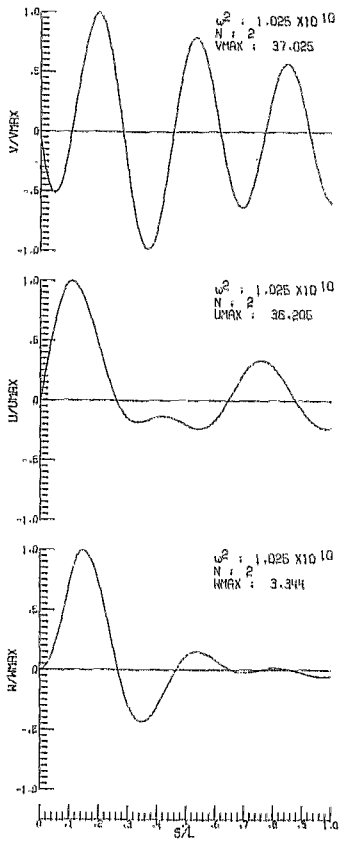

(j) Five nodal circles in w displacement

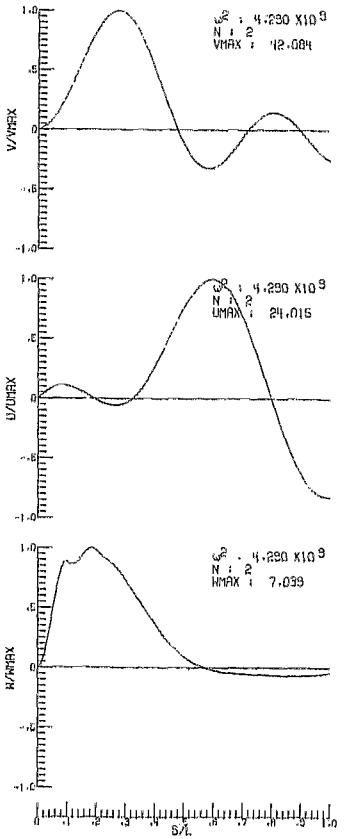

(k) One nodal circle in w displacement

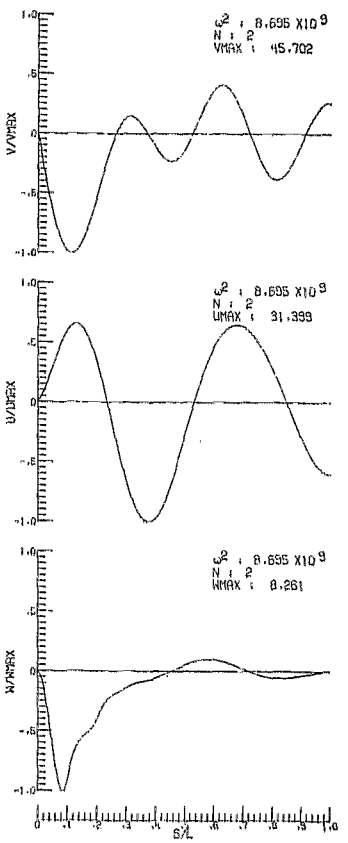

(l) Three nodal circles in w displacement

Figure 17.- Continued.

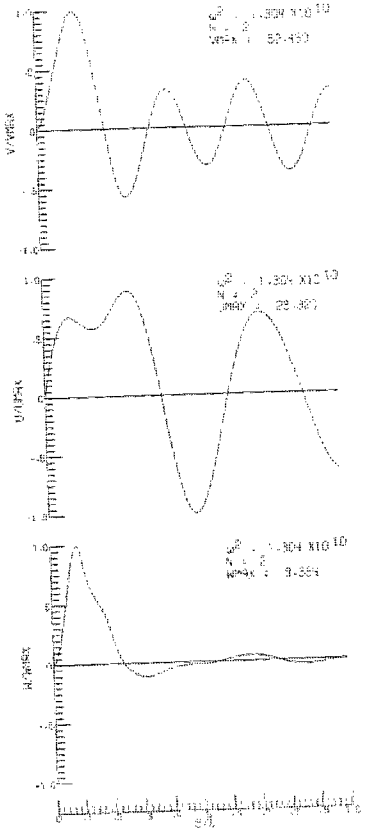

(m) Four nodal circles in w displacement

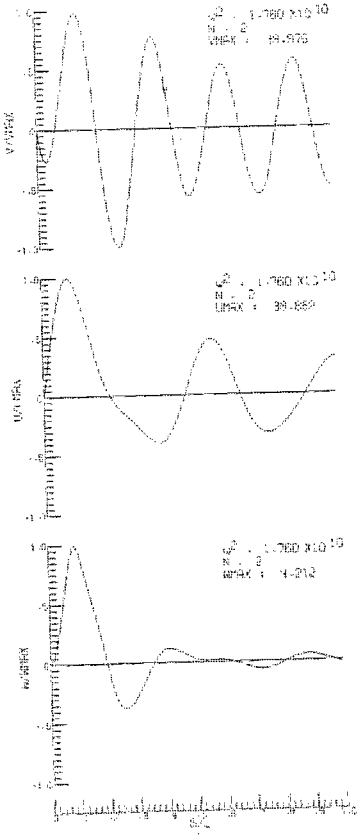

(n) Five nodal circles in w displacement

Figure 17.- Concluded.

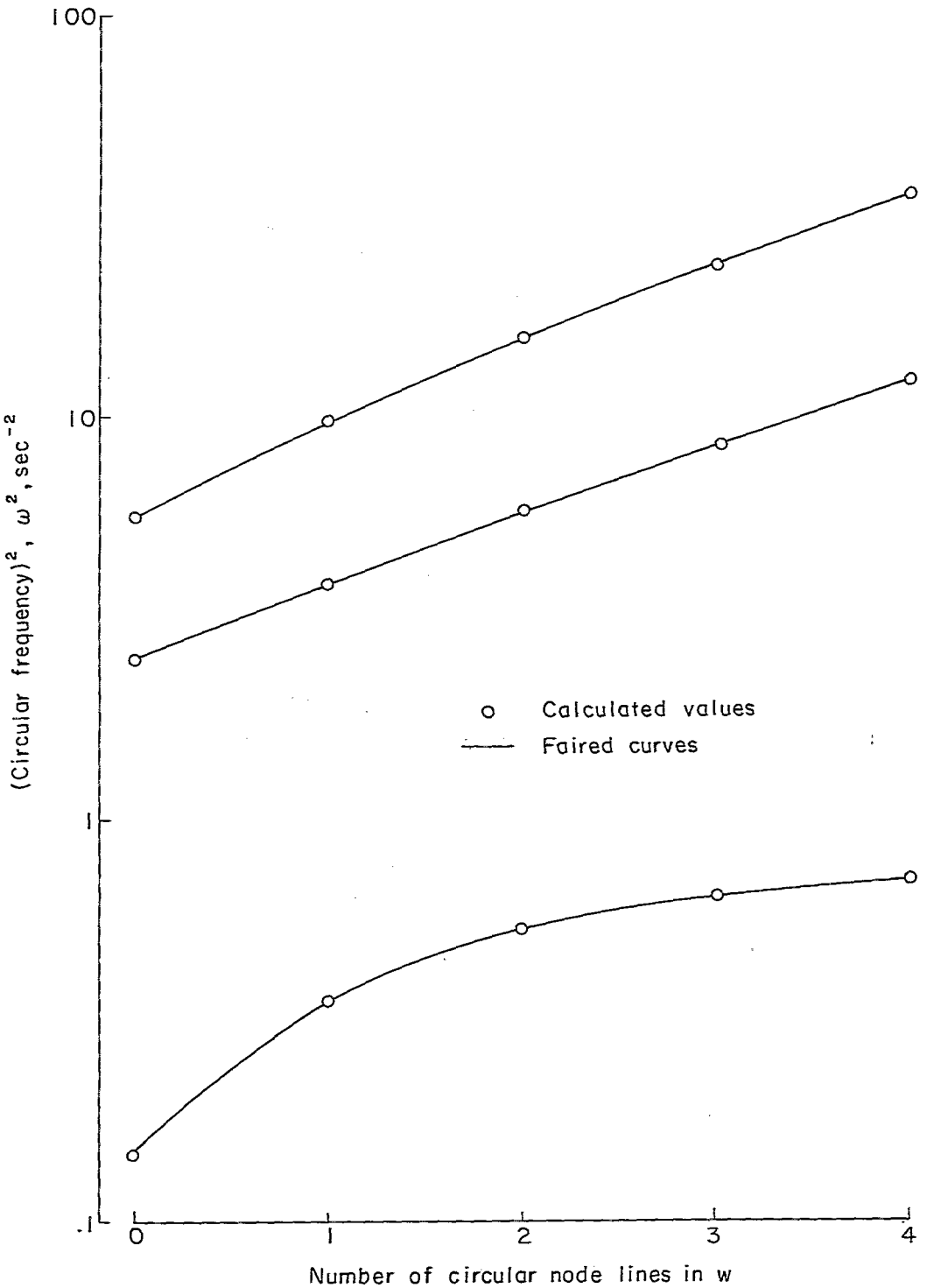

Figure 18.- Circular frequencies of a shell with positive Gaussian curvature with freely supported edges. n = 2.

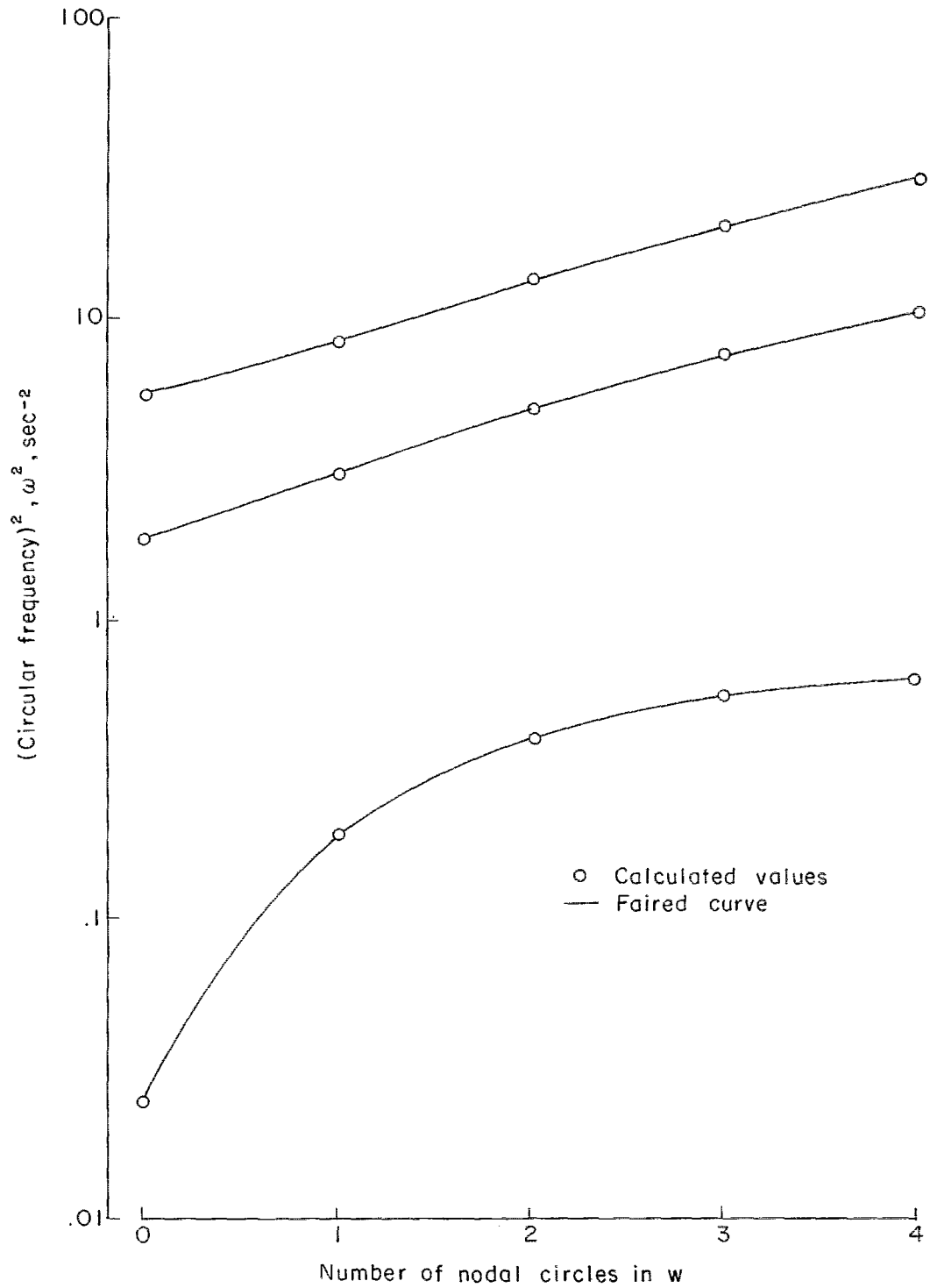

Figure 19.- Circular frequencies of a shell with negative Gaussian curvature having freely supported edges. n = 2.

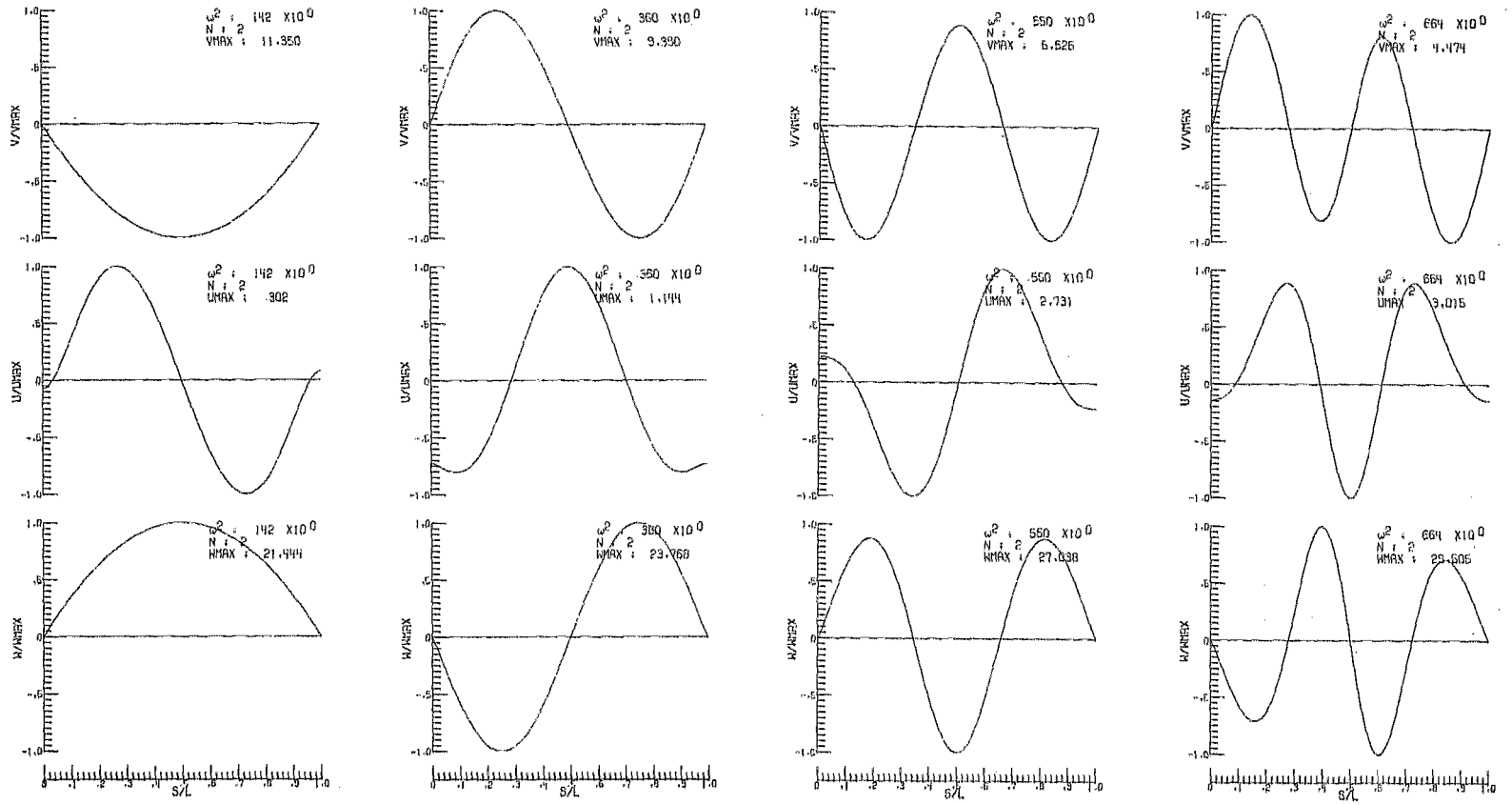

(a) Zero nodal circles in w displacement

(b) One nodal circle in w displacement

(c) Two nodal circles in w displacement

(d) Three nodal circles in w displacement ,

Figure 20.- Natural mode shapes of a shell of positive Gaussian curvature corresponding to the frequencies shown in figure 18.

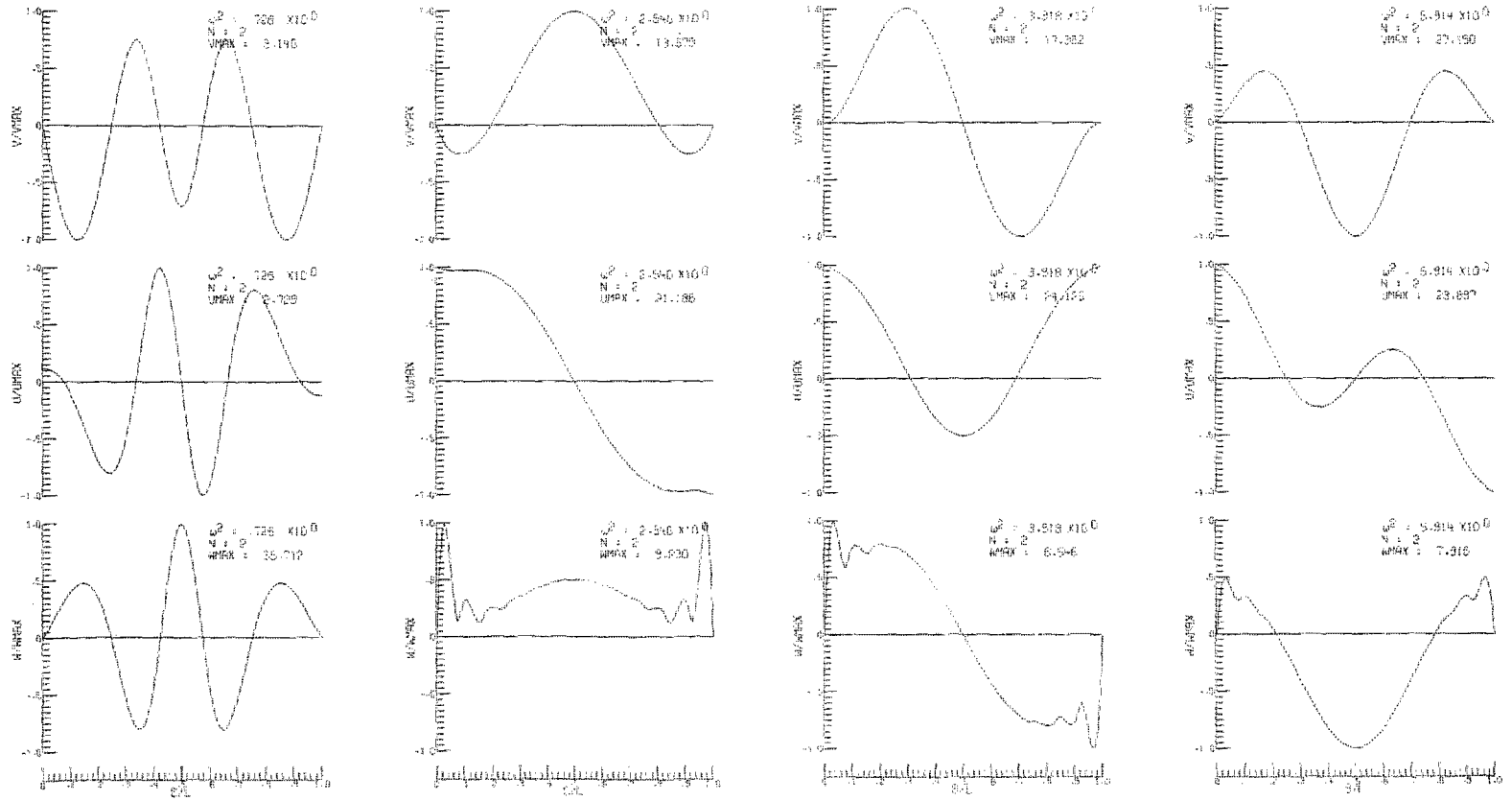

(e) Four nodal circles in w displacement

(f) Zero nodal circles in w displacement

(g) One nodal circle in w displacement

(h) Two nodal circles in w displacement

Figure 20.- Continued.

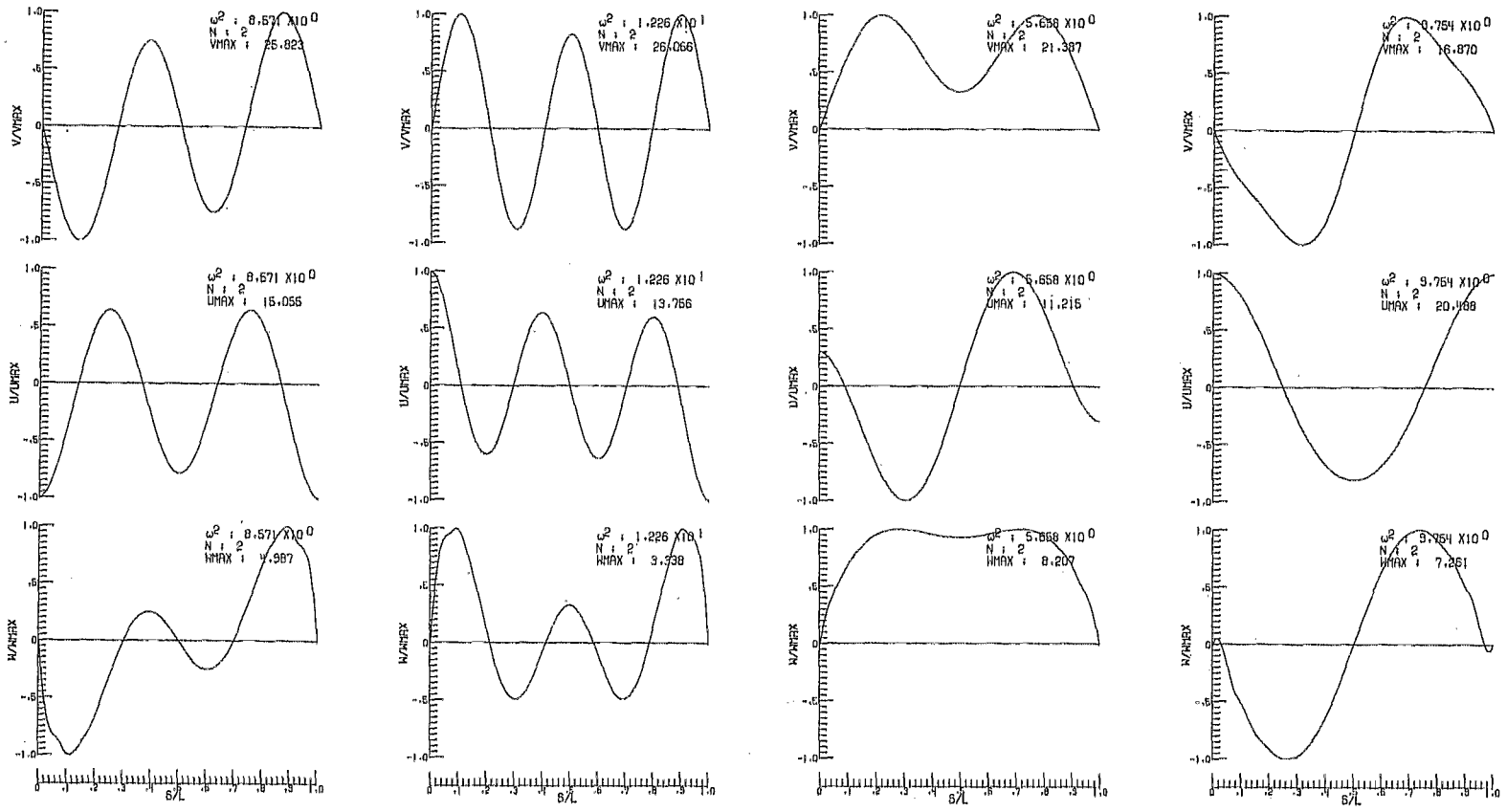

(i) Three nodal circles in w displacement

(j) Four nodal circles in w displacement

(k) Zero nodal circles in w displacement

(l) One nodal circle in w displacement

Figure 20.- Continued.

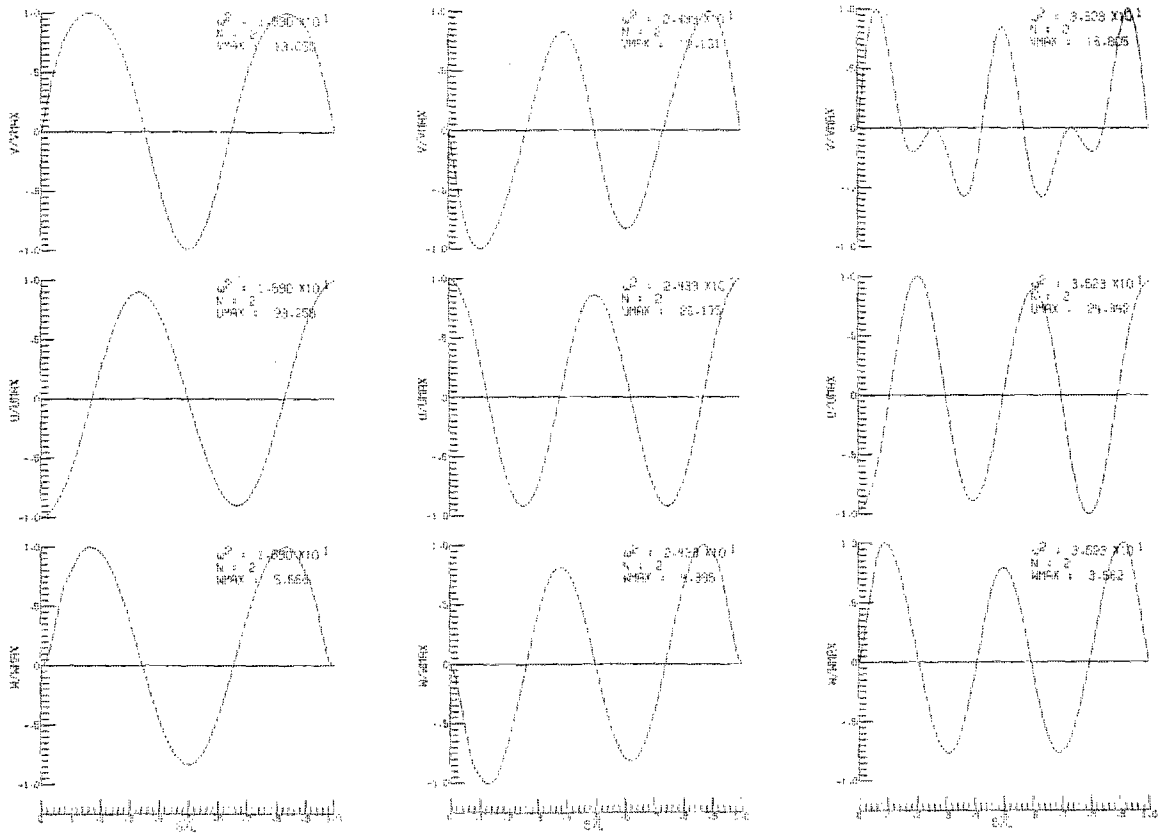

(m) Two nodal circles in w displacement

(n) Three nodal circles in w displacement

(o) Four nodal circles in w displacement

Figure 20.- Concluded.

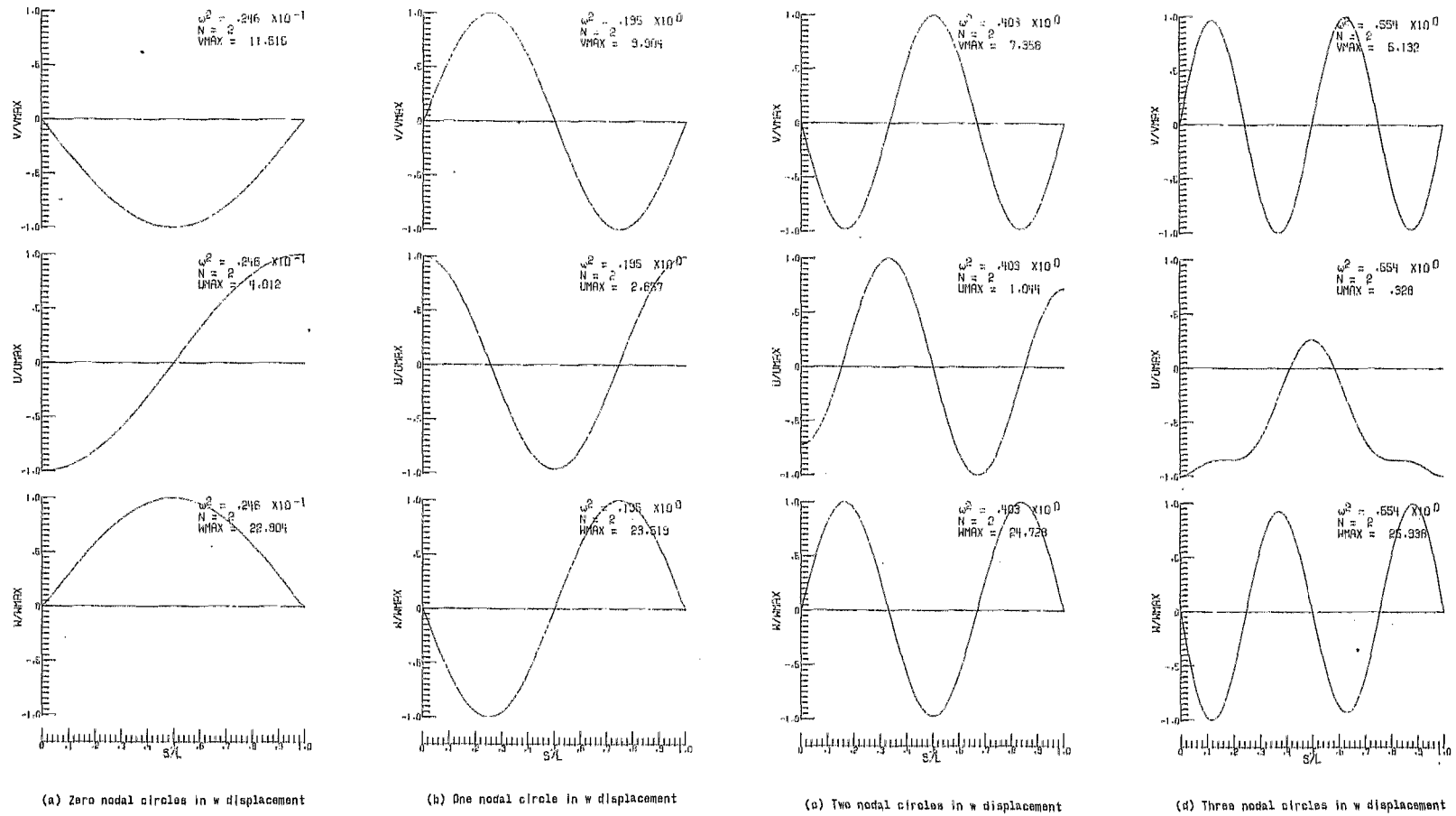

(a) Zero nodal circles in w displacement

(b) One nodal circle in w displacement

(c) Two nodal circles in w displacement

(d) Three nodal circles in w displacement

Figure 21.- Natural mode shapes of a shell having negative Gaussian curvature corresponding to the frequencies shown in figure 19.

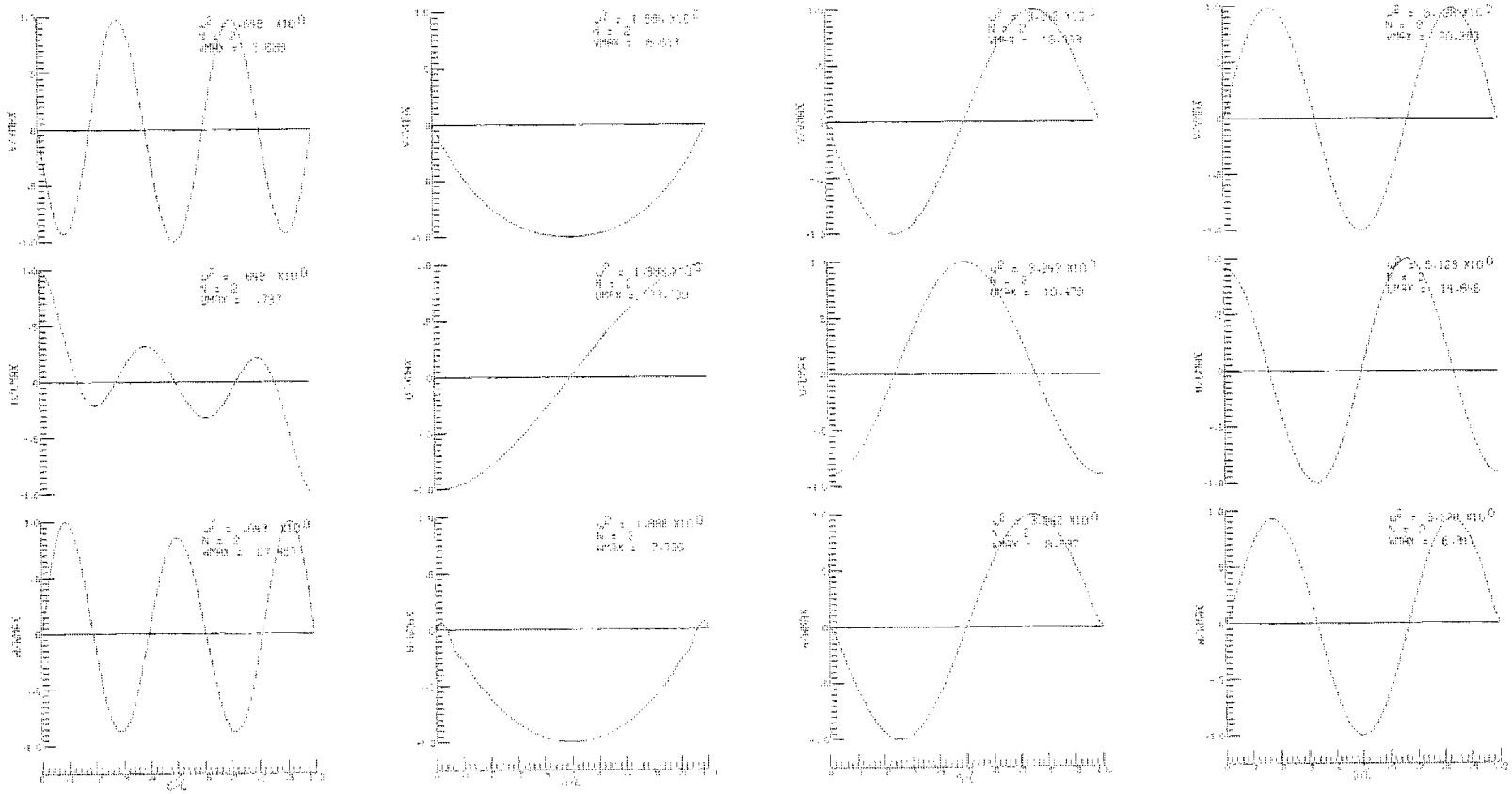

(e) Four nodal circles in w displacement

(f) Zero nodal circles in w displacement

(g) One nodal circle in w displacement

(h) Two nodal circles in w displacement

Figure 21.- Continued.

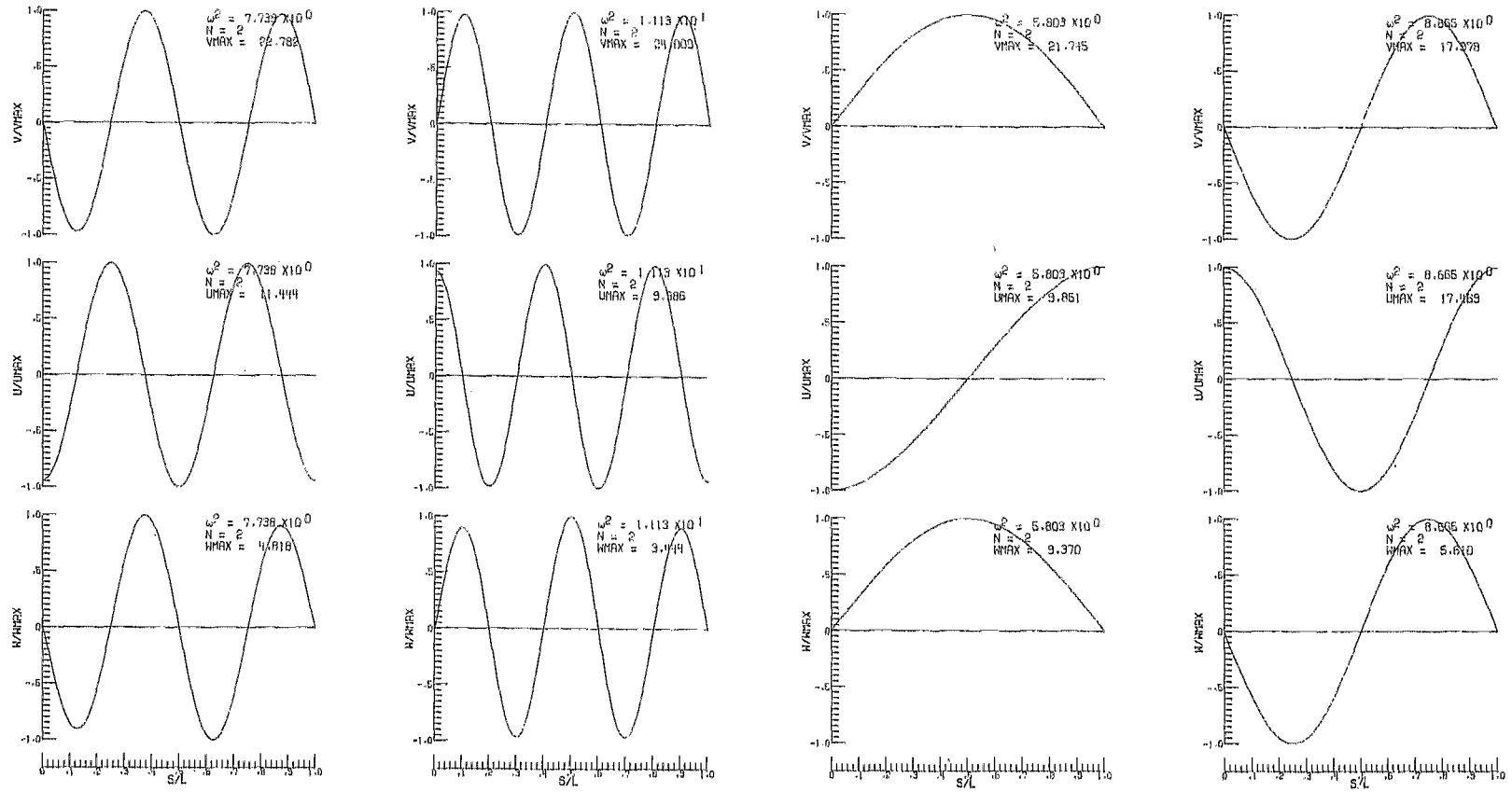

(i) Three nodal circles in w displacement

(j) Four nodal circles in w displacement

(k) Zero nodal circles in w displacement

(l) One nodal circle in w displacement

Figure 21.- Continued.

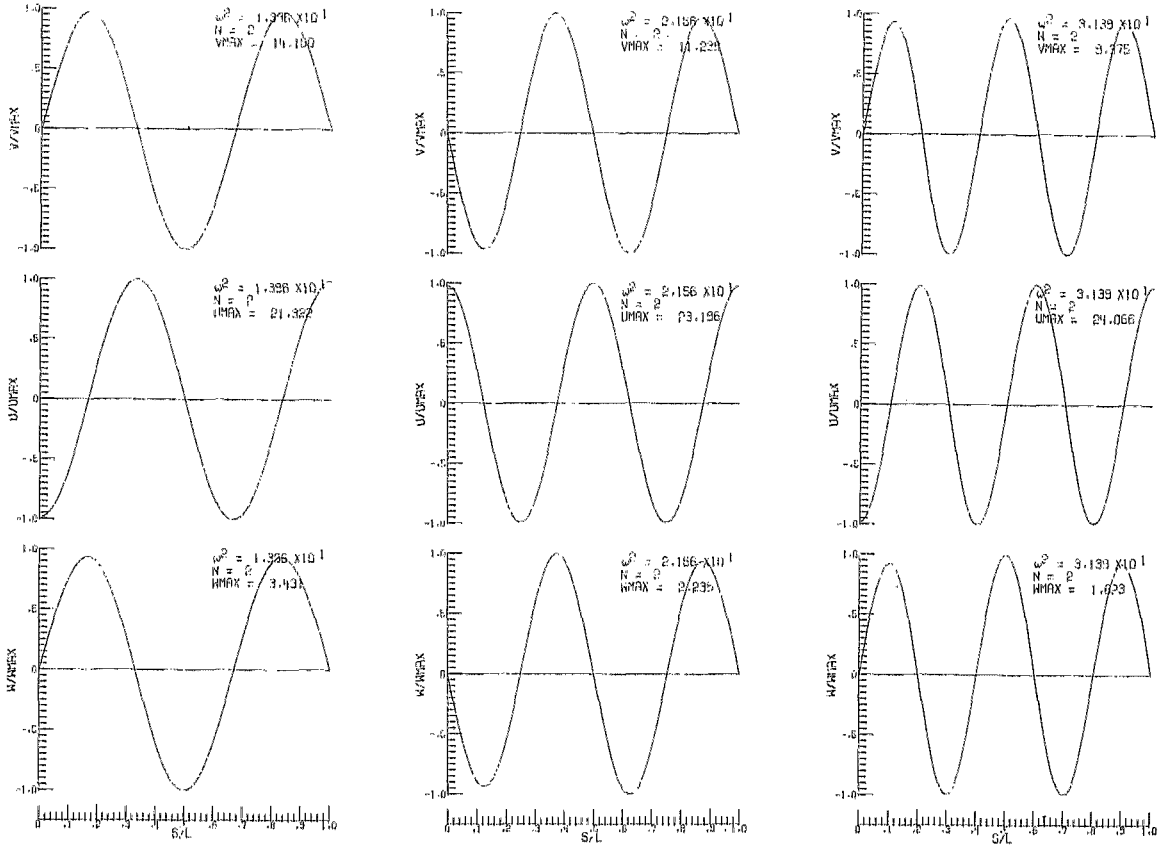

(m) Two nodal circles in w displacement

(n) Three nodal circles in w displacement

(o) Four nodal circles in w displacement

Figure 21.- Concluded.

NATIONAL AERONAUTICS AND SPACE ADMINISTRATION
WASHINGTON, D. C. 20546

OFFICIAL BUSINESS

FIRST CLASS MAIL

POSTAGE AND FEES PAID
NATIONAL AERONAUTICS AND
SPACE ADMINISTRATION

"The aeronautical and space activities of the United States shall be conducted so as to contribute . . . to the expansion of human knowledge of phenomena in the atmosphere and space. The Administration shall provide for the widest practicable and appropriate dissemination of information concerning its activities and the results thereof."

—NATIONAL AERONAUTICS AND SPACE ACT OF 1958

NASA SCIENTIFIC AND TECHNICAL PUBLICATIONS

TECHNICAL REPORTS: Scientific and technical information considered important, complete, and a lasting contribution to existing knowledge.

TECHNICAL NOTES: Information less broad in scope but nevertheless of importance as a contribution to existing knowledge.

TECHNICAL MEMORANDUMS: Information receiving limited distribution because of preliminary data, security classification, or other reasons.

CONTRACTOR REPORTS: Scientific and technical information generated under a NASA contract or grant and considered an important contribution to existing knowledge.

TECHNICAL TRANSLATIONS: Information published in a foreign language considered to merit NASA distribution in English.

SPECIAL PUBLICATIONS: Information derived from or of value to NASA activities. Publications include conference proceedings, monographs, data compilations, handbooks, sourcebooks, and special bibliographies.

TECHNOLOGY UTILIZATION PUBLICATIONS: Information on technology used by NASA that may be of particular interest in commercial and other non-aerospace applications. Publications include Tech Briefs, Technology Utilization Reports and Notes, and Technology Surveys.

Details on the availability of these publications may be obtained from:

SCIENTIFIC AND TECHNICAL INFORMATION DIVISION

NATIONAL AERONAUTICS AND SPACE ADMINISTRATION

Washington, D.C. 20546